The Fermilab Antiproton Source Design Report

April, 1981

Second Printing May, 1981

Fermi National Accelerator Laboratory

Batavia, Illinois

Operated by Universities Research Association Inc.

Under Contract with the United States Department of Energy

The Fermilab Antiproton Source Design Report

DRAFT

April, 1981

Second Printing May, 1981

Fermi National Accelerator Laboratory

Batavia, Illinois

Operated by Universities Research Association Inc.

Under Contract with the United States Department of Energy

<u>Contents</u>

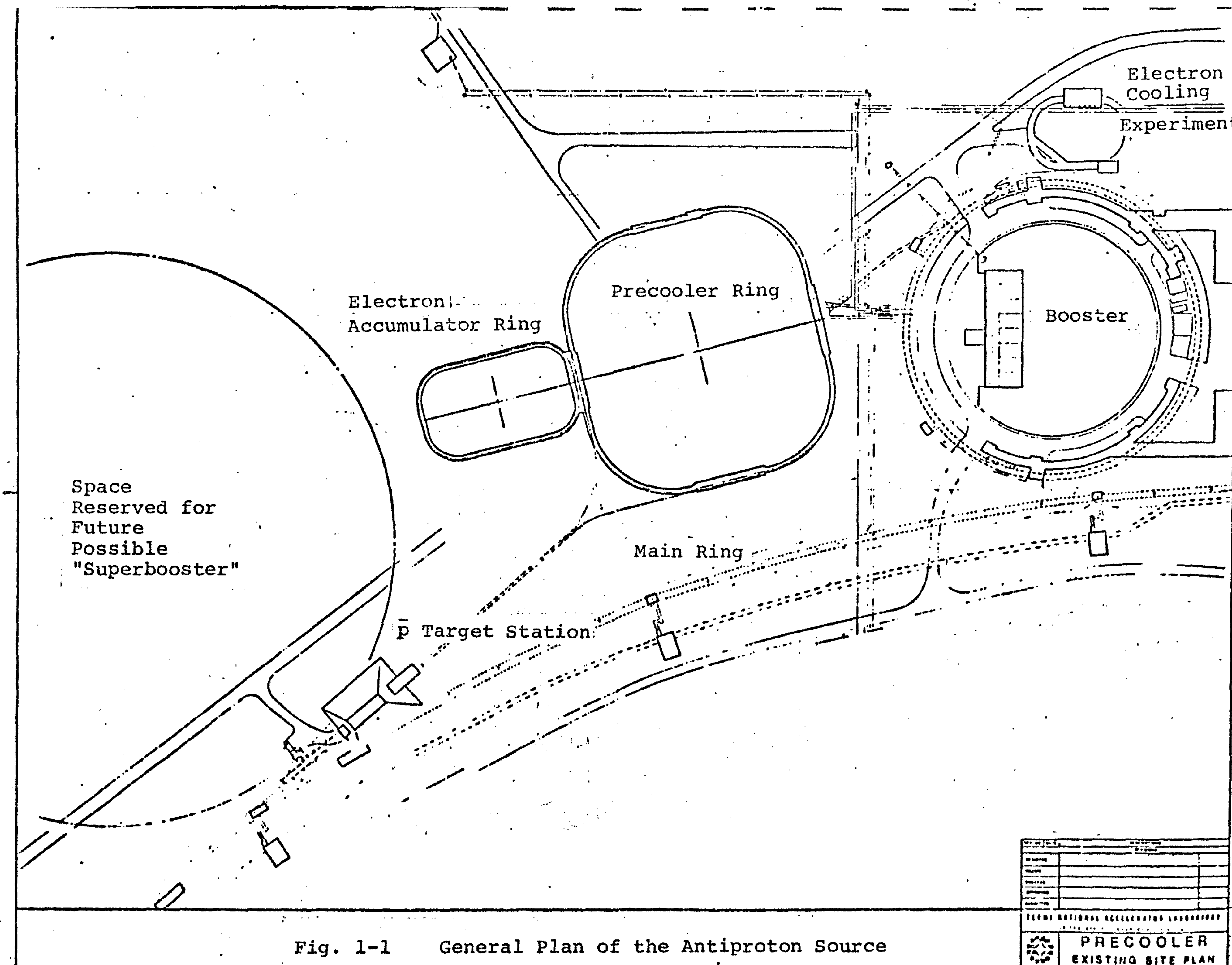

Fig. 1-1 General Plan of the Antiproton Source

1. Introduction and Summary

1.1 Purpose of the Antiproton Source

The purpose of the Fermilab Antiproton source is to provide at least 10^{11} cooled, accumulated antiprotons for acceleration in the Main Ring and Tevatron for colliding-beams experiments with 1-TeV protons. This will provide the highest available energy in the world for particle-physics experiments through at least the 1980's. Collisions at 2 TeV in the center of mass will provide a unique experimental tool in a new energy range.

The design of the Antiproton Source has been carried out by the Colliding Beams Department of the Accelerator Division in collaboration with Argonne National Laboratory, Lawrence Berkeley Laboratory, the Institute of Nuclear Physics at Novosibirsk, and the University of Wisconsin.

A project of similar purpose is under way at CERN. Its objective is to achieve colliding proton-antiproton beams at 540 GeV in the center of mass in the CERN SPS. The Antiproton Accumulator (AA), a ring that is roughly equivalent in function to the Precooler and Accumulator described here, has been built and is in operation. The AA is a different design solution to different design problems. The most important reason for the differences between the two projects is the different length of the proton beam that is the original source of antiprotons. The CERN PS beam proton beam is approximately 628 meters long, but the Fermilab Main Ring beam is 6280 meters long, a factor 10 larger. The larger size of our Precooler comes from the fundamental need to fold this longer beam into small pieces. It would be possible to extract the Main Ring beam in more batches and fill a Precooler of smaller radius, but the momentum spread of the $\bar{p}$ beam would increase and would soon go beyond what is possible to cool.

1.2 Overview of the System

Accumulation of antiprotons in a small enough phase-space volume to be usefully accelerated requires beam cooling. The system designed and described here makes use of both electron cooling and stochastic cooling in the energy and intensity ranges for which they are best suited, electron cooling at low energy and higher intensity both longitudinally and transversely, stochastic cooling longitudinally and at higher energy and low intensity.

Protons are accelerated to 80 GeV in the Main Ring in the time-honored fashion and the ring is flat-topped. The 80-GeV proton beam is extracted sequentially at F17 in Booster-length batches at 100-msec intervals, while the remaining batches circulate in the Main Ring. Each extracted batch is transported to the Antiproton Target Hall and targeted. Antiprotons of 4.5-GeV kinetic energy are collected and focused by a lithium lens and transported to the Precooler, a storage ring of Booster length (75.47 m average radius) to be built on a presently unoccupied site next to the Main Ring, as shown in Fig. 1-1. Each batch of beam is rotated in phase space to reduce its momentum spread and stacked with the previous antiproton batches. Depletion of the target by shock heating during the pulse limits the combination of intensity, pulse length, and spot size on the target. We have therefore split up the Main Ring pulse into batches of smaller length to preserve the target. The proton and antiproton beams will also be scanned approximately 0.5mm across the target during the pulse to spread the heating. This will make possible a smaller proton beam spot size. Within the limits imposed by target integrity, it is estimated that approximately 1.6×10^7 antiprotons per Main Ring pulse can be collected and stacked in the Precooler within a total relative momentum spread of 2% and transverse emittances of 5π mm-mrad in each plane.

The batch is now taken through a sequence of longitudinal stochastic cooling and deceleration steps. Each cooling step is continued until the cooling rate slows significantly because of bad mixing, then decelerated to re-establish mixing. After three such steps, the $\bar{p}$ batch is at 200 MeV with a total relative momentum spread of 0.55% and transverse emittances of 40π mm-mrad from adiabatic antidamping during deceleration. At this point, the batch is transferred into the Electron Cooling Accumulator, a smaller ring (32.35 m average radius) to be located south of the Precooler as shown in Fig. 1-1. This ring will be built in a new tunnel using magnets and other components taken from the present Electron Cooling Ring.

In the Electron Cooling Accumulator, the $\bar{p}$ batch will be injected, cooled both longitudinally and transversely by an electron cooling system, then accumulated with other $\bar{p}$ batches in a stack and cooled continually by the electron system. The cycle time for each batch is 9.85 sec and we therefore expect to accumulate 10^{11} antiprotons in 18 hours. The stack will have a total relative momentum spread of 0.1% and an emittance of 1π mm-mrad in each plane.

After accumulation has been completed, the antiprotons will be sequentially unstacked in 3 bunches. Each bunch is sequentially transferred to the Precooler and accelerated to 8 GeV, transferred to the Main Ring in the atypical (counterclockwise) direction, accelerated to 150 GeV, then transferred to the Tevatron. Protons will have been previously injected and accelerated to 150 GeV in the clockwise direction, then coalesced into three bunches and transferred to the Tevatron. After all three $\bar{p}$ bunches are stored in the Tevatron, the $\bar{p}$ and p bunches are accelerated together to 1 TeV for colliding-beams experiments. The luminosity goal of $10^{30}/\mathrm{cm}^2$-sec will be reached in 23 hours of accumulation. We will shorten this time by electron cooling at 400 MeV, rather than 200 MeV.

It should be noted that there is a large amount of flexibility possible in this system. The Electron Accumulator Ring will hold antiprotons up to 1 GeV in energy and it is possible to vary the cooling steps within wide limits to optimize the process. It is also possible to use the same rings in different electron and stochastic cooling scenarios.

2. General Scenario

2.1 Introduction

In this chapter, we give for reference a sequential listing of the scenario of antiproton accumulation and comment on possible variations.

2.2 Scenario Listing

(i) Proton Acceleration in Main Ring

Proton energy	80 GeV
No. of protons	2.6×10^{13}
Total no. of occupied buckets	975
Harmonic no.	1113
Flat-top length	1.3 sec
Total cycle time	9.85 sec

(ii) Proton Beam Extraction and Transport

Septum location	F17
No. of sequential batches	13
Batch interval	100 msec
No. of bunches per batch	75
No. of protons per batch	2×10^{12}
Extraction style	Single-batch
Transport to target	18 EPB dipoles 11 quadrupoles

(iii) Targeting

Target	Tungsten-rhenium
Target length	5 cm
Target diameter	8 cm, rotating at 47 rpm
Projected rms spot size (protons)	0.22 mm
$\bar{p}$ momentum	5.3567 GeV/C
$\bar{p}$ kinetic energy	4.5 GeV
$\bar{p}$ momentum spread (full)	1%
$\bar{p}$ emittance (each plane)	5π mm mrad
$\bar{p}$ bunch area	0.15 eV-sec
Invariant $\bar{p}$ cross section per nucleus	$0.0206/\mathrm{GeV}^2$-W nucleus
Proton absorption length	9.86 cm
$\bar{p}$ absorption length	9.09 cm
Yield $N\bar{p}/Np$ (includes Li lens loss)	0.6×10^{-6}
Total $\bar{p}$ per MR cycle	1.56×10^{7}
Accumulation rate	5.7×10^{9} $\bar{p}$/hr

(iv) RF Rotation in Precooler

Initial rms bunch length	21 cm
Harmonic number	84
RF capture voltage at 53MHz	400 kV
Phase-oscillation period	367 μsec
Phase-space rotation time	91 μsec
Momentum displacement in stacking	4%
Energy change	213 MeV
Stacking time	85 msec
Final momentum spread (full stack)	2.16%
Total $\bar{p}$ stacked per MR cycle	1.56×10^7

(v) Stochastic Momentum Cooling and Deceleration

(a) Cooling step 1

Energy	4.5 GeV
Initial momentum spread	2.1%
Final momentum spread	0.28%
Cooling time	4.5 sec

(b) Deceleration 1

Initial energy	4.5 GeV
Harmonic number	9
Peak rf voltage	84.4 kV
Final energy	2.4 GeV
Deceleration time	0.54 sec

(c) Cooling step 2

Energy	2.4 GeV
Initial momentum spread	0.5%
Final	0.13%
Cooling time	1.25 sec

(d) Deceleration 2

Initial energy	2.4 GeV
Harmonic number	10
Peak rf voltage	45.5 kV
Final energy	0.9 GeV
Deceleration time	0.435 sec

(e) Cooling step 3

Energy	0.85 GeV
Initial momentum spread	0.28%
Final momentum spread	0.046%
Cooling time	0.75 sec

(f) Deceleration 3

Initial energy	0.85 GeV
Harmonic number	14
Peak rf voltage	11.8 kV
Final energy	0.204 GeV
Deceleration time	0.4 sec

(g) 200-MeV bunching

Harmonic number	1
RF voltage	4 kV
Final momentum spread	0.44%
Final bunch length	1.0 μsec
Bunching time	5 msec
Total cycle time	9.85 sec

(vi) Electron Cooling and Accumulation

Kinetic energy	0.2 GeV
Initial momentum spread	0.44%
Initial emittance (each plane)	40π mm-mrad
Precooling	
Final momentum spread	0.1%
Final emittance	1 π mm-mrad
Cooling time	2 sec

Stack is cooled between precoolings to maintain $\Delta p/p = 10^{-3}$ and emittances of 1π mm-mrad

$\bar{p}$ per cycle	1.56×10^{7}
Total accumulation time	23 hr
time for $L=10^{30}/cm^2$-sec	

(vii) Reacceleration

Number of $\bar{p}$ bunches	3
Method of rebunching	RF unstacking
Precooler acceleration time	1 sec
Harmonic number	14
Frequency range	5.01-8.80 MHz

The 3 bunches are individually recooled, accelerated to 8 GeV, transferred to the Main Ring, accelerated to 150 GeV and injected into the Tevatron. Protons have previously been accelerated, rebunched, and stored in the Tevatron.

(viii) Colliding Scenario

Number of $\bar{p}$ bunches	3
Number of p bunches	3
Number of $\bar{p}$ per bunch	4×10^{10}
Number of p per bunch	10^{11}
β^*	2 m
RMS $\bar{p}$ beam size	<0.1 mm
RMS p beam size	0.1 mm
Luminosity per intersection region	$10^{30}/cm^2$-sec
Luminosity lifetime	several days
RMS bunch length ($\bar{p}$)	<45 cm
RMS bunch length (p)	45 cm
Beam-beam tune shift	0.003

2.3 Other Scenarios

There is a great deal of inherent flexibility in the design discussed in this report. It is believed that this is a considerable advantage of the design, because knowledge of beam cooling is expanding rapidly, both theoretically and experimentally.

This flexibility can be used in other cooling schemes with the same equipment. One such scheme that has been investigated would inject antiprotons into the Precooler, stack them, and cool the stack by stochastic cooling without precooling or deceleration. The performance of this scheme is limited because the stochastic cooling rate decreases as the number of antiprotons in the stack increases. Estimates show that the cooling rate becomes unmanageably long when the number of antiprotons accumulated is of the order of 3×10^9, with a collection time of the order of 1 hour. Such a beam will give a luminosity of approximately $2 \times 10^{28}/\text{cm}^2$ sec, which can be valuable for initial exploratory experiments. Higher-luminosity all-stochastic schemes would require a separate Accumulator ring.

It is also possible to vary the energy of electron cooling and accumulation. It is believed that 400 MeV $\bar{p}$ energy may be a practical upper limit without extensive electron-gun development; the Electron Accumulator Ring can store antiprotons up to 1 GeV. If development of a 550-keV electron gun (corresponding to 1-GeV antiprotons) appears feasible, the present rings will be adequate for this higher-energy cooling.

3. Targeting and Transport

3.1 Main Ring Extraction

Extraction of 80 GeV protons from the Main Ring for the production of antiprotons is to take place at location F17. At this location, a Lambertson magnet will deflect the extracted beam vertically towards the transport line, located imediately above the Main Ring magnets.

The geometry and expected beam sizes at the Lambertson location are shown in Fig. 3-1. The relevant parameters of the Main Ring Lattice are listed in Table 3-I.

TABLE 3-I PROPERTIES OF SELECTED MAIN RING MINISTRAIGHTS

Radial Plane Lattice Functions

Location	β[m]	α	Phase Relative to F17 Modulo 360°)	Space Available (in.)
C48 Kicker	102.414	0.46696	-90.11°	(Existing)
F11	67.258	1.1745	-214.27°	0.0
F12	29.601	-0.5731	-168.30°	0.0
F13	95.356	1.8584	-135.74°	0.0
F14	28.383	-0.5893	-99.29°	34.0
F15 (Bump 1)	97.247	1.8396	-66.32°	42.5
F16	30.093	-0.6239	-31.47°	42.0
F17 (Bump 2) (Extraction)	99.648	1.9388	0.00°	32.0
F18 (Bump 3)	28.865	-0.5582	35.20°	52.0
F19	94.322	1.8156	68.92°	0.0
F21	28.912	-0.6177	104.71°	28.0
F22 (Bump 4)	99.541	1.8926	136.92°	27.5
F23	30.073	-0.5983	171.32°	35.0
F24	97.400	1.9056	203.21°	0.0
F25	28.365	-0.5666	239.23°	35.0
F26	95.244	1.8100	272.60°	43.5

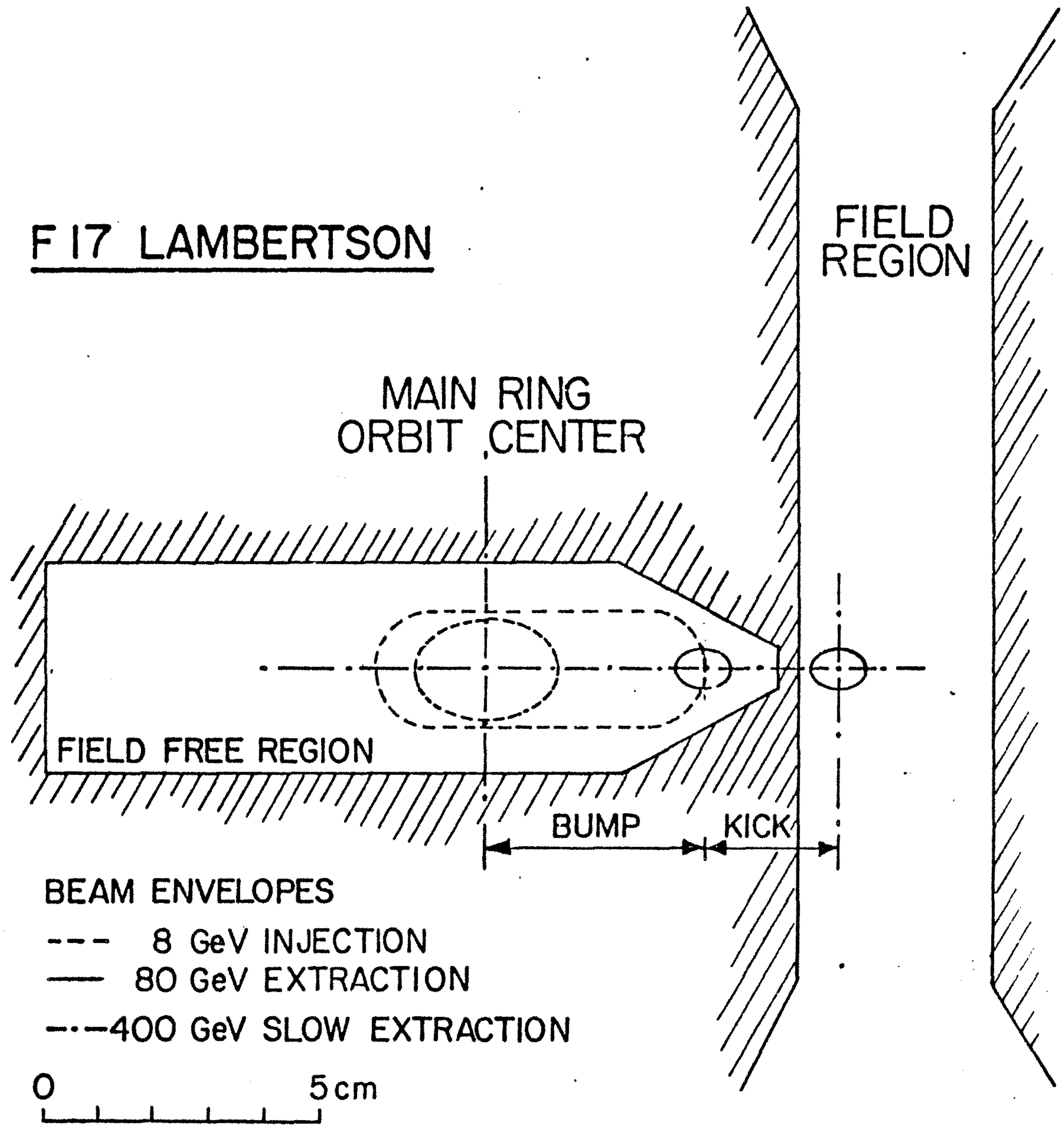

Fig. 3-1 Main Ring Extraction Geometry

The existing kicker at location C48 will be utilized to provide the necessary horizontal displacement of approximately 25 mm to jump the Lambertson septum. The present kicker power supply is designed for single-turn Main Ring extraction. A simple modification is required to shorten this pulse to extract 1/13 of the Main Ring circumference at a time, a batch 1.6 μsec long. The required angular kick at C48 is -0.238 mrad or a voltage at the supply of 21.0 kV, well within the present operating range. Given the Main Ring lattice characteristics, the displacement at F17 will result also in an angular displacement of 0.467 mrad.

In order to compensate for the angle resulting from the kick across the septum and to have flexibility in the location of the Main Ring beam with respect to the F17 Lambertson during 8-GeV injection prior to 80-GeV extraction, and to allow for room during 400-GeV extraction (see Fig. 3-1) we have designed a local 4-magnet slow orbit bump to be installed at locations F15, F17, F18 and F22. This 4-magnet combination will permit independent adjustment of the beam position and angle at F17. For the configuration of -38 mm displacement and compensation for the angle resulting from the C48 kick (-25 mm at F17) the required angular kicks and magnets bending power are indicated in Table 3-II. The required apertures in Main Ring have been measured during machine studies.

TABLE 3-II FOUR-MAGNET ORBIT-BUMP PARAMETERS

MR Location	Bump angle (mrad)	Bend strength (kG-m)
F15	-.42	-1.134
F17	-1.04	-2.808
F18	+1.04	+2.808
F22	-1.03	-2.781

The configuration described here will permit the two following modes of operation:

(i) Dedicated 80-GeV running: The Main Ring will operate on a 80-GeV ramp. Allowance is to be made at F17 for 8-GeV injection aperture. Only the desired number of Booster batches to be extracted towards the $\bar{p}$ target will be injected.

(ii) Parasiting on 400-GeV operation: Probably only 1 Booster batch could be extracted towards the $\bar{p}$ target at 80 GeV for tests. Allowance is to be made at F17 for 8-GeV injection aperture and 400-GeV extraction aperture requirements.

The F17 Lambertson has been installed and operated in the Main Ring since January, 1981. It is equipped with remote positioning devices, beam monitors and loss monitors. Power supply, controls and electronics are located in service building F1. Extraction studies are to take place during June and October 1981 to determine the best Lambertson location with respect to the center of the Main Ring orbit. Although the Lambertson can be moved away from the orbit, its location will remain fixed during 80-GeV extraction, due to the fixed location of the 80-GeV transport line; the variations in operating modes will be accomodated by the four-magnet bump to position the Main Ring orbit with respect to the Lambertson septum.

Vertical extraction was chosen at F17 to minimize the angular deflection required to clear the first Main Ring magnet downstream of the Lambertson. The return coil on the upstream end of this magnet has been modified to permit the extracted 80-GeV beam pipe to be located close to the magnet steel. This space restriction will limit the maximum energy that can be extracted at F17 to below 125 GeV. An upgrade to 125 GeV would require a second Lambertson magnet and major modifications of the upstream end of the transport line described below.

3.2 Proton Transport

The layout of the 80-GeV proton-beam transport is shown in Fig. 3-2. From the extraction point at F17, the line extends to location F25. The transport elements are located just above the Main Ring magnets. At location F25, the 80-GeV beam exits the Main Ring tunnel toward the pretarget area, $\bar{p}$ Hall, and the antiproton target area, $\bar{p}$ Target Hall.

The transport line is assembled from External Proton Beam (EPB) type magnets. Two dipoles, V1 and V2, are utilized to set the beam horizontal (19.0 in. above the Main Ring orbit) following the extraction Lambertson. Thirteen dipoles are utilized to follow the Main Ring radius by distributing them uniformly between locations F18 and F23. Five dipoles are used to provide the reverse bend to exit the Main Ring tunnel at a convenient place in location F25. This last requirement forces the beam to the inside of the Main Ring between F23 and F25, reducing some of the tunnel free space. A small-diameter pipe connects the Main Ring tunnel to the upstream end of $\bar{p}$ Hall, where a remotely operated beam stop will permit access to most of $\bar{p}$ Hall, and $\bar{p}$ Target Hall during Main Ring operation.

The transport line includes eleven EPB quadrupoles with water-cooled coils upgraded to match the power supplies obtained to power them. Element Q7B is a type 5Q36 (ANL) quadrupole. The location of the elements in $\bar{p}$ Hall is shown in Fig. 3-3.

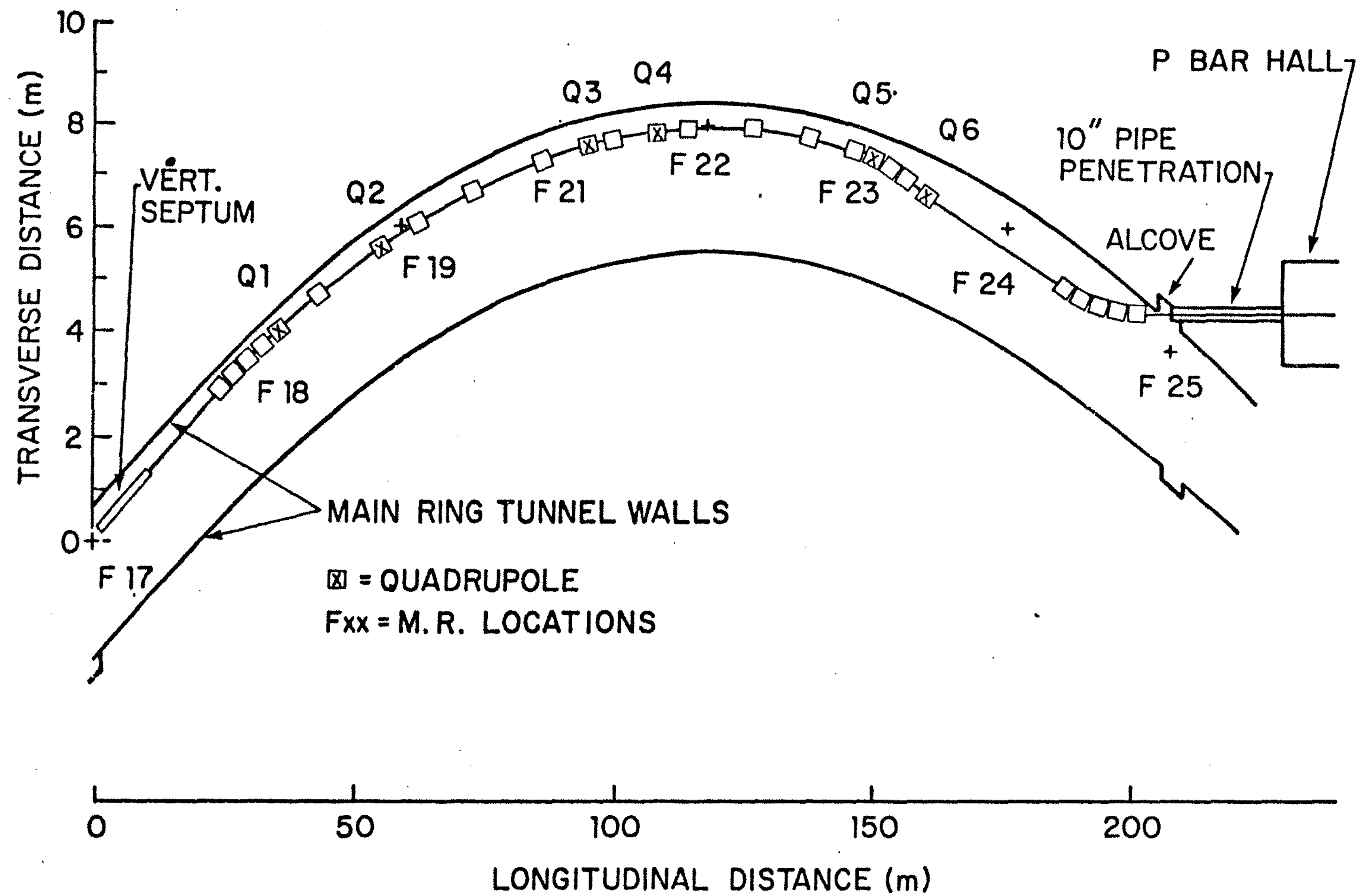

Fig. 3-2 EXTRACTED-PROTON BEAM-TRANSPORT LAYOUT

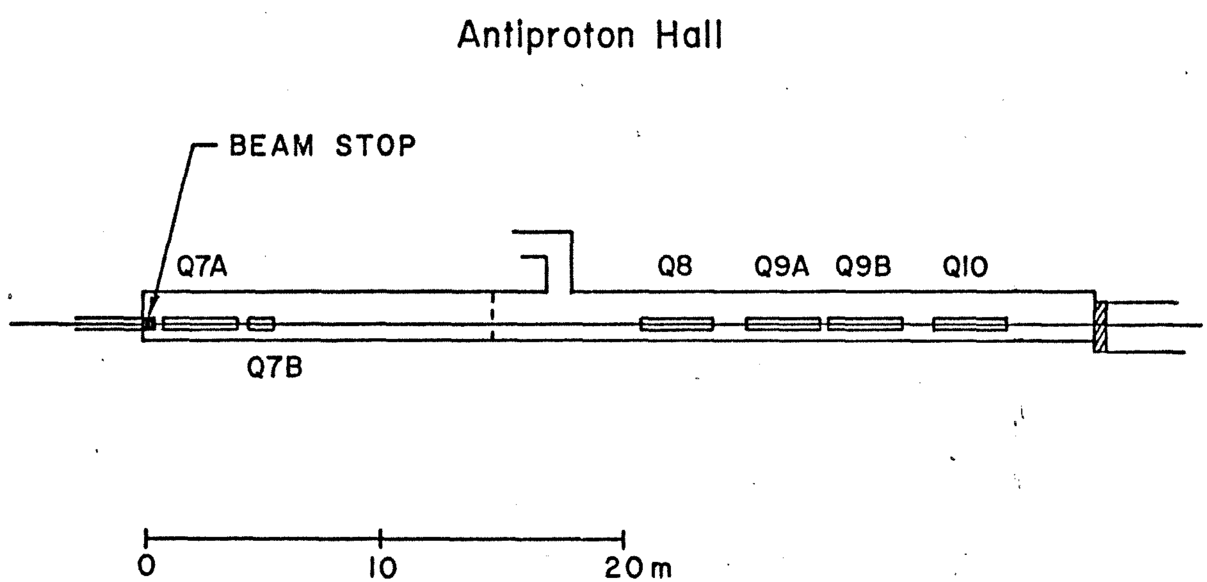

Fig. 3-3 $\bar{p}$ Hall

The details of the transport line are given in Table 3-III.

TABLE 3-III PROTON TRANSPORT LINE

Distance to F17(inches)	Element	Type	Field/Gradient (T)/(T/m)	Bend
210	Lambertson		1.083	UP
916	H1	EPB	1.272	RIGHT
1048	V1	EPB	0.920	DOWN
1180	V2	EPB	0.920	DOWN
1312	H2	EPB	1.272	RIGHT
1444	Q1	3Q120A	-5.07	
1706	H3	EPB	1.272	RIGHT
2126	Q2	3Q120A	5.07	
2426	H4	EPB	1.272	RIGHT
2946	H5	EPB	1.272	RIGHT
3466	H6	EPB	1.272	RIGHT
3854	Q3	3Q120A	-5.07	
3986	H7	EPB	1.272	RIGHT
4246	Q4	3Q120A	3.88	
4506	H8		1.272	RIGHT
5033	H9	EPB	1.272	RIGHT
5559	H10	EPB	1.272	RIGHT
5944	H11	EPB	1.272	RIGHT
6142	Q5	3Q120A	-3.88	
6274	H12	EPB	1.272	RIGHT
6406	H13	EPB	1.272	RIGHT
6646	Q6	3Q120A	3.88	
7453	H14	EPB	1.272	LEFT
7585	H15	EPB	1.272	LEFT
7717	H16	EPB	1.272	LEFT
7849	H17	EPB	1.272	LEFT
7981	H18	EPB	1.272	LEFT
9185	Q7A	3Q120A	15.20	
9280	Q7B	5Q36	14.81	
9968	Q8	3Q120A	-15.20	
10142	Q9A	3Q120A	9.96	
10274	Q9B	3Q120A	14.34	
10448	Q10	3Q120A	-15.20	
10688	Target Center			

As shown, six quadrupoles in $\bar{p}$ Hall are utilized to produce the desired beam spot at the target. Alternative designs including a Lithium lens in the proton beam have also been considered. For the present requirements, the quadrupole solution suffices, because the minimum spot size at the target is expected to be limited by target lifetime.

One above-ground power-supply service building at location F23 houses power supplies, controls, instrumentation, vacuum and water for the section of transport line within the Main Ring tunnel. A second above-ground building at location F27 will provide services for the $\bar{p}$ Hall and $\bar{p}$ Target Hall enclosures.

Access to $\bar{p}$ Hall is by a hatch and labyrinth. Because of the limited amount of earth between the upstream end of the hall and the Main Ring tunnel, that end will not be accessible during Main Ring operation. The downstream end will be sealed by a 30 cm thick iron shield required to minimize soil exposure due to backward radiation from the target. Residual radiation levels in $\bar{p}$ Hall are expected to be low enough to permit maintenance in place.

Completion of the 80-GeV beam transport line to F25 is expected by summer 1981, and to the target station by October, 1981.

3.2.1 $\bar{p}$ Target Hall. The antiproton producing target, proton beam dump and antiproton collection system will be located in an existing vault downstream of $\bar{p}$ Hall of dimensions 1.5 m wide and 40 m long. The floor is 6.4 m below ground with a beam elevation 1.2 m above it. An elevation view is shown in Fig. 3-4.

The upstream end of the hall, containing the target, vertical bend, and dump will be an area of high residual radiation and limited access. During normal operation of the $\bar{p}$ source, greater than 2×10^{12} protons per second are to be incident on the target and dump. Shielding configurations, taking into account soil irradiation, outdoor dose rate and muon fluxes have been studied to permit operation with average intensities of up to 10^{13} protons per sec.

The target will be just downstream of the thick iron shield separating $\bar{p}$ Target Hall from $\bar{p}$ Hall. The target design and the $\bar{p}$ collection system are described in detail below. As shown in Fig. 3-4, antiprotons are collected by a lithium lens before a vertical bend up (BV1) of 6° separates them from the 80-GeV protons (-0.4°). A vertical translation by 2.485 m, required to get to the level appropriate for Precooler injection, takes place within $\bar{p}$ Target Hall. The antiprotons emerge from the Li Lens as a nearby parallel beam.

The proton beam dump will be made of steel, approximately 5 m long, 1.5 wide and of a height to accomodate the antiproton transport line. It will contain a water-cooled graphite core capable of absorbing in excess of the 25 kW presently required. A closed loop water cooling system will be located in $\bar{p}$ Hall.

Access to the elements in the Target Hall is from above, possible within a structure, that will straddle the present roof hatch. As part of this structure an additional 1.8 m of shielding

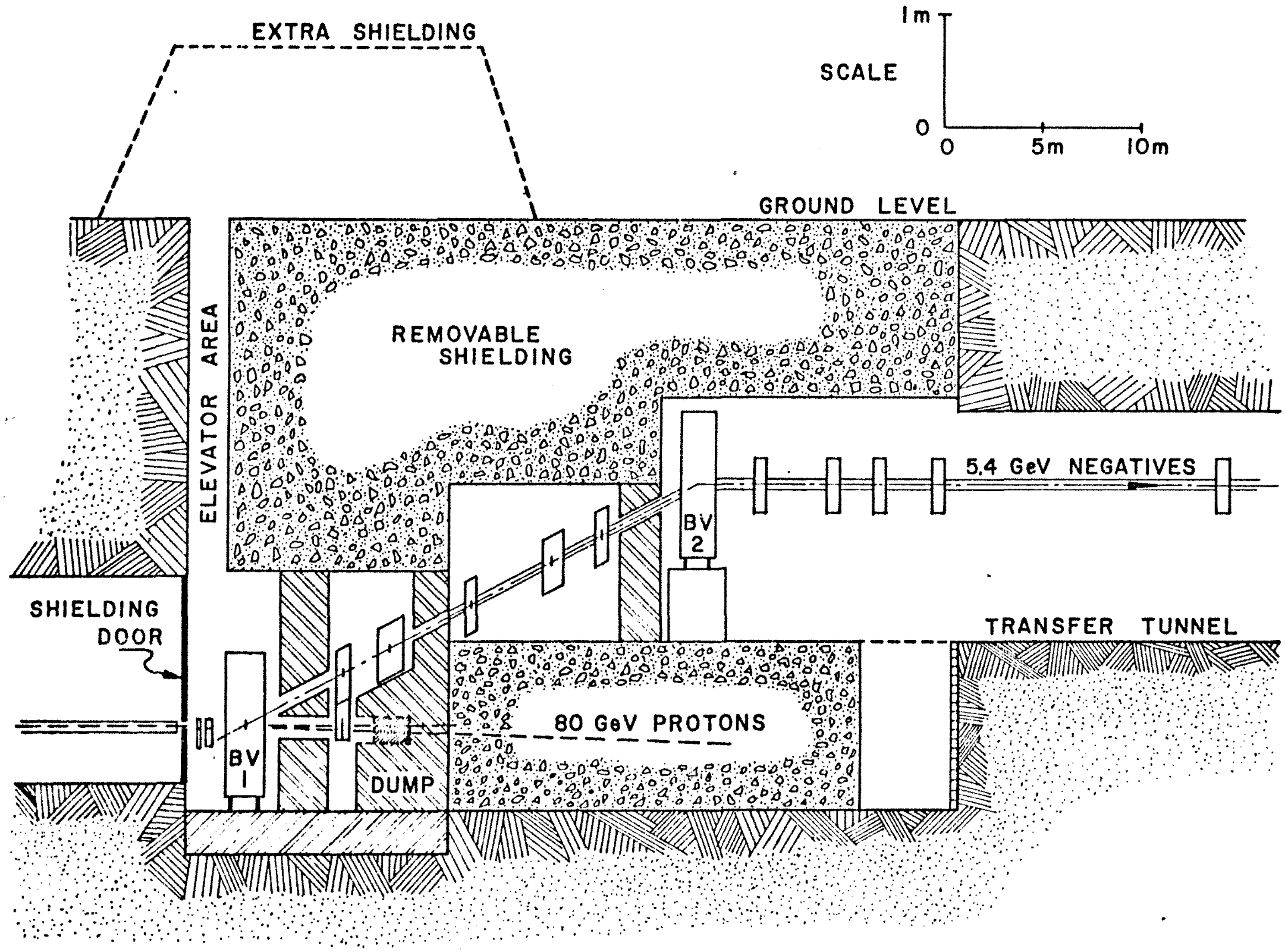

Fig. 3-4 $\bar{p}$ Target Hall

will be incorporated to keep the above-ground dosage level well below 50 mrem/hour.

From the point of view of accessibility, we have identified two different regions within $\bar{p}$ Target Hall:

(i) Upstream of BV1: This area contains the target itself, the lithium lens, instrumentation to monitor target performance, target, lens remote-positioning mechanism and lens electrical devices. We expect the need of relatively frequent accesses, especially during the commissioning phases of the project. Elements are to be located within elevators that will include that section of the shielding directly above them. Services are to be through the shielding. In the down position, the elevator platform will rest on alignment pins on the floor. In the up position, the elevator will place the radioactive elements for remote transfer to shielded containers. These containers, with relatively light and small components, can then be transferred to the Neutrino area remote-handling facility for maintenance. Highly radioactive components can be stored within $\bar{p}$ Target Hall shielding for cooling.

(ii) Downstream and including BV1: This region contains only dipole and quadrupole magnets. Access is expected to be very infrequent both during and after commissioning. Access for maintenance will require the removal of shielding blocks and lifting of the beam-transport elements with a crane.

3.3 $\bar{p}$ Production Rate

Several independent calculations exist that estimate the number of antiprotons to be captured within a given precooler acceptance. These calculations have been extended with a Monte Carlo program that includes a fit to available data on antiproton production cross sections, hadronic shower development in the target, multiple scattering, absorption and a lithium lens collector. The result of these calculations are summarized in Table 3-IV.

TABLE 3-IV PARAMETERS FOR ANTIPROTON FLUXES INTO PRECOOLLER ACCEPTANCE

Precooler acceptance (each plane)	5π mm-mrad
Proton beam momentum	80 GeV/c
Proton beam β:	1 m
Proton beam size	$\sigma x = \sigma y = 0.02$ cm
Antiproton momentum	5.39 GeV/c
Target material	Tungsten
Target length	5cm

Li lens gradient	1000 T/m
Li lens radius	1cm
Li lens length	10 cm
Lens face to target center	14.75 cm
$\frac{1}{\sigma_i} E \frac{d^3\sigma}{dp^3}$	0.0206 GeV^{-2} per W nucleus
Proton absorption length	9.86 cm
Antiproton absorption length	9.09 cm
Antiproton yield	1.1×10^{-5} p^{-1} GeV^{-1}
Antiproton yield for $\Delta p/p = 1\%$	6×10^{-7} $proton^{-1}$

The antiproton yield increases with decreasing proton beam size. The choice of $\sigma = 0.02$cm is based on the limiting behaviour of the target due to the energy density deposited (see below).

The choice of a 5-cm long high-density target (tungsten) is dictated by a 20% increase in antiproton yield of shower development vs the depth of field effect due to the very short focal distance of the lithium lens.

The antiproton yield increases with increasing Li lens gradient. An increase of 5% to 10% could be achieved by increasing this gradient. The choice of 1000 T/m permits a reasonable distance between the target and the lens.

A reduction on the lithium lens radius from 1cm to 0.25cm will result in a 20% decrease of yield for a $5\pi \times 10^{-6}$m acceptance.

The yield in Table 3-IV corresponds to an invariant cross section per inelastic interaction of ~ 0.66 mb GeV^{-2} Other estimates of antiproton yields have been previously based on 0.80 mb/GeV^{-2}. This difference reflects the uncertainties in the production cross sections, including the dependence on the target nucleus and the scaling variable x.

3.4 Antiproton Target

The yield of antiprotons into a given precooler acceptance increases as the proton beam spot decreases, until multiple scattering in the target material starts to contribute to beam-size growth. Smaller proton beam sizes will result in increasing energy density deposition in the target material. A compromise must be made between the brightness of the antiproton beam and the expected lifetime of the target itself.

3.4.1 Material Choice. With the requirements that the target material be of high density and high melting point a compilation of mechanical properties for different materials was performed. A figure of merit to compare the mechanical properties was obtained from the yield stress divided by the coefficient of thermal expansion and the modulus of elasticity. On this basis rhenium, tungsten and tungsten-rhenium alloys are in increasing order for this figure of merit. The coefficient of heat conductivity could also be included in the figure of merit without significant altering the choice of material.

The high-temperature behavior of tungsten-rhenium alloys shows considerable increase of yield stresses with respect to tungsten, but little change on the coefficient of thermal expansion or the modulus of elasticity.

Tungsten-rhenium alloys are utilized in industry for high-temperature applications (e.g. incandescent-lamp wire and targets for high-power x-ray tubes) and a significant amount of experience and technology for their fabrication exist. Other tungsten and/or rhenium alloys exhibit interesting mechanical properties. Tungsten will be used for the following calculation, although a number of target configurations are to be tested during the R & D phase of the target-station development.

3.4.2 Energy Deposition. The energy deposition in tungsten was calculated using the computer code CASIM. The total energy deposited per proton vs target length is shown in Fig. 3-5.

The energy density deposited vs radius for Gaussian beams, is shown for $\sigma_x = \sigma_y = 0.02$ cm in Fig. 3-6, 0.03 cm in Fig. 3-7, and 0.04 cm in Fig. 3-8. The radial distribution is wider on the downstream face of the target due to the shower development. Also shown is the energy density expressed in (Joules gm^{-1} $pulse^{-1}$) for 2×10^{12} protons per pulse, to be compared with the integral of the enthalpy reserve for tungsten. This quantity, the integral of the heat capacity from 20°C to a given temperature, is shown in Fig. 3-9. A summary of this data is presented in Table 3-V.

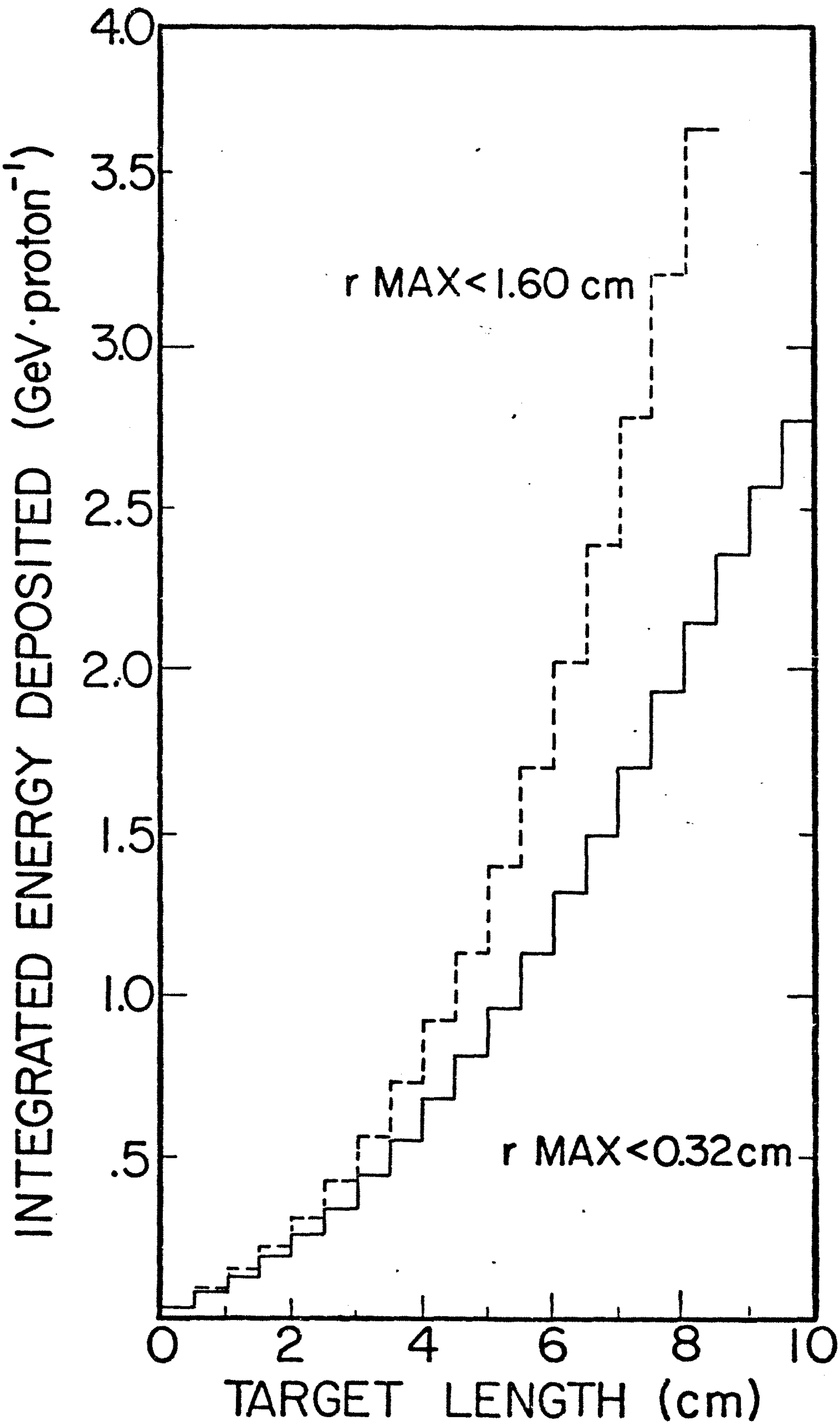

Fig. 3-5 Energy Deposition by Protons vs Target Length

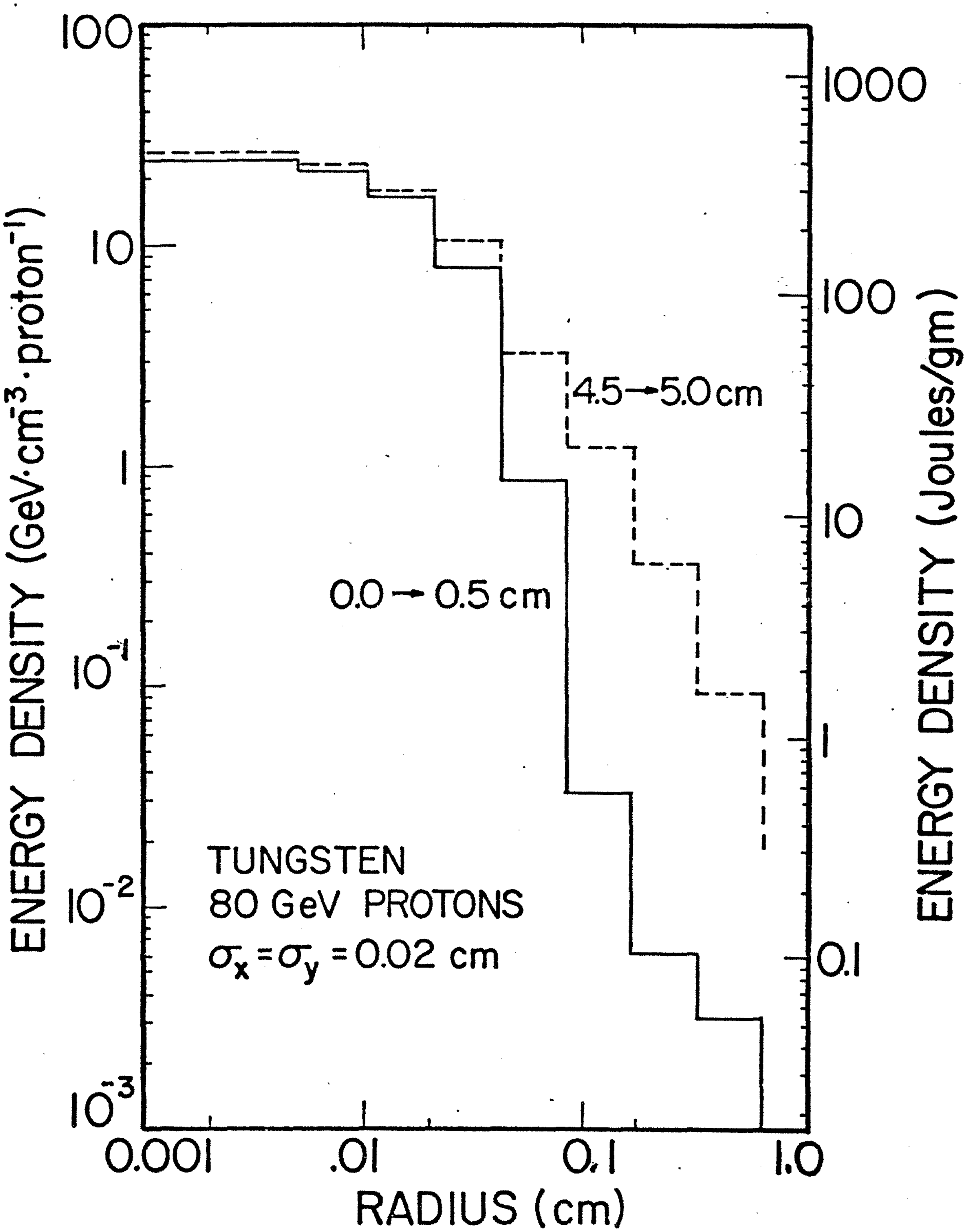

Fig. 3-6 Energy Deposition by Protons vs Radius; σ = 0.2 mm

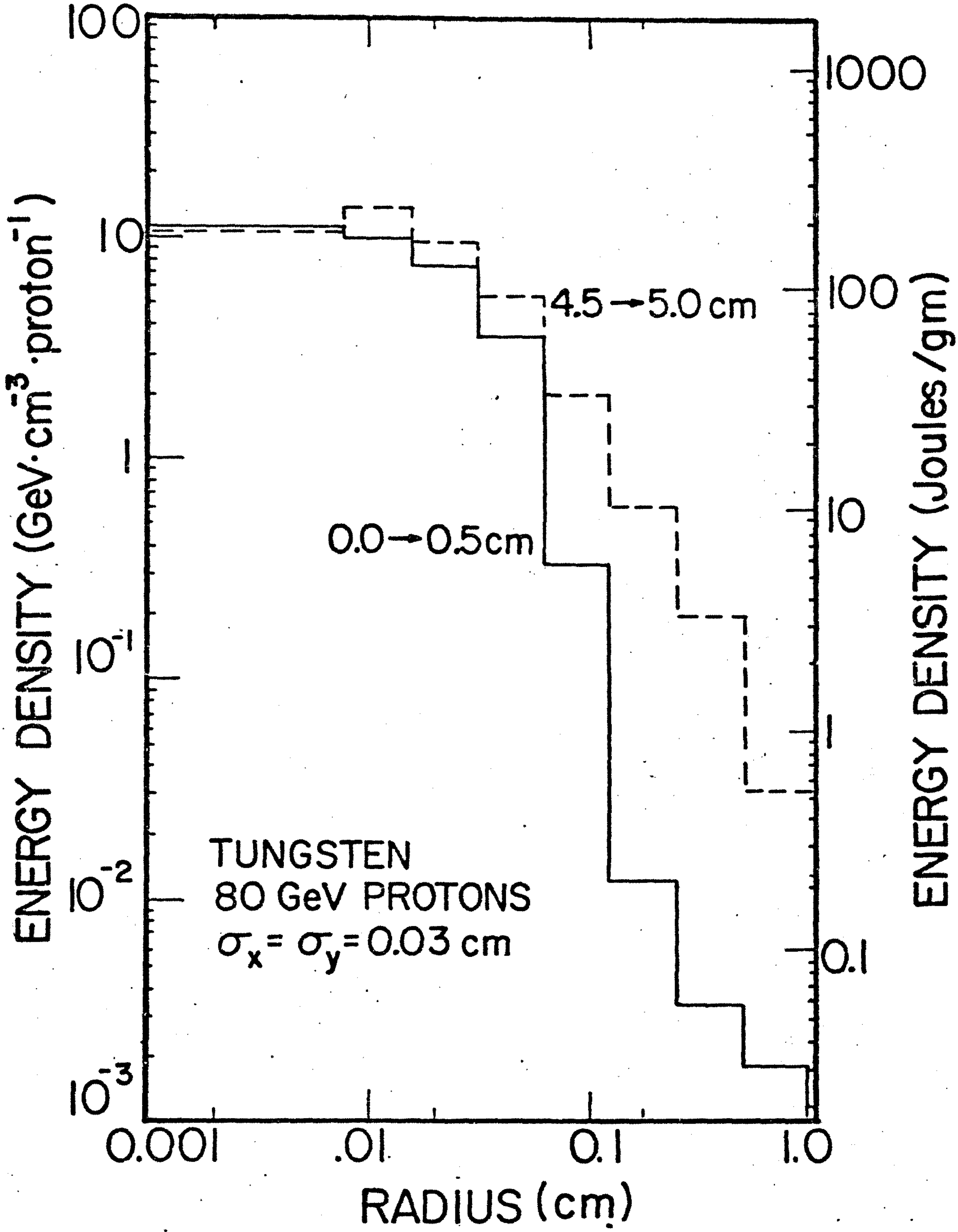

Fig. 3-7 Energy Deposition by Protons vs Radius; $\sigma = 0.3$ mm

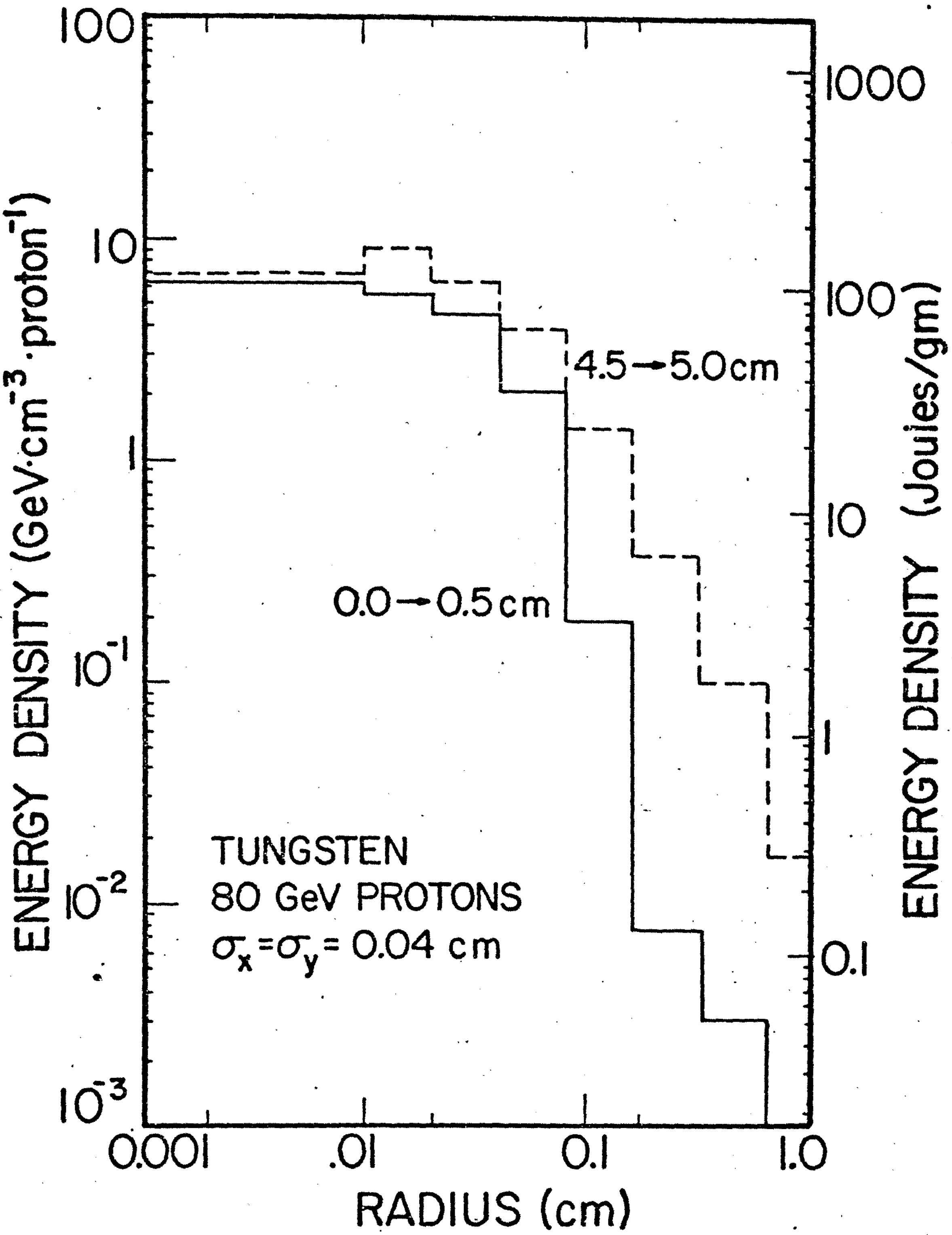

Fig. 3-8 Energy Deposition by Protons vs Radius; σ = 0.4 mm

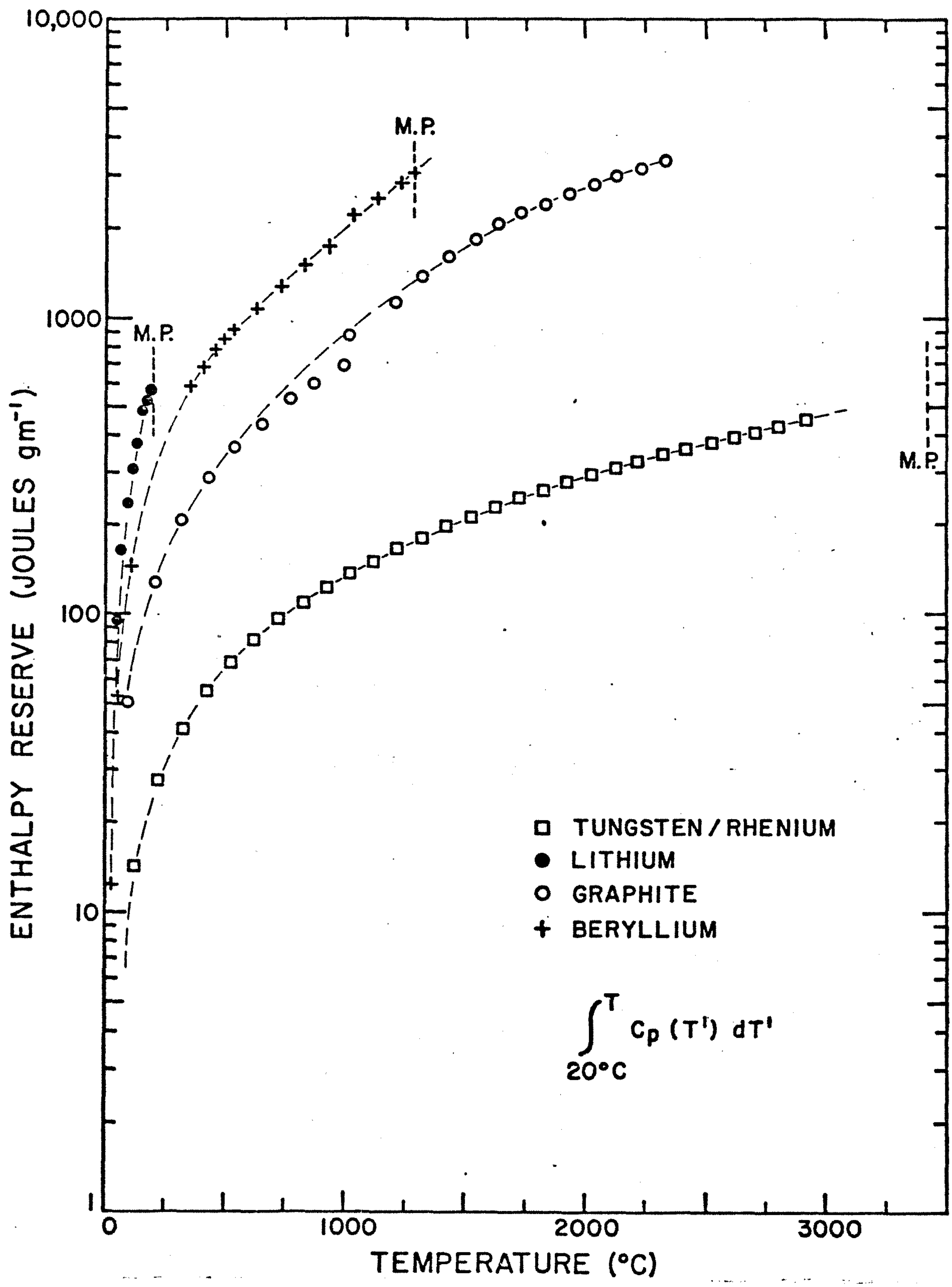

Fig. 3-9 Enthalpy Reserve for Several Materials

TABLE 3-V ENERGY DEPOSITION IN TARGET

Target Material			Tungsten/Tungsten Alloys
Length			5cm
80 GeV protons/pulse			2.0×10^{12}
Total Beam Energy			25960 Joules
Pulses/Burst			13
Burst Interval			11 s
Beam Pulse Duration			1.6×10^{-6} s
Energy Deposited/proton		1.13 GeV	1.82×10^{-10} Joules
Energy Deposited/pulse			368 Joules
Energy Deposited/burst			4778 Joules
Average Energy Deposited			434 Watts
Average Temperature			<100°c
dE/dx			376.6 J/gm
Beam Size ($\sigma x = \sigma y$)	0.02	0.03	0.04cm
Peak Energy Density/proton	25	11.0	9.0 $GeV.cm^{-3}$
Peak Energy Density/pulse	430.0	210.0	150.0 $Joules.gm^{-1}$
Peak Temperature rise	2800	1500.	825. °C
CERN Peak Energy Density			>185 Joules gm^{-1}
Peak Temperature rise			1500°C
Average Temperature			800°C
SLAC Peak Energy Density			81 Joules gm^{-1}
Peak Temperature rise			600°C(SLAC Report 480°C)
Average Temperature			600°C

The operational target at the CERN Antiproton Source has been designed for a peak energy density in excess of 185 Joules gm^{-1} and a peak temperature rise of 1500°C above an average temperature of 800°C. This rhenium target has been operational for some time with no reported failures.

The SLAC Linear Collider will use a tungsten-rhenium target with peak energy densities of up to 81 joules gm^{-1} and peak temperature rise of 600°C over an average temperature of 600°C.

High energy density-deposition in targets was the subject of a workshop at Fermilab. Energy-density depositions well in excess of the ones considered here are expected to result in melting, vaporization and the depletion of the target material in a time short compared with the beam pulse of 1.6 μsec. General rules indicate the onset of shock waves for energy densities in excess of 200 Joules gm^{-1} and energy deposition in the nanosecond range.

We will lower the energy density to less than 200 J/gm by sweeping the proton beam across the target during the pulse by several beam diameters. The acceptance of the antiproton beam will be similarly pulsed to follow.

Based on the discussion above, the expectation is that after some target-development effort, one should be able to operate with beam spot $\sigma_x = \sigma_y$ of less than 0.03 cm.

3.4.3 Target Design. Elastic stress calculations for Tungsten-Rhenium alloys, utilizing the temperature profiles resulting from the energy-density deposition discussed above will result in the formation of a plastic zone (material compressed to above yield point) concentric to the beam. The diameter of this zone is expected to be of the order of 0.3 mm for a beam of $\sigma_x = \sigma_y = 0.4$ mm, and grow to approximately 0.6 mm for $\sigma_x = \sigma_y = 0.2$ mm.

The failure mechanism for a solid target will probably be the following:

1. Development of a plastic zone with each heat pulse.

2. Flow of material within the plastic zone with each repeated pulse. The flow direction will be from inside to face of target.

3. Swelling at target face followed by surface cracking.

4. Surface cracks extending into the volume of the material.

In order to decrease the thermal cycling of the same volume of material, targets will be rotated at approximately 46 rpm, during the 13 beam-pulse sequence, resulting in a distribution of the beam impact point around the circumference. Target translation could provide an even larger number of impact points.

The target geometry of Fig. 3-10 is composed of a number of wedges to decrease the cost of the target manufacturing with respect to a circular rim. During the development stage, wedges could contain different designs for comparative testing. The target geometry of Fig. 3-11 results from available powder technology for the construction of high-power x-ray tubes. Because of the low average, power deposited in the target, forced-air cooling should suffice for both geometries.

In order to achieve targets that would survive smaller beam spots (larger energy density deposited) the following approaches to target design are under study:

Laminated targets with the plane of the laminations perpendicular to the proton beam. The purpose would be to decrease the amount of material flow within the plastic zone.

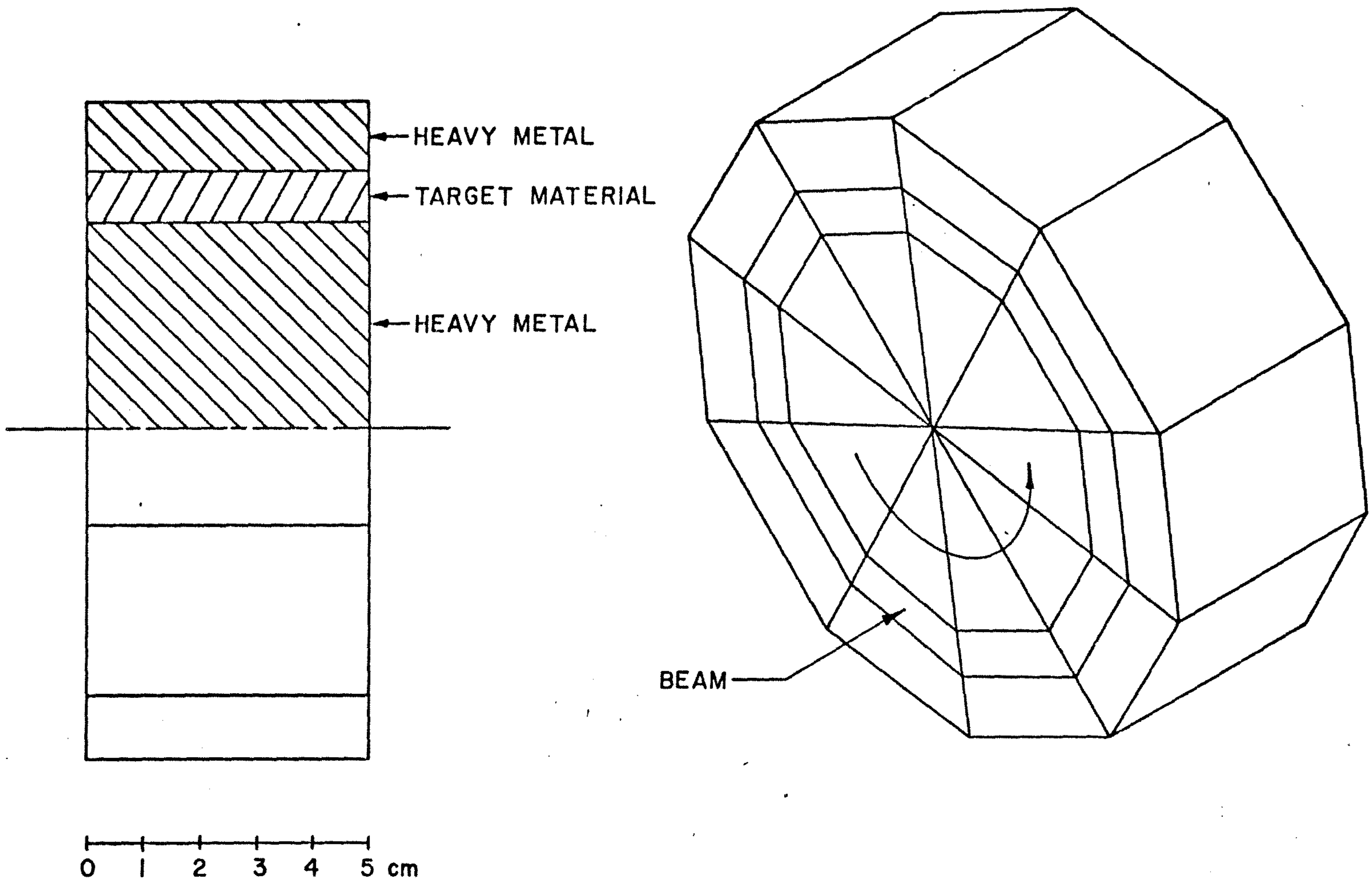

Fig. 3-10 Target Geometry

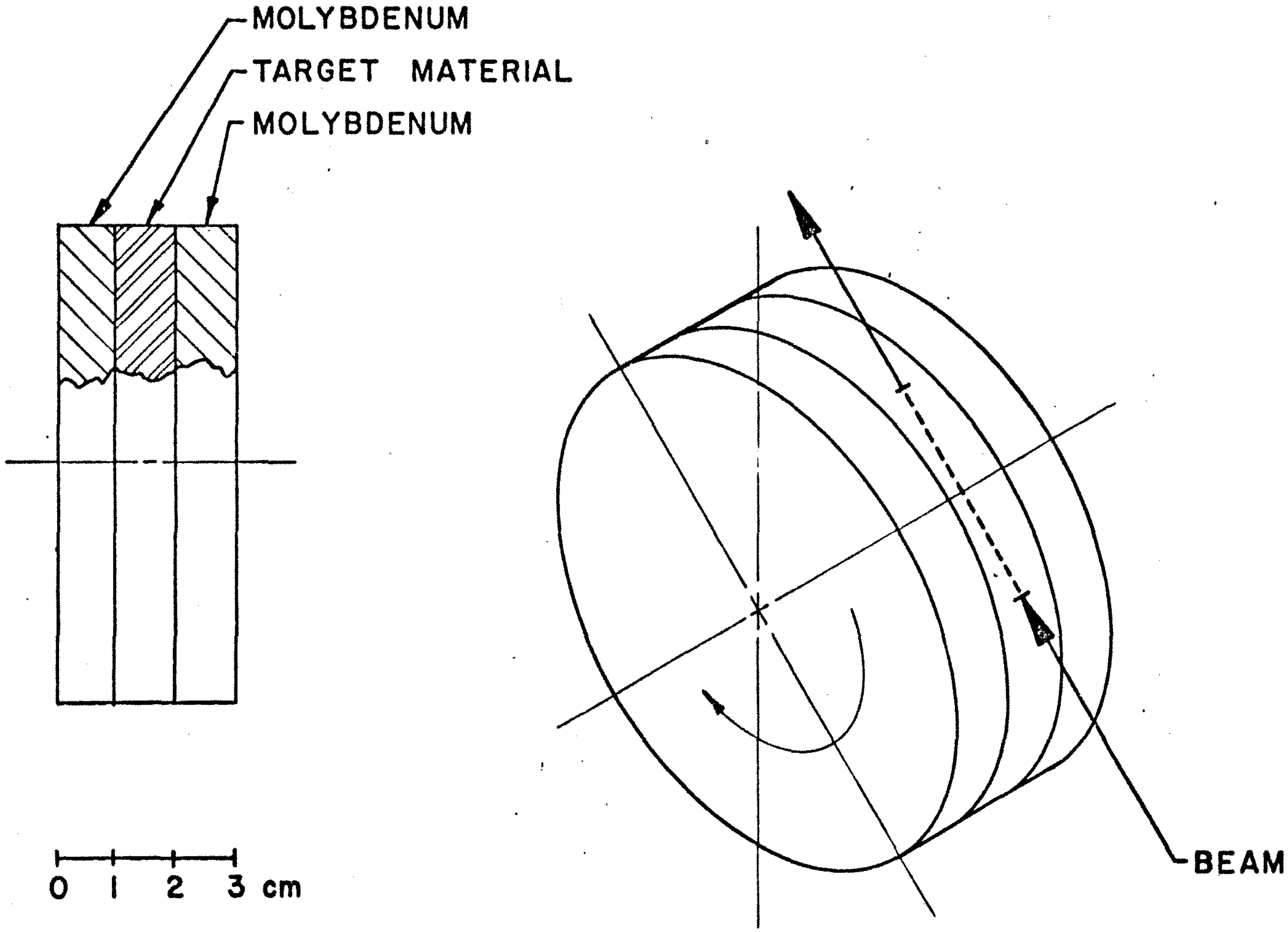

Fig. 3-11 Target Geometry using Powder Technology

Filamented targets will allow the introduction of slip planes across large temperature gradients, resulting in a lowering of the stresses.
Powder targets high density particles embedded in graphite by powder metallurgy would incorporate the excellent shock and high-temperature properties of graphite, allowing enough energy deposition to melt the metal particles. The lower antiproton yield resulting from the lower average target density could be overcome by the much smaller beam spot.

A research and development program is underway to test these ideas. Beam is expected to be available after October 1981.

3.4.4 The Lithium Lens Collector. Antiprotons diverging from the target are to be collected by a 10-cm long lithium lens of 1cm radius. The basic principle of this device is that an electric current uniformly distributed in a cylindrical conductor produces an azimuthal magnetic field with a constant radial gradient inside the conductor. Thus, such a conductor is an axially symmetric focusing device for a particle beam passing through the conductor axially. To produce the desired gradient of 1000 T/m, current pulses of 0.5 MA are required. Current uniformity is secured by adjusting the pulse length to make the skin depth close to the radius; nearly 1 msec full width is required for a sinesoidal pulse. A lens capable of handling such pulses at a 10 Hz repetition rate has not yet been built, and its design will in fact require some extension of the present technology. The lens now under development at the Institute for Nuclear Physics (Novosibirsk) is intended for operation at a maximum of 0.5 Hz. On the other hand, Fermilab has already received from INP four lenses of 0.25 cm radius that are conservatively rated for the required gradient and a 13 Hz cycle. These lenses cannot fulfill the plan to provide an antiproton transport system with 20π mm mrad acceptance, but do in fact serve rather well to meet the more immediate need for 5π. A lens of this design and its immediate appurtenances have been life tested for $>10^7$ pulses, and destructive testing has established that the short-term maximum sustainable gradient is about 50% above the operating value. Tests of the optical performance and beam effect on service life will be made in the fall of 1981 when protons are brought to the target station.

3.5 Antiproton Transport to Precooler

The antiproton beam from the target is collected by the lithium lens and made close to parallel as input to the transport system. The entire transport system is designed to contain an antiproton beam of transverse emittance 20π mm-mrad in each plane and momentum spread 4%.

The transport line can be thought of as two distinct sections:

(i) a vertical translation of 2.485 m using 6-deg bends followed by a periodic array of quadrupoles. This section is also utilized for the return journey of cooled 8-GeV antiprotons;

(ii) a horizontal bend (essentially a section of a Precooler quadrant) followed by a vertical translation of 1.966 m to put the beam parallel to the Precooler and 50 in. above it. The beam is then bent down and injected in the South straight section. Elements and strengths of the elements are given in Table 3-VI.

TABLE 3-VI TRANSPORT LINE FROM TARGET TO PRECOOLER

Beam Emittances (H and V): $\varepsilon = 20\pi\ 10^{-6}$m
Momentum Spread: $\Delta p/p$ = 4% full

Sequence of Magnets

1. Vertical Translation After Target
2. Matching and FODO Transport
3. Matching
4. Dispersion Suppressors
5. Two Regular Cells
6. 1 Cell With 2 Missing Dipoles
7. 1 and 1 1/2 Regular Cells
8. Long Straight Matching
9. Vertical Translation

1. Vertical Translation after Target

D1 V1 D2 Q1 D3 Q2 D4
Q1 D4 Q2 D3 Q1 D2 $\overline{\text{V}}$1 D1

Drifts	Length(m)
D1	-0.915
D2	3.8359
D3	1.5
D4	3.50

Quadrupoles	Effective Length(ft)	Strength (B'/Bp)(m^{-2})
Q1	2	0.5025
Q2	4	-0.41262

Vertical Dipoles	Effective Length(m)	Strength (B/Bp)(m^{-1})
V1	1.83	(up) 0.05726
$\overline{\text{V}}$1	1.83	(down) 0.05726

2. Matching and FODO Transport

D5 (in the middle of $\overline{\text{V}}$) Q3 D6 Q4
D7 QD D8 QF D9 QD ^{1}D9
QF D9 QD D9 QF/2

Drifts	Lengths(m)
D5	3.0
D6	3.1962
D7	1.6916
D8	2.574
D9	14.0757

Quadrupoles	Effective Strength(ft)	Strength $(B'/B\rho)(m^{-2})$
QF/2	1	0.1602
Q3	2	-0.52436
Q4	2	0.34452
QD	2	-0.1602
QF	2	0.1602

3. Matching

QF/2 D4 Q14 D14 Q13 0 $\overline{V}3$ D15
Q15 D16 Q16 D17 Q17 D16 Q18 D18

Drifts	Lengths(m)
D4	1.500
D14	1.354
0	0.50
D15	12.719
D16	0.9144
D17	5.2461
D18	0.3048

Quadrupoles	Effective Length(ft)	Strength $(B'/B\rho)(m^{-2})$
QF/2	2	0.1502
Q14	2	-0.005054
Q13	2	not energized
Q15	2	-0.5
Q16	2	0.47270
Q17	2	-0.1662
Q18	2	0.2584

Vertical Bends	Effective Length(m)	Strength $(B/B\rho)$
$\overline{V}$	1.3716	not energized

4. Dispersion Suppressor

06 B 0 B 05 QD 04 B 03
QF 02 B 01 QD/2

Drifts	Lengths(m)
01	0.450
02	2.2609
o3	1.8025
04	0.9083
05	0.2172
06	0.8172

4. Dispersion Suppressor

06 B 0 B 05 QD 04 B 03
QF 02 B 01 QD/2

Drifts	Lengths(m)
01	0.450
02	2.2609
03	1.8025
04	0.9083
05	0.2172
06	0.8172

Quadrupoles	Effective Length(ft)	Strength $(B'/B\rho)(m^{-2})$
QD	2	-0.53522
QF	2	0.54216

Dipole	Effective Length(m)	Strength $(B/B\rho)(m^{-1})$
B	1.3716	0.0409

5. Two Regular Cells

QD/2 0 B 0 B 00 QF/2
QF/2 00 0 B 0 B QD/2

This is repeated twice.

Drifts	Lengths(m)
0	0.3048
00	0.72963

Quadrupole	Effective Length(ft)	Strength $(B'/B\rho)(m^{-2})$
QF	2	0.54216
QD	2	-0.53522

Dipole	Effective Length(m)	Strength $(B/B\rho)(m^{-1})$
B	1.3716	0.0409

6. 1 Cell with 2 Dipoles Missing

QD/2 000 QF 0 B 0 B 00 QD/2

Drifts	Lengths(m)
0	0.3048
00	0.72963
000	4.08243

Quadrupoles	Effective Length(ft)	Strength $(B'/B\rho)(m^{-2})$
QF	2	0.54216
QD	2	-0.53522

Dipole	Effective Length(m)	Strength $(B/B\rho)(m^{-1})$
B	1.3716	0.0409

7. 1 and 1/2 Regular Cells

QD/2 0 B 0 B 00 QF2 0 B 0 B
00 QD2 0 B 0 B

Quadrupoles	Effective Length(ft)	Strength $(B'/B\rho)(m^{-2})$
QD2	2	-0.42353
QF2	2	0.40420
QD	2	-0.53522

Dipole	Effective Length(ft)	Strength $(B/B\rho)(m^{-1})$
B	1.3716	0.0409

8. Long Straight Matching

D19 Q19 D20 Q20 D21 Q21
D22 Q22 D21 Q23 D22

Drifts	Lengths(m)
D19	0.75
D20	5.32814
D21	1.250
D22	3.00

Quadrupoles	Effective Length(ft)	Strength $(B'/B\rho)(m^{-2})$
Q19	2	0.47357
Q20	2	-0.7990
Q21	4	0.82195
Q22	4	0.62407
Q23	2	-0.8490

9. Vertical Translation

V4 D23 Q24 D24 Q25 D25
Q26 D26 Q27 D27 Q28 D28
V5 D29

Drifts	Lengths(m)
D23	3.5046
D24	0.75
D25	1.15113
D26	0.8840
D27	0.60754
D28	2.1712
D29	-1.8788

Quadrupoles	Effective Length(ft)	Strength $(B'/B\rho)(m^{-2})$
Q24	2	0.82608
Q25	4	-0.80589
Q26	2	0.78407
Q27	4	-0.89608
Q28	2	0.72807

Septum Dipole	Effective Length(m)	Strength (B/Bρ)(m^{-1})
V5	3.6576	(up) 0.021884

4. PRECOOLER DESIGN

4.1 General Structure and Layout

4.1.1 Lattice. The Precooler is a storage ring for antiprotons of energy between 200 MeV and 4.5 GeV. It must be capable of slow acceleration and deceleration for antiproton energies between 200 MeV and 8 GeV in order to be able to inject into the Main Ring at a suitable energy. The Precooler is to have large acceptances, $40\pi\times10^{-6}$ m-rad in each transverse plane and a momentum spread $\Delta p/p$ of 4.5%. These acceptances are chosen to give flexibility for later development in injection and cooling methods.

The general size of the Precooler is determined by its relation to the Main Ring. A smaller Precooler would require that the Main Ring proton beam be split into smaller segments for targeting, which would in turn increase the momentum spread of the collected antiproton beam in the Precooler, making cooling more difficult (in fact impossible for a momentum spread much larger than 4%). Within the limits of feasibility, it is economical to keep the Precooler as small as possible. A radius of approximately 75m appears to be optimal and we choose R=75.4717m (exactly the Booster radius) in order to match rf frequencies exactly with the Main Ring. Long straight-section space is also required for injection, stochastic cooling, acceleration, deceleration, and extraction and is available at this radius.

Parameters of the lattice design that has evolved are given in Table 4-I.

TABLE 4-I PRECOOLER PARAMETERS

A. GENERAL

Peak Kinetic Energy	8.0 GeV
Momentum	8.8889 GeV/c
Magnetic Rigidity	296.5 kG-m
Bending Field	12.127 kG
Bending Radius	24.449255 m
Average Radius	75.4717m
Revolution Time: 8.0 GEV	628.71 kHZ
4.5 GEV	622.72 kHZ
200 MEV	357.93 kHZ
Superperiodicity	2
Focusing Structure	Separated Function
Normal Cell Structure	FODO
Horizontal Betatron Tune	11.415
Vertical Betatron Tune	11.393
Transition Energy γ_T	10.246
Natural Chromaticity: Horizontal	-18.35
Vertical	-17.68

B. Magnets

Number of Dipoles	112
Length of Dipoles	-
Effective Length of Dipoles	1.3716 m
Sagitta	0.962 cm

Quadrupoles:

Type	Number	Effect. Length	Strength $B'/B\rho(m^{-2})$
QF	24	2	.542162
QD	18	2	-.535217
1Q1	4	4	.325417
1Q2	4	4	-.352206
1Q3	4	4	.552459
QD1	4	4	-.371853
QF1	4	2	.518653
QD2	4	2	-.42353
QF2	4	2	.40420
QF9	4	4	.308953
2Q1	4	4	-.359801
2Q2	4	4	.361397
2Q3	4	4	-.406104

C. Drift Lengths (m)

0	.3048
00	.72963
000	4.08243
LL	10.00000
L11	1.96582
L1	1.1159
L2	2.67062
L3	.3048
01	.45
02	2.26083
03	1.80250
04	0.90833
05	0.217213
06	.817217

D. Lattice Structure

D1. Cells:

.BB:	00	B	0	B	0		
.C :	QD	.BB	QF	QF	.BB	QD	
.C1:	QD1	000	QF1	QF1	.BB	QD2	
.C2:	QD2	.BB	QF2	QF2	.BB	QD	
.C3:	QD	.BB	QF	QF	000	QD	
.C8:	QD	01	B	02	QF		
	QF	03	B	04	QD		
.DF9:	QD	05	B	0	B.	06	QF9

Cell Length: 9.3841 m

D2. Long Straight Section:

With Dispersion

.S1	LL	1Q1	1Q1	0	1Q2	1Q2
	L1	L2	1Q3	1Q3	L3	QD1

Without Dispersion

.S2	QF9	L3	2Q3	2Q3	L2	L11
	2Q2	2Q2	0	2Q1	LL	

D3. Arc Sector:

.Arc	.C1	.C2	.C3	.C	
	.C	.C	.C	.C8	.DF9

D4. Quadrant Structure:

.Sph		.S1	.Arc	.S2

D5. Superperiod:

.Sph Reflect (.Sph)

E. Lattice Functions

	β_H (m)	β_V (m)	η (m)
Maxima	60.22	55.76	-2.74
Regular Cell:			
Max	16.	16.	1.3
Min	2.5	2.5	0.6
Middle of long straight with dispersion (.S1)			
	9.9854	10.0512	-2.7426
Middle of long straight without dispersion (.S2)			
	10.3516	6.0185	0.00

The lattice is shown in Fig. 4-1 where the locations of functions are labelled. The orbit functions are graphed in Fig. 4-2. A normal cell is shown in Fig. 4-3. The long straight section insertions are shown in Figs. 4-4 through 4-7. The detailed SYNCH output is included as Appendix 2.

The lattice has 2-fold symmetry; it is symmetric about the center of each long straight section. In addition to the long straight-section insertions, there are missing magnets in the first, third, and eighth cells in each direction from the South and North straight sections.

4.1.2 Nomenclature. Locations and components in the Precooler are labelled by a four-place code. The meaning of each place is:

(i) Place 1: Quadrant label
Each quadrant begins at the center of a long straight section and ends at the center of the next long straight section. Quadrant 1 begins at the center of the South (injection) straight section.

(ii) Place 2: Device Label
B: bending magnet
Q: quadrupole
L: straight section
S: sextupole
T: trim magnet

(iii) Place 3: Period Label
a. In long straight sections, this label is S, W, N, or E.
b. In bending sections, this label is 1 through 9

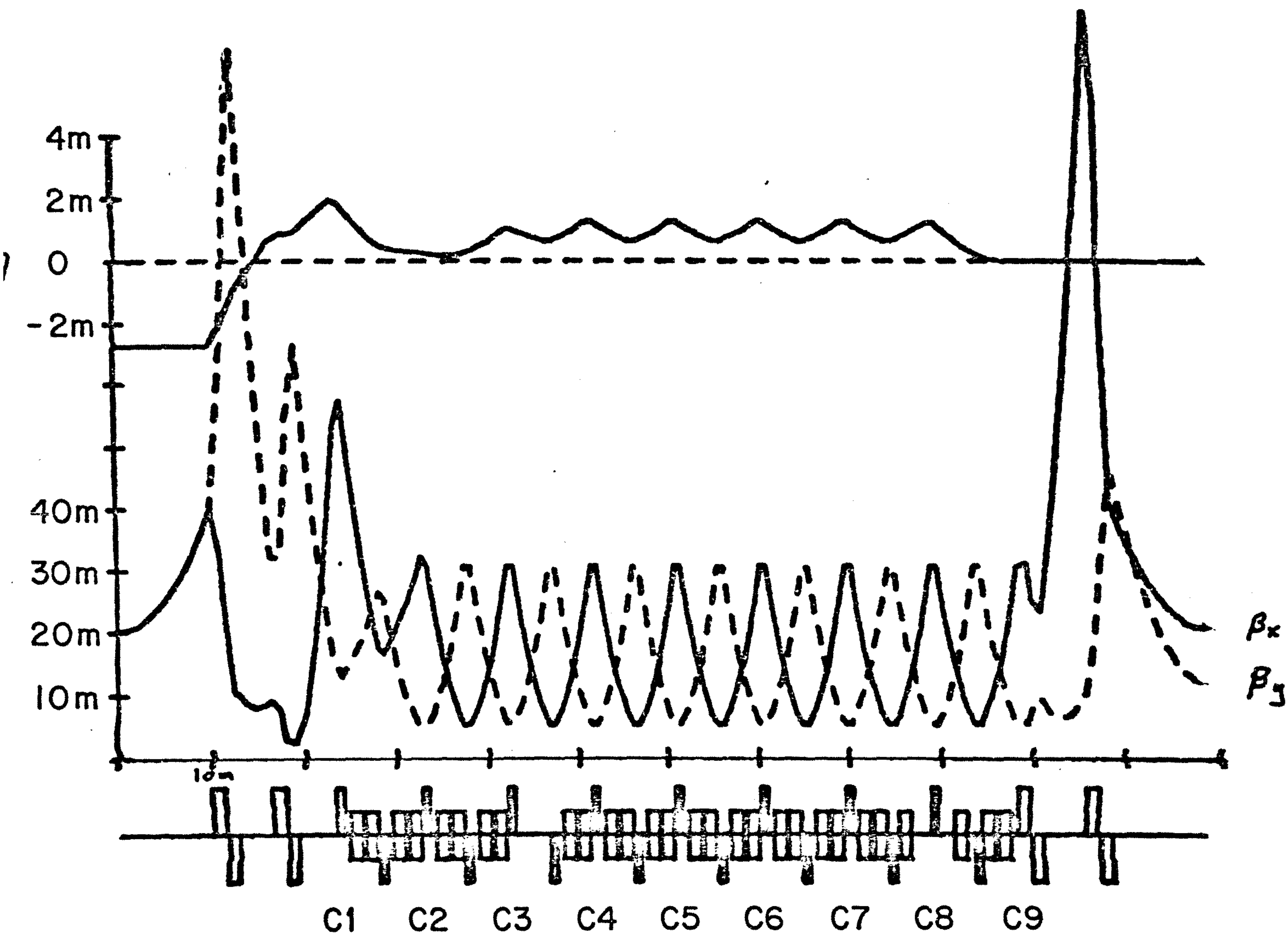

Fig. 4-2 Precooler Orbits

a) Amplitude and dispersion functions

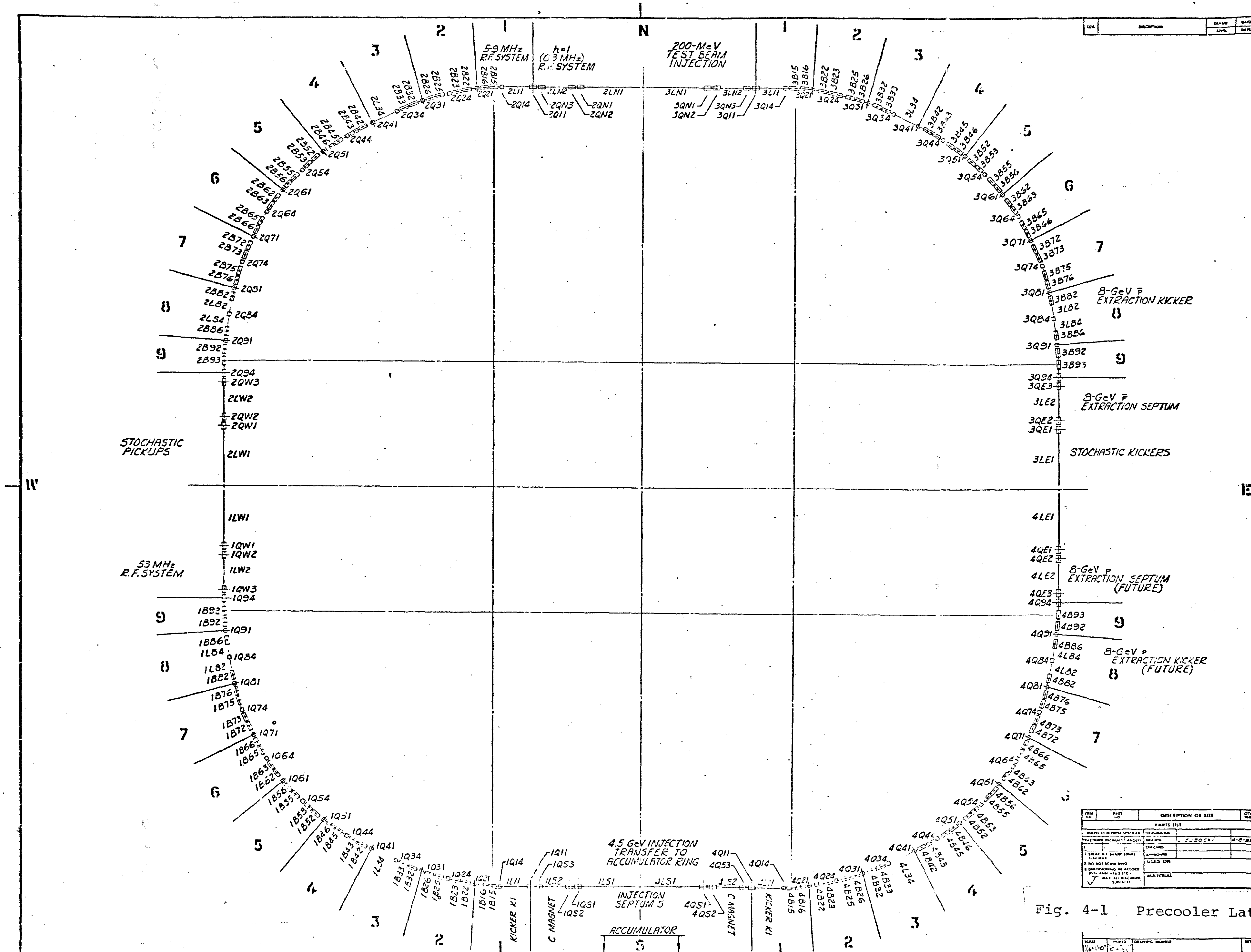

Fig. 4-1 Precooler Lattice

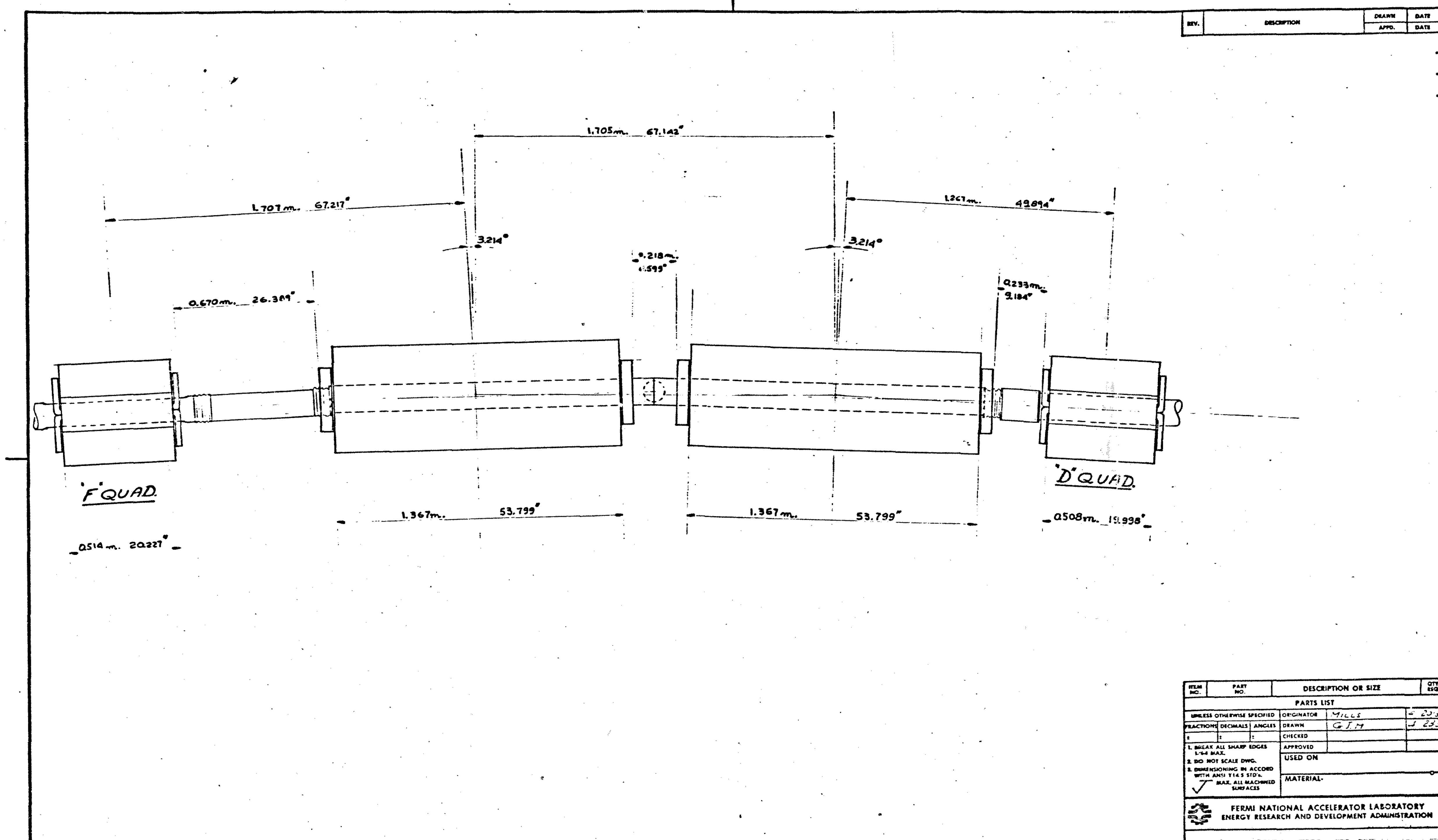

Fig. 4-3 Precooler Normal Cell

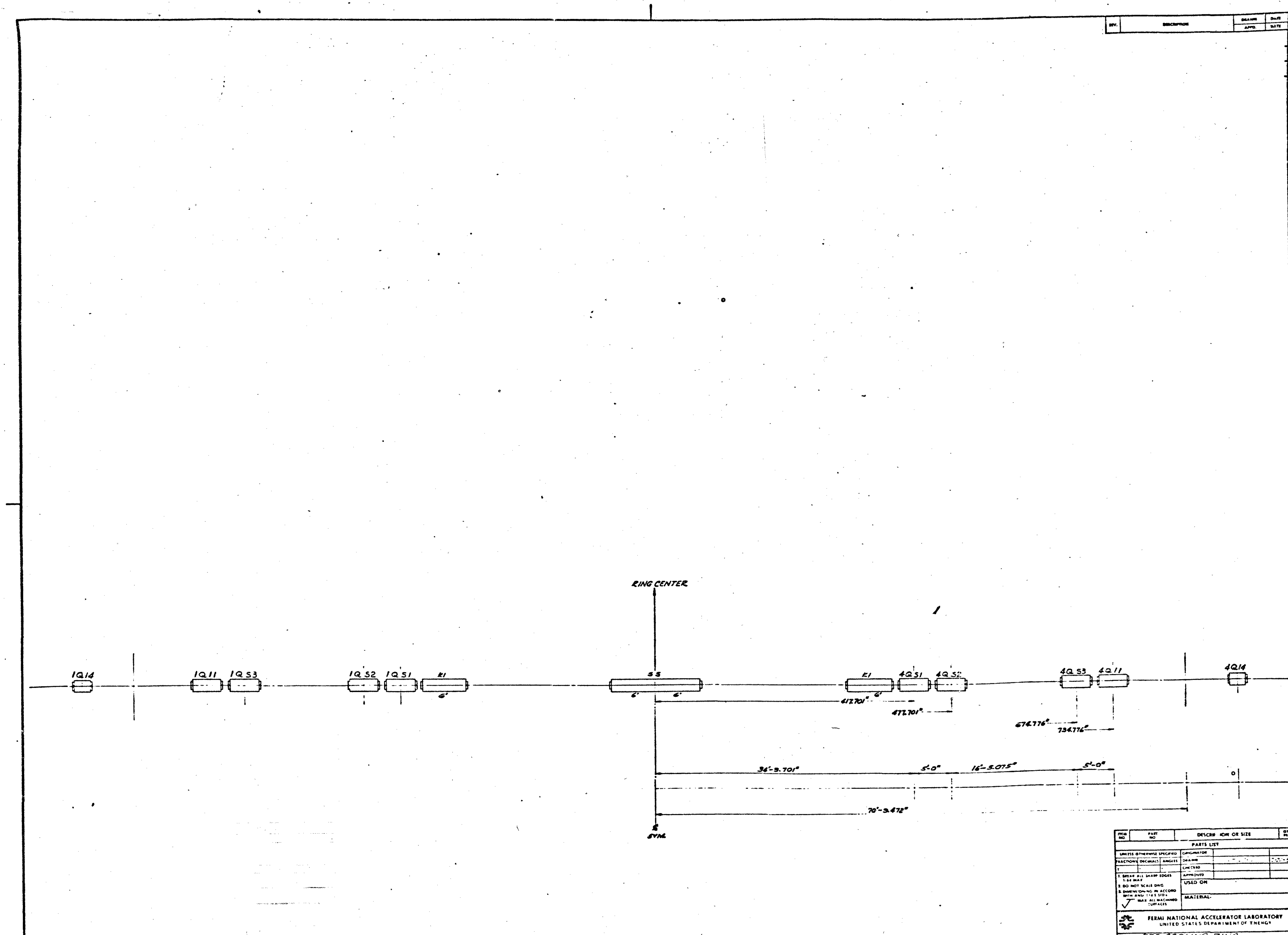

Fig. 4-4 South Long Straight Section

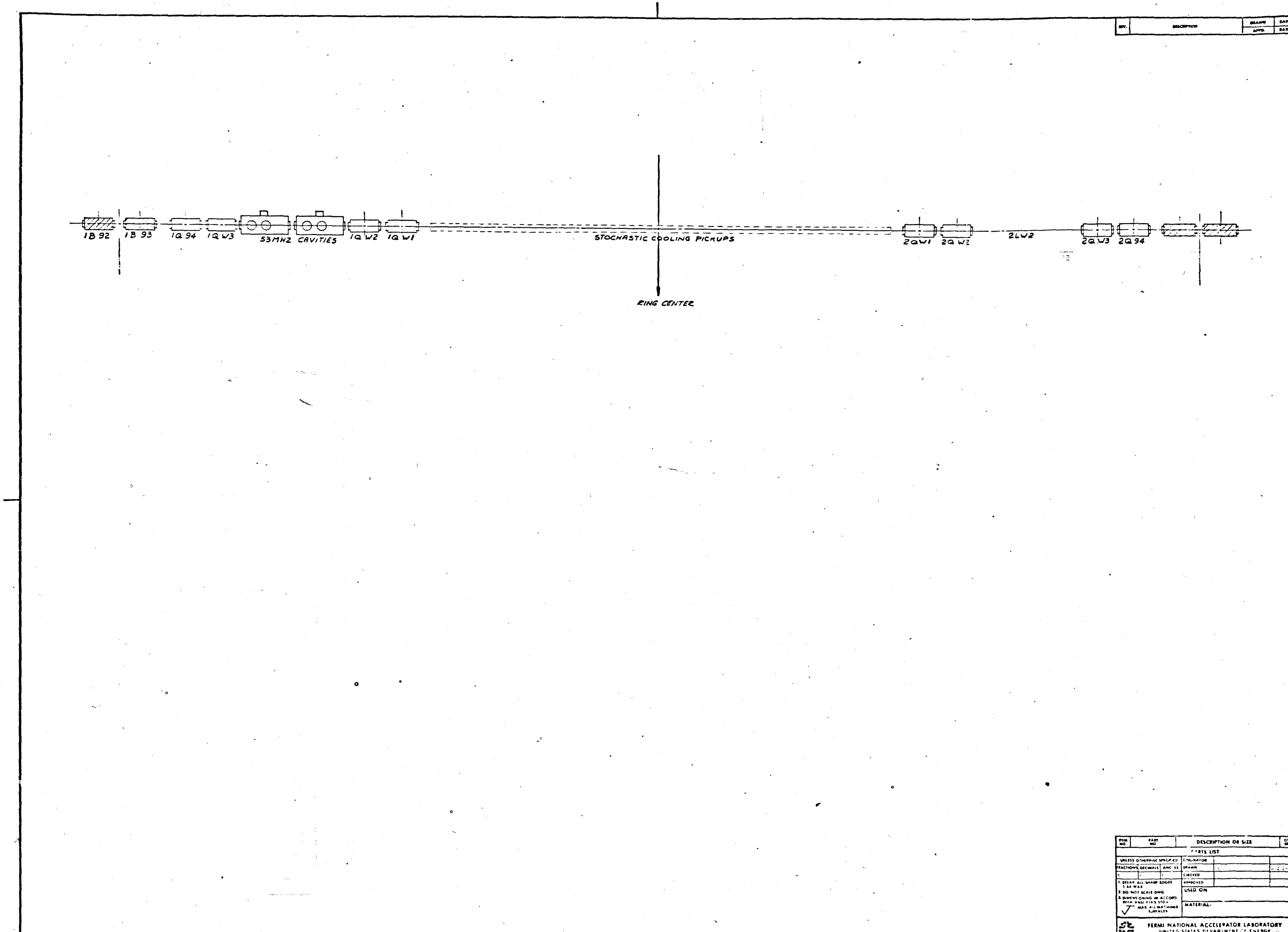

Fig. 4-5 West Long Straight Section

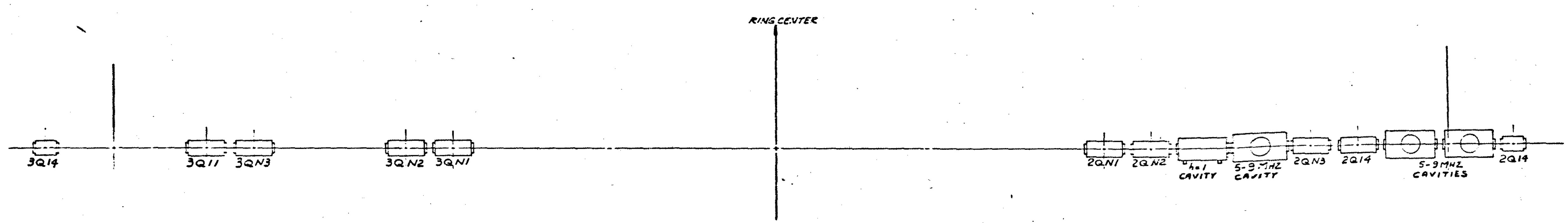

FERMI NATIONAL ACCELERATOR LABORATORY
UNITED STATES DEPARTMENT OF ENERGY

Fig. 4-6 North Long Straight Section

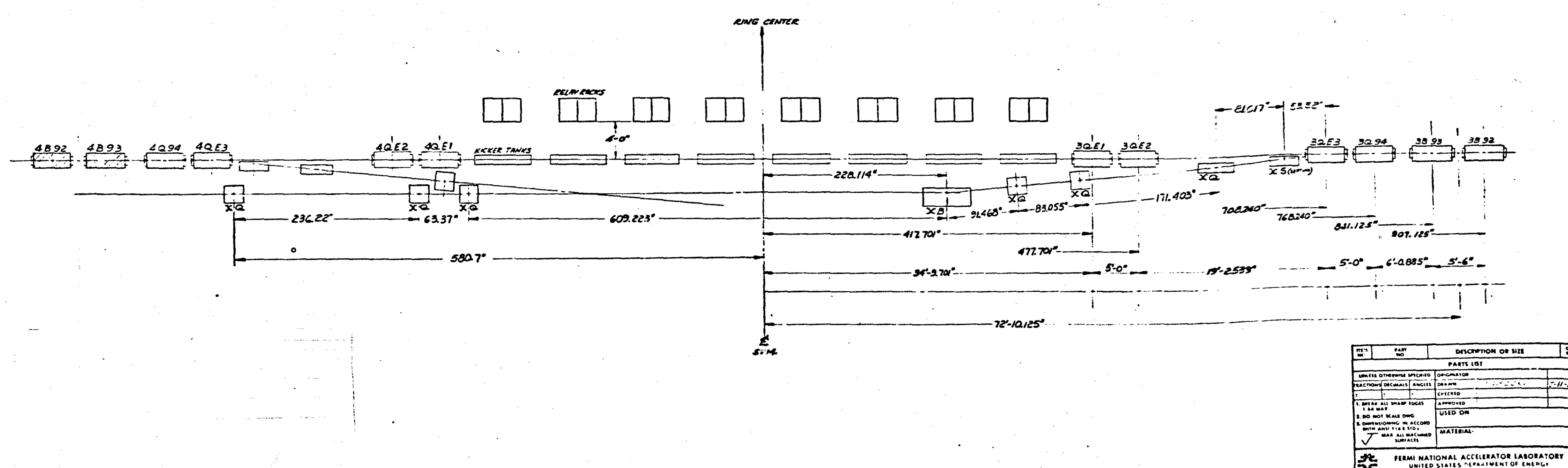

Fig. 4-7 East Long Straight Section

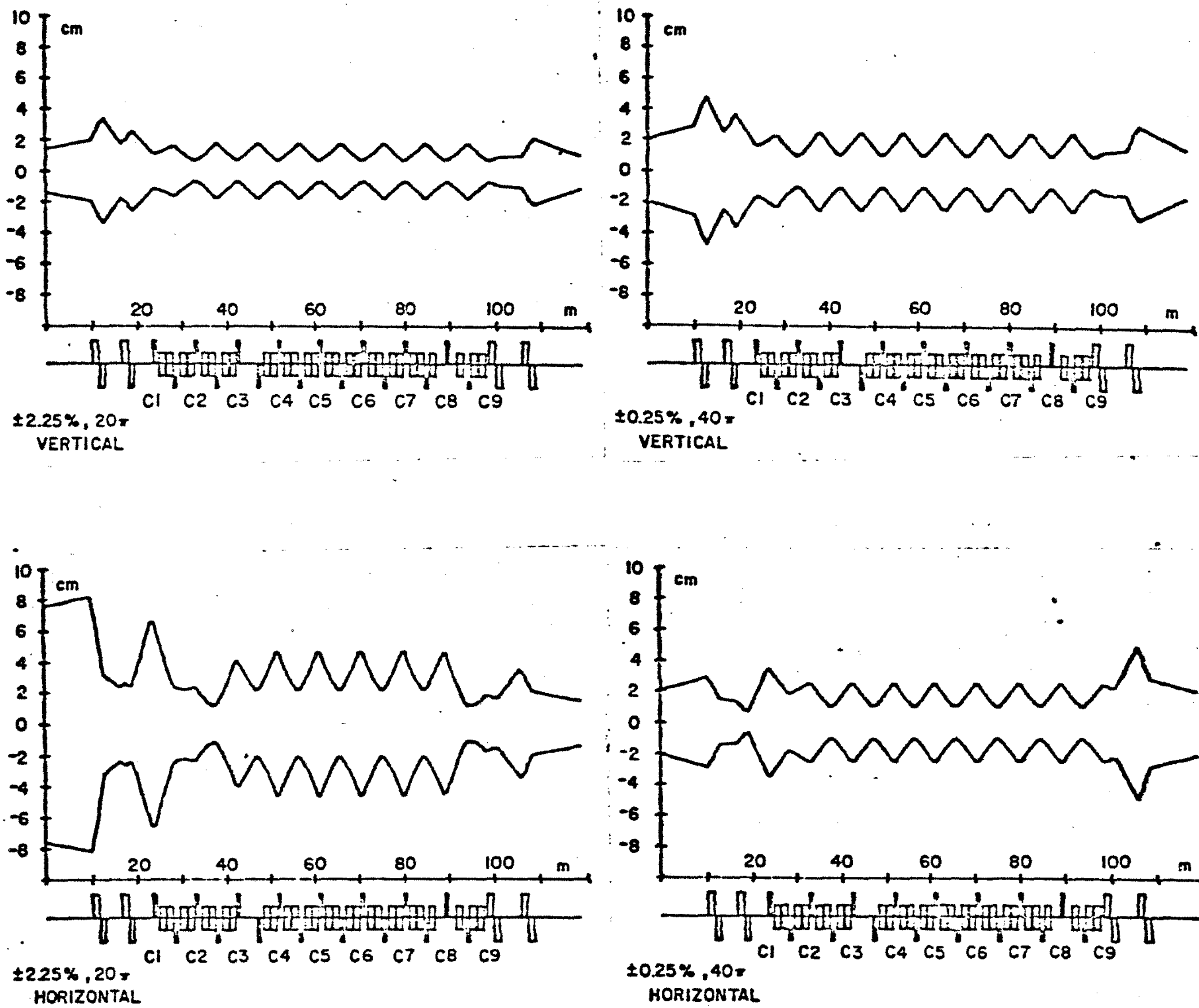

b) Horizontal and vertical beam envelopes for the cell number. Note that as one proceeds in the direction of beam, the period label increases from 1 to 9 in quadrant 1, decreases from 9 to 1 in quadrant 2, increases from 1 to 9 in quadrant 3, then decreases from 9 to 1 in quadrant 4. This reflects the symmetry of the lattice.

(iv) Place 4: Location Label
This label is sequential within a cell. Note that all radially focusing quads have even numbers and all radially defocusing quad have odd numbers. These labellings are shown in Figure 4-1.

4.2 Injection and Stacking

4.2.1 Injection. The 4.5-GeV injection transport line is shown in Fig. 4-4 and its parameters are given in Table 4-II.

TABLE 4-II PRECOOLER INJECTION

Kinetic Energy at Injection	4.5 GeV
Momentum	5.3567 GeV/c
Magnetic Rigidity	178.7 kG-m
Emittance Injected (H and V)	20 π mm-mrad
Momentum Spread Injected, Full DP/P	1.0 %
Method	Vertical Injection on a Full-Aperture Horizontal Orbit Bump
Location of Horiz. Bump	South Long Straight
Location OV Vertical Inject.	Middle of South Long Straight
Orbit Separation at Septum	6.5
Structure of Horiz. Bump:	

2(QF1) K3 0 K2 2(QD1) 0 2(1Q3) L2 L1
2(1Q2) 0 2(1Q1) 0 K1 LL* S/2 -- Reflect

Kickers: K1, K2, K3

Effective Length	6 ft
Strength	600 G
Rise Time	150 nsec
Horiz. Aperture, Full	9 in.
Vertic. Aperture, Full	3 in.

Septum Magnet: S

Septum Thickness	10 mm
Effective Length	12 ft
Strength	4 kG

Vertical Separation Between Beam Axes 50 in.

Drift Elements:

0 L1 L2	(See Table 4-I)
LL*	8.1712 m

Quadrupoles:

QF1 QD1 1Q1 1Q2 1Q3	(See Table 4-I)

In order to leave space in the South straight section for transfer of beams between the Precooler and the Electron Accumulator, injection is vertical. The $\bar{p}$ beam from the target is raised 112 in. to an elevation of 734 ft 8 in. It then is kicked downward to the Precooler elevation of 730 ft 6 in. In order to inject later $\bar{p}$ pulses from the target, it is necessary to have kickers K1 and K2 move the injection closed orbit into the septum magnet S.

4.2.2 Stacking. After each of the 13 bunches is injected, it is captured by the 53-MHz rf system, rotated in longitudinal phase space through one-fourth of a phase-oscillation period to reduce its momentum spread from 1% to 0.24%, then moved to the stack and deposited. The loss of $\bar{p}$ in this process is less than 5%. The process is outlined step-by-step in Table 4-III.

TABLE 4-III RF ROTATION AND STACKING

Kinetic Energy	4.5 GeV
Momentum	5.3567 GeV/c
Magnetic Rigidity	178.7
Precooler Ring Radius	75.4717
RF Frequency	52.31 MHz
Harmonic Number	84
Transition Energy γ_T	10.24624
Capture:	
Bunch Area (95% of Beam)	0.15 eV-sec
Momentum Spread (Full Uniform Distr.)	1.0%
Bunch Length	21.0 cm
RF Voltage at Capture (Stationary Bucket)	400 kV
Phase-Oscillation Period	0.367 msec
Bunch Rotation:	
Time Period for Rotation	94 μsec
Bucket Reduction:	
Final Voltage (Stationary Bucket)	19 kV
Bucket Half-Height	0.12%
Bucket Area	0.154 eV-sec
Time to Drop Voltage to Final Value At the End of Rotation	8 μsec
Phase Oscillation Period	1.68 msec
Transformation to Moving Bucket:	
RF Voltage for Moving Bucket	33.0 kV
RF Phase for Moving Bucket	173 deg
Moving Bucket Area	0.154 eV-sec
Moving Bucket Half-Height, DP/P	0.18%
Phase Oscillation Period	1.29 msec
Time for Transformation	1.6 msec

Stacking With Moving Bucket:

Momentum Variation Swept	4.0 %
Energy Variation	213 MeV
Energy Gain Per Turn	4 keV
No. of Revolution During Stacking	53,000
Time for Stacking	85 msec
Relative Frequency Swing	$8.0 \cdot 10^{-4}$
Variation of RF Frequency	500 Hz/msec

Transformation to Stationary Bucket:

RF Voltage for Stationary Bucket	19 kV
RF Phase for Stationary Bucket	180 deg
Stationary Bucket Area	0.154 eV-sec
Stationary Bucket Half-Height, DP/P	0.12%
Phase Oscillation Period	1.68 msec
Time for Transformation	1.6 msec

Adiabatic Debunching

Final Voltage	0.0 V
Time Required to Turn Off RF	1.5 msec
Final Beam Momentum Spread	0.17%

Overall Stacking Parameters

No. of Pulses Stacked/Main Ring Cycle	13
No. of $\bar{p}$'s Per Pulse	$1.62 \cdot 10^{6}$
Final Momentum Spread	2.16%
Stacking Efficiency (Including Dilution During Bunch Rotation)	0.88
Fraction of Overall Beam Loss	5.0%

RF Cavities Requirement

No. of Cavities Required (Voltage Programmed by Paraphasing)	2
Frequency Tuning Range	10^{-3}
Total Length of System	4.3 m

There will be surplus Main Ring rf cavities when the Tevatron is in operation and we will use two of these, with associated power amplifiers, bias supplies, modulators, and local controls, for the stacking rf system. They will be installed at the upstream end of the West long straight section, so the tunnel has been made wider to provide this access. Experience in the Main Ring has shown that access to the back of the cavities is useful. For purposes of space allocation, we show in Figs. 4-8 an outline drawing of the cavities.

4.3 Magnets

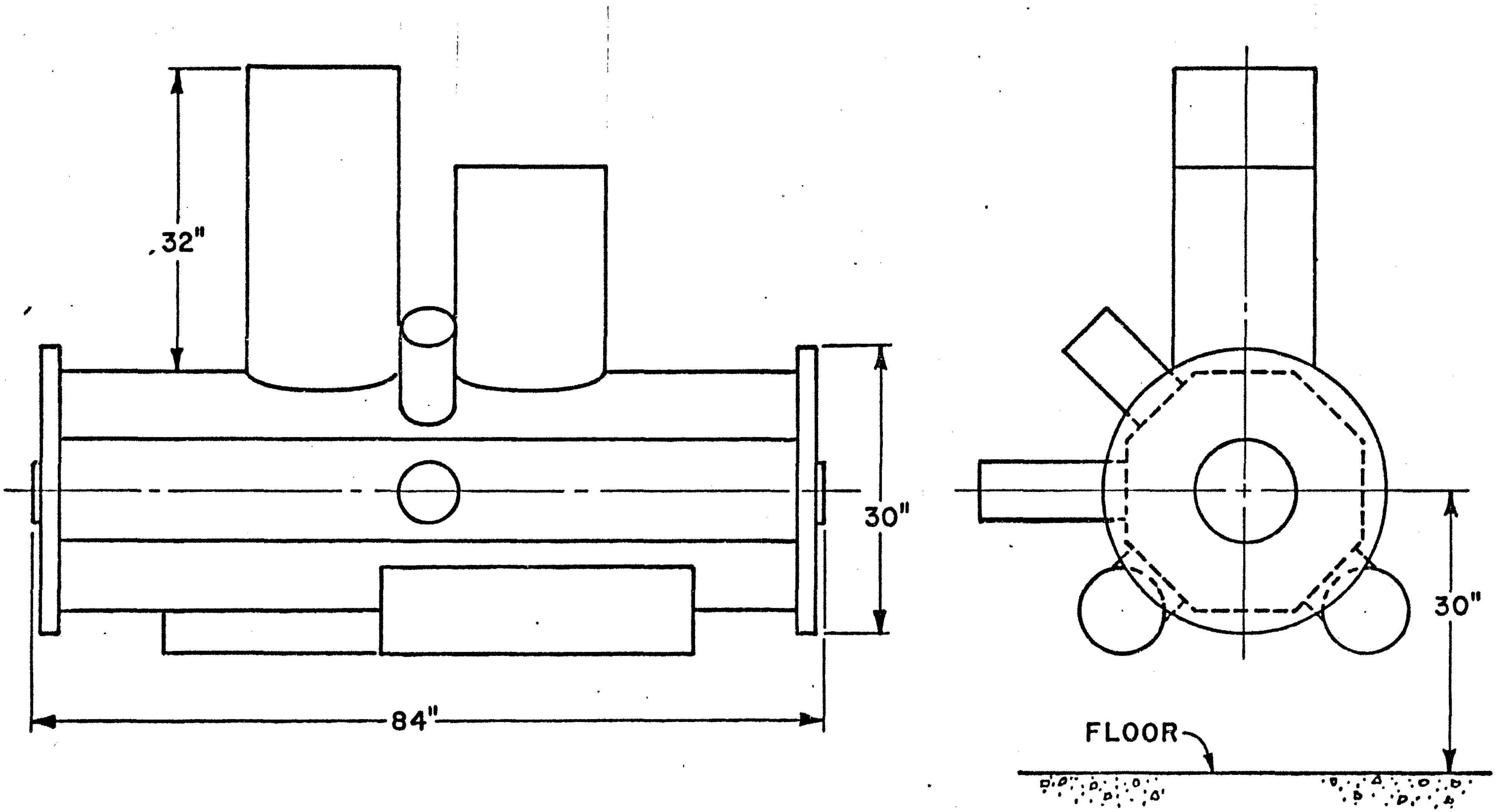

PHYSICAL DIMENSIONS

BUNCH CAPTURE/ROTATION CAVITY (53 MHz)

(SUPPORTS NOT SHOWN)

Fig. 4-8 52-MHz RF Cavity

<u>4.3.1 Main Magnets.</u> The Precooler magnet design and plan for construction follow closely the successful magnets of the Electron Coolng Ring (which are to be absorbed into the Electron Accumulator). The same methods of bolted assembly and construction in the Fermilab magnet factory will be followed. The only difference will be that the dipole coil ends will be bent up at 90^0 to save space, rather than 45^0 as in the Electron Ring dipoles. Table 4-IV gives the parameters of the main dipoles and quadrupoles.

TABLE 4-IV MAIN MAGNET PARAMETERS

<u>Dipoles</u>	
Number	112
Length (effective)	1.3716m
Length (steel)	1.2903m
Steel Weight	1270kg
Copper Weight	175kg
Gap Height	6.4cm
Gap Width	18cm
Good Field	12.8 x 6.0cm^2
Width	48.7cm
Height	28.9cm
No Turns	40
Peak Field	1.21T
Peak Current	1540A
<u>Quadrupoles</u>	
Number	52
Effective Length	0.610m
Steel Length	0.56m
Peak Gradient	16.6T/m
Poletip Field	0.79T
Bore	9.55cm
Steel Weight	920kg
Copper Weight	110kg
No Turns	44
Peak Current	1540A
Average Total Magnet Power in Normal Cycle	2.23 MV

The dipole assembly is shown in Fig. 4-9. The quadrupole assembly is shown in Fig. 4-10.

There are in addition special quadrupoles of different length and the same aperture or of larger aperture (bore=15cm) to accommodate large beam envelopes in straight sections. These are

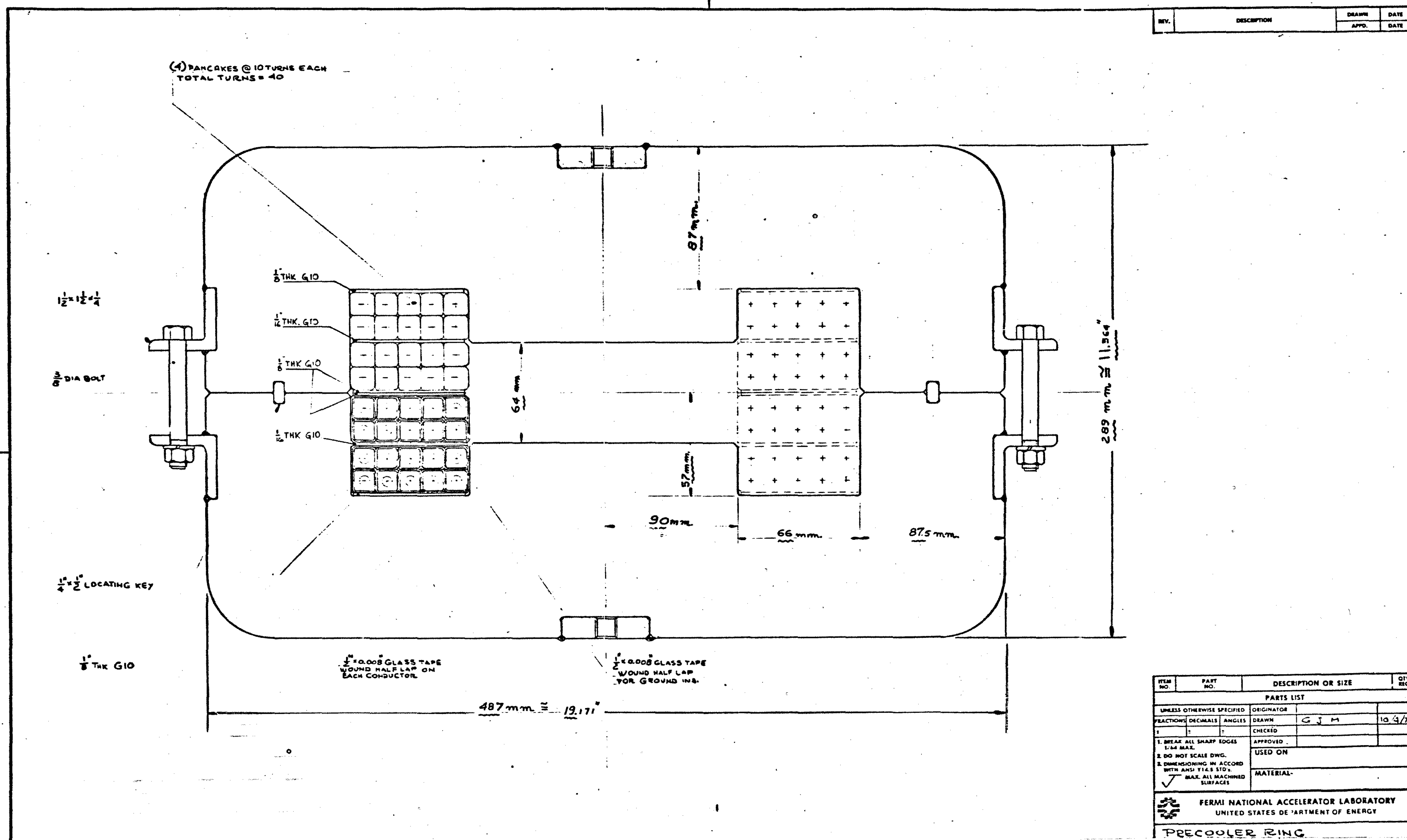

Fig. 4-9 Precooler Dipole

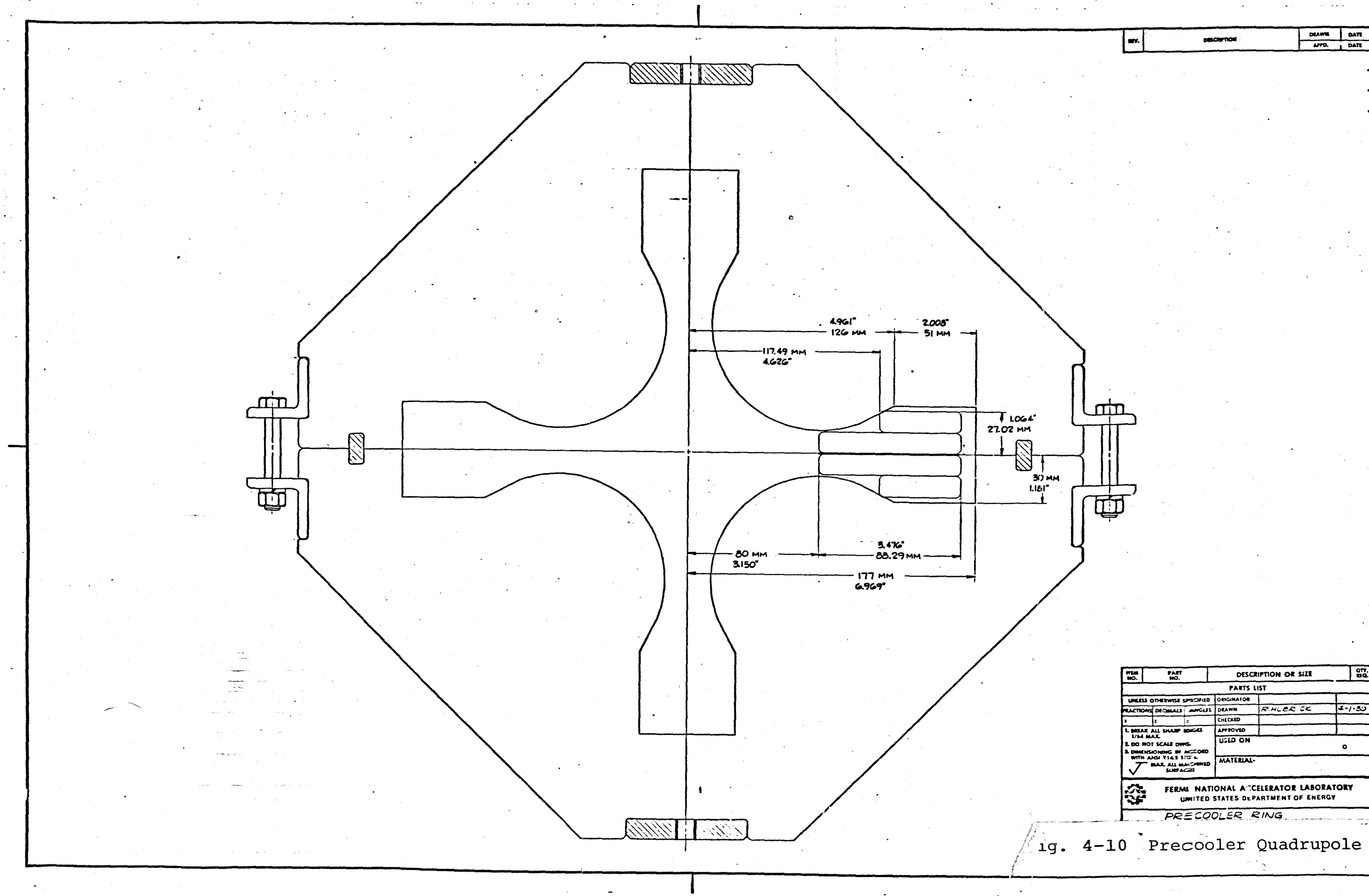

ig. 4-10 Precooler Quadrupole

designed to have lower field in order to keep poletip fields within reasonable limits.

Magnet support and alignment systems will follow the successful Electron Cooling Ring practice.

4.3.2 Main Magnet Power Supply. Eight power supplies will energize the antiproton Precooler ring. There will be two series-connected supplies per quadrant. These supplies will power 32 dipole and 19 quadrupole magnets. The resistance and inductance per quadrant is $R=1.4045\ \Omega$ and $L=0.466$ H. Each power supply will hve 12-phase series bridge rectifiers and will be energized from the 480-V 3-phase grid.

The total of eight power supplies are numbered IA, IIA, IIIA, IVA, and IB, IIB, IIIB, and IVB. Each quadrant will contain one "A" and one "B" supply. A block diagram of the Precooler ring with its power supplies is shown in Fig. 4-11. We discuss below the supply use in various cycles.

1. Cooling Cycle
During the cooling cycle, only the "A" supplies will be used. The "B" supplies will be bypassed.

1.1 112A (0.2 GeV) Flattop (Bunch and transfer to ECR)
The injection current level of 112A, (0.2 GeV) (8.2% of peak current), requires a voltage of 130 V, (8.9% of peak voltage), per quadrant. This level can be maintained by either charging the power-supply filter capacitors with current spikes or by bypassing most of the power supplies in the other quadrants. We could also operating half the power supplies as rectifiers and half as inverters.

1.2 112A (0.2 GeV) to 928 A(4.5 GeV) (Begin new cycle)
To raise the current from 112 A to 928 A in 0.5 sec requires a voltage jump from 130 V to 663 V and then an exponential voltage rise to 1458 V (928 A) per quadrant. The "A" supplies will operate under phase control following a B reference.

1.3 928 A (4.5 GeV) Flattop (First Cooling)
To maintain the 928 A current level the "A" supplies willl be phased back to $\alpha = 50°$.

1.4 928 A (4.5 GeV) to 555 A (2.4 GeV)
To go from 928 A to 555 A at a rate of 1139 A/s requires the voltage per quadrant to drop from 925 V ($\alpha = 50^0$) to 395 V ($\alpha = 74^0$) and then decrease exponentially to 82.5 V ($\alpha = 86^0$). The "A" supplies will operate under phase control from a B reference.

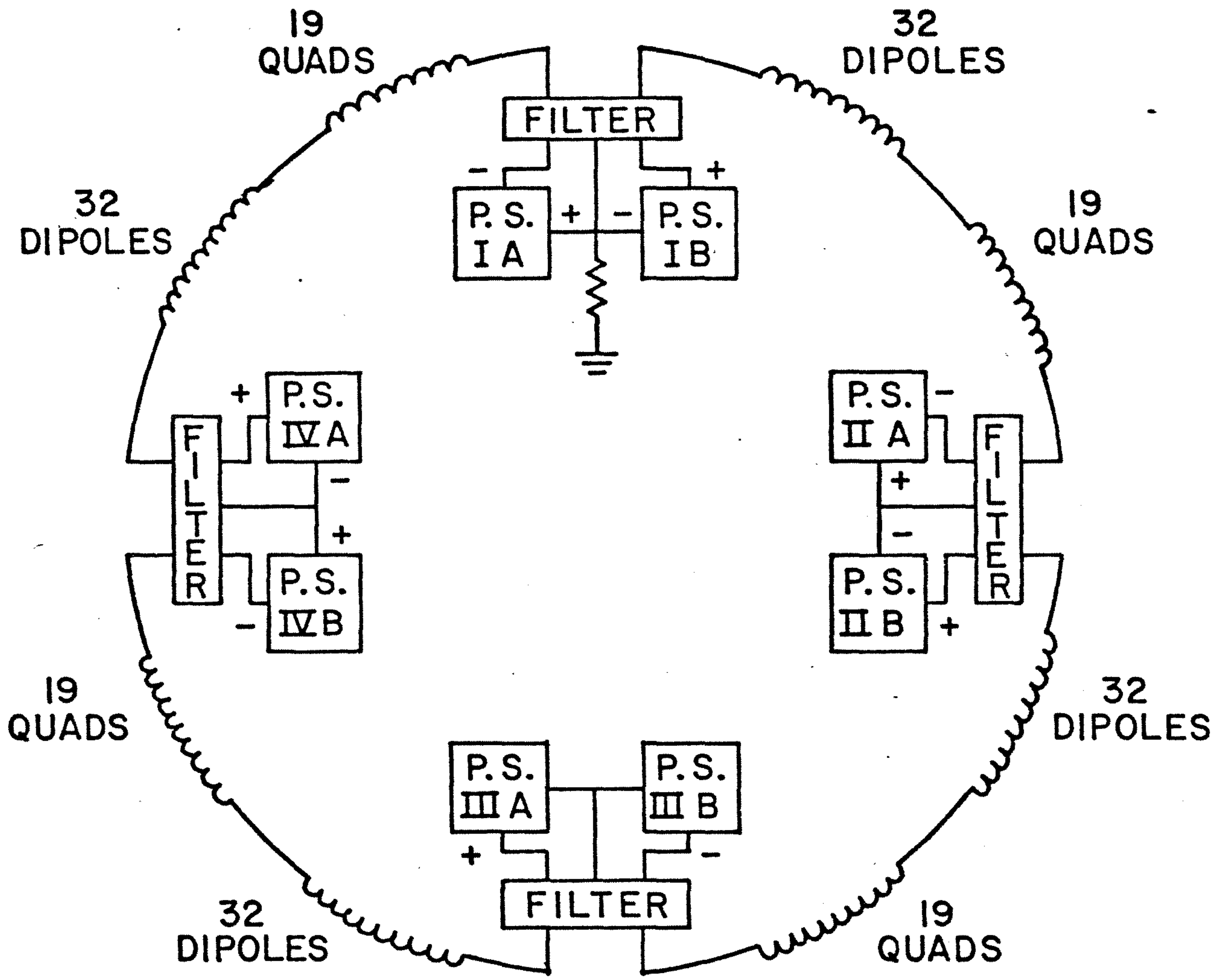

Fig. 4-11 Power-Supply Schematic

1.5 555A (2.4 GeV) Flattop (Second Cooling)
When the current reaches 555 A the voltage per quadrant must jump from 82.5 V (α =86^0) to 600 V (α = 69^0). For a better power factor, the supplies in two quadrants could operate as rectifiers while the other two supplies operate as inverters. One could also bypass the supplies in two quadrants and operate the remaining two supplies as rectifiers at a phase angle of α = 35^0 providing 1200 V for two quadrants.

1.6 555 A (2.4 GeV) to 246 V (1.3 GeV) (Deceleration)
The voltage across a quadrant of magnets must drop from 600 V to 82.5 V and then decrease exponentially to -185 V. If all four "A" supplies are on and operating at 600 V (α = 69^0), the phase angle must increase to α = 86^0 for 82.5 V, and then to α = 97^0 for -185 V. If two supplies are bypassed, the remaining two supplies must operate at α = 83^0 for 165 V, (2 x 82.5 V), and α = 105^0 for -370 V, (2 x -165 V). The "A" suplies will operate under phase control for a B reference.

1.7 274 A (0.9 GeV) Flattop (Third Cooling)
When the current has decayed to 274 A, the four "A" power supplies are phased to operate with α = 76^0 providing 345 V per quadrant. If only two supplies are operating, the phase angle of each supply would be α = 61^0 for 690 V for two quadrants.

1.8 274 A (0.9 GeV) to 112 A (0.2 GeV) (Deceleration)
To decrease the current from 274 A to 112 A requires a voltage drop from 345 V, per quadrant, to -185 V and then an exponentially decreasing voltage to -398 V. With four "A" supplies operating, the phase angle of each supply must go from α = 76^0 for 345 V to α = 97^0 for -185 V, and then to α = 106^0 for -398 V. If only two "A" supplies are operating, the phase angle of each supply must go from α = 61^0 for 690 V per two quadrants to α = 105^0 for -370 V per two quadrants, and then to α = 123^0 for -796 V per two quadrants. The "A" supplies will operate under phase control from a B reference.

2. Once Every 10 Hours Acceleration to 8 GeV

2.1 Injection Current of 112 A (0.2 GeV) (Raise field to injection level)
Either the type "A" or the type "B" supplies can be used to obtain the injection current of 112 A. If the "B" supplies are used, they must be phased on to produce a voltage of 530 V per quadrant (α = 37^0) and then exponentially increased to produce 663V (α

= 9^0) per quadrant. The current rises from zero to 94 A in 82 ms at a rate of 1139 A/sec.

2.2 112 A (0.2 GeV) Flattop (Injection)
When the current reaches 94 A, the "B" supplies are phased back to produce 130 V per quadrant ($\alpha = 78^0$). Alternatively the voltage for this level can be maintained, as described in 1.1 above.

2.3 112 A (0.2 GeV) to 1540 A (8.0 GeV) Acceleration
For acceleration to 8 GeV, the four "A" and the four "B" supplies are required. The power-supply output voltage per quadrant must jump from 130 V to 663 V and then rise exponentially to 2130 V. The current will rise at a rate of 1139 A/sec. The "A" and "B" supplies will operate under phase control following a B reference signal.

2.5 1540 A to 0 A (Discharge of Magnets)
By means of rectifier phase control, the output voltage of the power supplies is reduced, thereby forcing the current to zero at a rate determined by a B reference signal. Some of the 1.2 MJ stored in the magnets is returned to the power grid when the power-supply voltages go negative.

3. Tune-up Cycles
The antiprotons will be collected at 4.5 GeV (928 A) for precooling and transferred to the Electron Cooling Ring at 0.2 GeV (112 A). After electron cooling and accumulation, the antiprotons will be transferred back to the Precooler at 0.2 GeV, preaccelerated to 8 GeV (1540 A), and injected into the Main Ring. It may be desirable to experiment at one or more of the above energy levels during tune-up.

4.3.3 Correction Elements. The very large size of the Precooler momentum acceptance (4.5%) means that sextupole chromaticity correction will be important (only at lower field, because $\bar{p}$ beam accelerated to 8 GeV will have been cooled). Sextupoles will be located in the straight section downstream of each quadrupole. They will be powered in series with the main magnets and separately powered windings will be provided for adjustment.

The field lengths calculated to bring the chromaticities to zero are 20T/m at F locations and 35T/m at D locations. The two kinds of magnets will be built with one cross section, giving $B''=187T/m^2$ and a poletip field of 0.3T for a pipe diameter of 4.5 in. The effective lengths are then 4.15 in. (F) and 7.37 in. (D).

Quadrupole corrections will be provided by trim windings on the regular quadrupoles. Separate horizontal and vertical trim dipole and spew quadrupoles will be located downstream of the sextupole elements. We assume:

	Low Field	High Field
Dipole Error	10^{-3}	5×10^{-4}
Dipole Tilt	1 mrad	0.3 mrad
Position Error	5×10^{-4}	2.5×10^{-4}
Quad Tilt	10^{-3}	3×10^{-4}

The trim dipole strength needed is approximately 2×10^{-3} T-m and the skew quad strength needed is 2×10^{-3}T. We are designing a package 10 cm long to contain these elements.

4.4 Vacuum System

Beam will not be stored in the Precooler for periods of many hours, as is the case in the Electron Accumulator, but for periods of seconds or minutes. One might store for a few hours in the simple initial low-luminosity scenarios briefly mentioned at the end of Chapter 2. We see from the calculated lifetimes collected in Table 4-V that even this possible use does not put any severe constraint on pressure.

TABLE 4-V GAS-SCATTERING MEAN LIFETIMES AT 10^{-8} TORR

	Multiple Scattering	Single Scattering	Nuclear Scattering
4.5 GeV	4 hrs	21 hrs	89 hrs
200 MeV	2 min	11 min	154 hrs

An average pressure below 10^{-8} Torr, achievable with a low-temperature bake, is adequate. Quite aside from this possible low-luminosity use, we desire a pressure in the 10^{-9} Torr range in our real scenarios in order that beam broadening from scattering be negligible compared with cooling. The vacuum system designed to achieve this pressure is described in Table 4-VI.

TABLE 4-VI VACUUM-SYSTEM PARAMETERS

Valves - each end of each long straight section	8
- each rf system location	2
Gauges - 2 per quadrant	8
Mass spectrometers - 2 per straight section	8
Roughing stations - each long straight section	4
- each rf system location	2
Pumps - one 60 l/sec per cell	36
- 8 per long straight section	32

Normal Cell

Chamber cross section	5.6x12.5 cm^2
Effective diameter	8.9 cm
Half-cell conductance	18.4 ℓ/sec
Outgassing rate	$3x10^{-12}$ T-ℓ/cm^2-sec
Total flux per pump	$16x10^{-9}$ T-ℓ/sec
Pump location	between dipoles
Mean Pressure	10^{-9} T

4.5 Stochastic Cooling System

4.5.1 Stochastic Cooling Sequence

The momentum precooling system must reduce the initial momentum spread of the antiproton beam at the end of rf stacking (± 1%) in a coordinated manner with deceleration so that the momentum spread of the beam at 200 MeV is compatible with the electron-cooled accumulation process. There is an optimum relationship between energy, momentum spread, lattice characteristics, and hardware placement in the ring for rapid initial cooling. This relationship depends on the frequency spread of the Schottky signals at the highest usable harmonic. As cooling proceeds, the cooling rate decreases quickly as the frequency spread is reduced, so that practical reductions in momentum are 10 or less in a few seconds of cooling time. The cooling sequence to be used in the Precooler calls for cooling periods interspersed with deceleration to lower energies. This re-establishes the desired Schottky signal spread, permitting resumption of rapid cooling.

Table 4-VII gives a sequence of cooling and deceleration which, from the computer simulation shown in Fig. 4-12, produces a more than sufficient amount of cooling.

TABLE 4-VII STOCHASTIC COOLING SEQUENCE

Cooling Steps:

STEP		#1	#2	#3	
Kinetic energy (GeV)		4.5	2.4	0.9	GeV
β		0.985	0.960	0.860	
γ		5.796	3.558	1.959	
η		0.020	0.065	0.225	
Revolution freq		622.72	606.78	543.74	kHz
Bandwith, MHZ	Low	100	100	100	MHz
	High	500	500	300	MHz

a) at 4.5 GeV

b) at 2.4 GeV

c) at 0.9 GeV

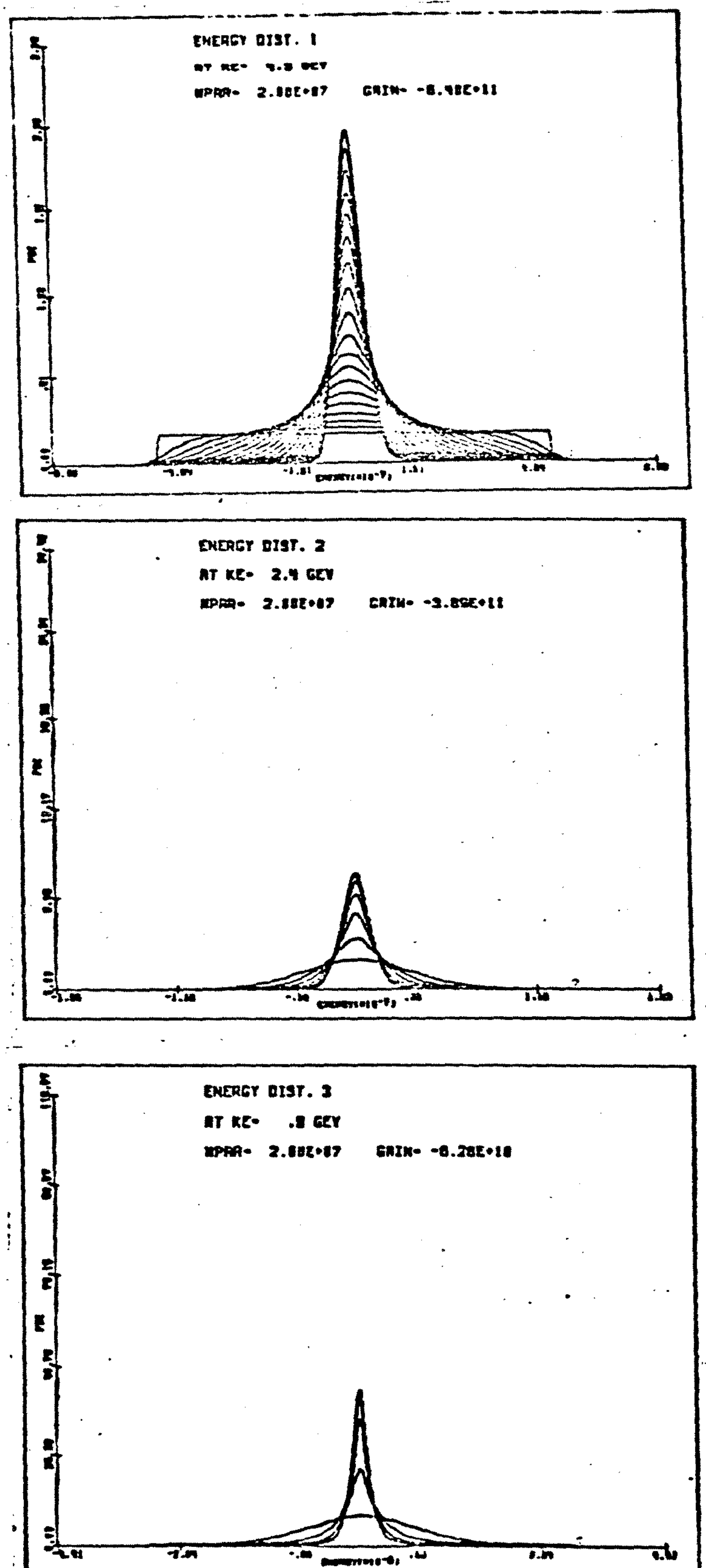

Fig. 4-12 Stochastic Cooling Simulation

Lower harmonic	160	164	180	
Upper harmonic	803	823	543	
Initial $\Delta p/p$, full	2.1	0.5	0.28	%
Final $\Delta p/p$, full	0.28	0.13	0.046	%
Cooling period	4.5	1.25	0.75	sec
RMS Schottky power	0.93	0.033	--	kW
RMS total power	3.62	0.97	0.04	kW
Overall amplifier gain	230	230	220	db
Total delay required	330	352	434	nsec

The inherent flexibility of the process could easily accommodate a fourth cooling step, should it be required, at the expense of having a slightly longer cooling cycle.

4.5.2 Hardware. Hardware for the precooling system is mostly conventional. Parameters are given in Table 4-VIII.

TABLE 4-VIII STOCHASTIC COOLING EQUIPMENT

Mode	Momentum
Beam	Debunched
No. of Cooling Steps (See Table 9)	3
Precooler Radius	75.4717 m
Transition Energy γ_T	10.24624
No. of Cooling Devices	1
Pickup Long Straight Section	20. m
Kicker Long Straight Section	20. m
No. of Particles Cooled	2.1×10^7
Notch Filter	Circumference Length Shorted
No. of Tanks of Pickups/Kickers	6
No. of Pickups/Kickers Per Tank	32
Total No. of Pickups/Kickers	192
Impedance Per Pickup/Kicker	50 Ω
Length Per Pickup/Kicker	10 cm
Overall Transverse Dimension of Tanks	2 ft
No. of Premplifiers	6
No. of Major Amplification Stations	1
Amplifier Total Rated Power	10 kW
Amplifier Delay Time	60 nsec
Distance Between Pickups and Kickers Normalized to Circumference	0.5
Location of Pickup Station	West Long Straight
Location of Kicker Station	East Long Straight
Time Distance Between Pickups And Kickers in Straight Line	470 nsec

The same pickups, amplifiers, filter, and kicker system can be used for all cooling steps, although either separate notch filters (high-quality long transmission lines) or a tunable system are required because of the variation of β, and consequently of the revolution frequency, during deceleration. Similarly, the delay between pickups and kickers, and between groups of pickups, must also be adjusted. This can be accomplished by switching delay lines in the system during the rf deceleration steps.

An effort has been made to use realistic parameters in calculations of expected system performance, particularly for "sensitive" parameters such as effective pickup coupling impedance, kicker impedance, amplifier noise, and so forth. For example, the 30-Ω impedance that has been assumed for the pickup is close to an experimental value achieved with a crude prototype constructed for cooling studies on the Electron Cooling Ring, and is consistent with (in units of impedance/pickup length) values achieved in the CERN AA cooling system. Similarly, the effective preamplifier noise figure of 1.4 db assumed in the calculations is justified by the commercial availability of suitable preamplifiers with noise figures of less than 1 db (when cooled). A modest supporting R & D program will almost certainly yield specific designs that will meet or exceed the assumed performance requirements.

It should be noted that the use of a full-wavelength notch filter is planned. This technique permits rapid cooling without excessive amplifier power and constitutes a distinquishing feature of the precooling system.

The layout of stochastic cooling equipment in the East and West straight sections is shown in Figs. 4-7 and 4-5.

4.6 Deceleration and Rebunching

4.6.1 Deceleration. Deceleration and subsequent acceleration of antiprotons in the Precooler is to be done with three slightly modified PPA accelerating cavities capable of operating over frequency range of 5 to 9 MHz. The dimensions of one of these cavities are shown in Fig. 4-13. The locations of these cavities in the North straight section is shown in Fig. 4-6. Each cavity can develop about 28kV effective gap voltage, so a total voltage of 84kV will be available. The deceleration will be done in three stages, each separated by a debunching and cooling period so each stage can be done at a different harmonic number. Harmonic numbers are selected such that the required bucket areas and deceleration rates are provided within the voltage and frequency ranges of the rf system. Except for transition periods from stationary field conditions, each deceleration is to be done at a constant rate of change of momentum and guide field.

The first stage of deceleration, from 4.5 GeV to 2.4 GeV, will be done at h=9 and cover a frequency range of 5.60 to 5.46 MHz. The deceleration rate dp/dt will be 4 GeV/c-sec.

PHYSICAL DIMENSIONS

PRECOOLER DECELERATION/ACCELERATION CAVITY (5-9 MHz)
(SUPPORTS NOT SHOWN)

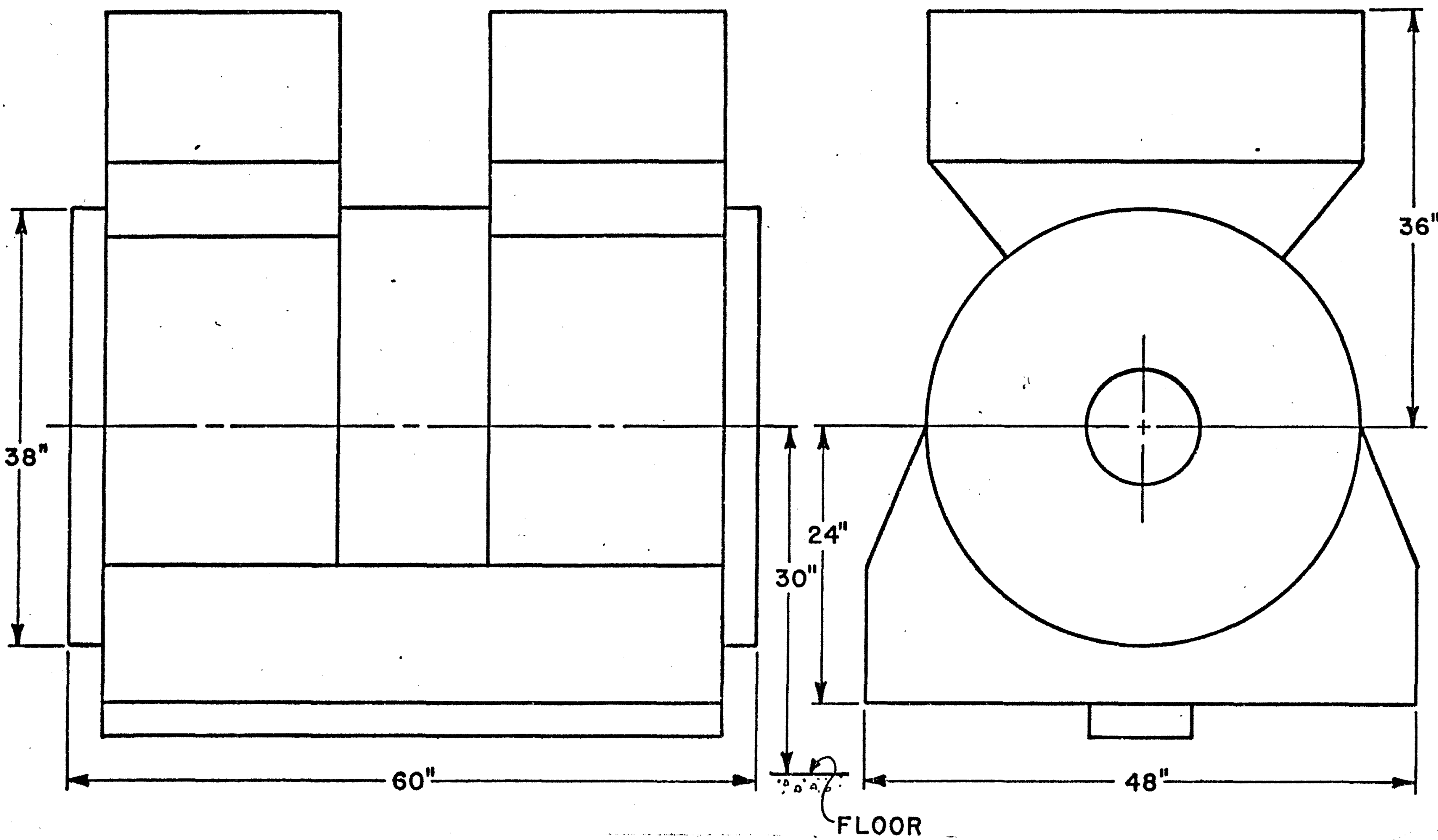

Fig. 4-13 5-9 MHz Cavity

After 4.5 sec of cooling at T=4.5 GeV, the momentum spread will be 0.28%. This results in a total energy spread ΔE=17.2 MeV and a longitudinal emittance of 27.6 eV sec.

At 4.5 GeV, a 30 eV-sec stationary bucket area is established at h=9 by 11.6 kV. In this case, $T\phi = 6.38 \times 10^{-3}$ sec, so the adiabatic capture period may nominally be 25 msec. Then $V\sin\phi_s = 6.33 \times 10^3$ volts.

Based on these considerations, the tabulations given in Table 4-IX are developed for the deceleration stages.

TABLE 4-IX DECELERATION PARAMETERS

First Stage

Kinetic energy range	4.5 - 2.5 GeV
Cooling time (4.5 GeV)	4.5 sec
Cooled momentum spread	±0.148 %
Energy spread (total)	17.2 MeV
Longitudinal emittance	27.6 eV-sec
Total bucket area allocated	30 eV-sec
Harmonic number	9
Frequency range	5.604 - 5.46 MHz
Deceleration rate c dp/dt	4 GeV/sec
V sin Θs	6.33×10^{3} V
Stationary bucket voltage (4.5 GeV)	11.6 kV
Phase oscillation period (4.5 GeV)	6.4×10^{-3} sec
Bunching time allocated	25×10^{-3} sec
Deceleration time required	0.54 sec
Stationary bucket voltage (2.4 GeV)	65.3 kV
Phase oscillation period (2.4 GeV)	1.1×10^{-3} sec
Debunching time allocated	10×10^{-3} sec

T(GeV)	φs(deg)	Γ	V(kV)	Freq(MHz)
4.5	0	0	11.6	5.604
4.4	12.3	0.213	29.7	5.601
4.0	10.4	0.181	34.9	5.59
3.5	8	0.139	45.5	5.56
3.0	6	0.104	60.8	5.52
2.5	4.3	0.075	84.4	5.47
2.4	0	0	65.3	5.46

Second Stage

K.E. range	2.5 - 1.0 GeV
Cooling time	1.5 sec
Cooled momentum spread	±0.064 %
Energy spread (total)	4.22 MeV
Longitudinal emittance	6.94 eV-sec
Bucket area allocated (total)	7.5 eV-sec
Harmonic number	10
Frequency range	6.067 - 5.322 MHz
Deceleration rate c dp/dt	4 GeV/sec
V sin Θs	6.33×10^{3} V
Stationary bucket voltage (2.4 GeV)	4.54 kV
Phase oscillation period (2.4 GeV)	4.1×10^{-3} sec
Bunching time	20×10^{-3} sec
Deceleration time	0.435 sec
Stationary bucket voltage (800 MeV)	35.3 kV
Phase oscillation period (800 MeV)	5×10^{-4} sec

Debunching time	2.5×10^{-3} sec

T(GeV)	ϕs(deg)	Γ	V(kV)	Freq(MHz)
2.4	0	0	4.54	6.067
2.0	16.8	0.289	21.9	5.99
1.5	12.6	0.218	29.0	5.835
1.0	8	0.139	45.5	5.54
0.8	0	0	35.3	5.322

Third Stage

K.E. range	800 - 200 MeV
Cooling time	1 sec
Cooled momentum spread	±0.0237%
Energy spread (total)	584.1 KeV
Longitudinal emittance	1.09 eV-sec
Bucket area allocated (total)	1.25 eV-sec
Harmonic number	14
Frequency range	7.45 - 5.01 MHz
Deceleration rate c dp/dt	2 GeV/sec
V sin Θs	3.17×10^{3} V
Stationary bucket voltage (800 MeV)	1.37 kV
Phase oscillation period	2.25×10^{-3} sec
Bunching time	13×10^{-3} sec
Deceleration time	0.409 sec
Stationary bucket voltage (200 MeV)	5.0 kV
Phase oscillation period (200 MeV)	6.2×10^{-4} sec
Debunching time	3×10^{-3} sec

T(GeV)	ϕs(deg)	Γ	V(kV)	Freq(MHz)
0.8	0	0	1.37	7.45
0.7	22	0.3746	8.46	7.26
0.6	21	0.3584	8.84	7.01
0.4	17	0.2927	10.8	6.31
0.3	15.5	0.2670	11.86	5.78
0.2	0	0	5.0	5.01

4.6.2 Bunching for Extraction. At the end of the deceleration cycle, the debunched beam must be re-bunched into a single bunch of length and momentum spread suitable for injection into the Electron Cooling Accumulator. A total bunch of 1 μsec will allow a kicker fall time in the electron ring of 200 n sec. We assume here a longitudinal emittance for the decelerated beam of 1.3 eV-sec. Such a beam, bunched at harmonic number one will have an energy spread of ±827 kV and a momentum spread of $\pm2.26 \times 10^{-3}$.

The bucket half-height required to match such a distribution is 1.55 MeV with ϕ=1.124 rad. An rf voltage of 7 kV at 357.9 kHz is required to create such a bucket. The phase oscillation period is 7.8×10^{-4} sec, so this bunching will require about 5 msec.

The 1-μsec bunch can be generated with slightly small rf voltage by first bunching the beam to $\Delta\phi^2$ ±π/2, or 1.4 μsec, then suddenly jumping the voltage slightly to an unmatched bucket in which the beam distribution rotates into the vertical position with a width of 1 μsec, one quarter of a phase-oscillation period. The rf voltages necessary for these two steps are 2 kV and 4 kV. The initial phase-oscillation period is 3.7 msec, so 10 msec will be allowed for initial bunching. The final phase-oscillation period is 2.7 msec, so the quarter rotation will occur in about 670 μsec. Dimensions of the h=1 cavity are shown in Fig. 4-14 and its location was shown in Fig. 4-6.

4.7 Transfer to and from the Electron Accumulator

The lines used to transfer 200-MeV beam from the Precooler to the Electron Accumulator and the line used to transfer cooled beam back to the Precooler are symmetric with each other, as can be seen in the layout of Fig. 4-15. Elements and parameters of the line back to the Precooler are given in Table 4-X, which could become the other line with only relabelling of elements.

TABLE 4-X TRANSFER-LINE ELEMENTS FROM

ELECTRON ACCUMULATOR TO PRECOOLER

	element	length	strength (200 MeV)
electron	1B21	(m)	
cooling	1K21	1.5240m	-240 G
ring	1QD2	0.6767	-10.97 kG/m
	1QF1	0.6787	5.73 kG/m
	C-magnet	1.5240	1.33 kG
transfer	XQ1	0.6767	2.21 kG/m
line	XQ2	0.6767	-8.20 kG/m
	XQ3	0.6767	12.88 kG/m
	XQ4	0.6767	-7.96 kG/m
precooler	C-magnet	1.5240	1.76 kG
	1Q3	1.5240	9.80 kG/m
	QD1	0.9905	-10.08 kG/m
	Kick	1.5967	88.8 G
	Kick	1.5967	88.8 G
	QF1		

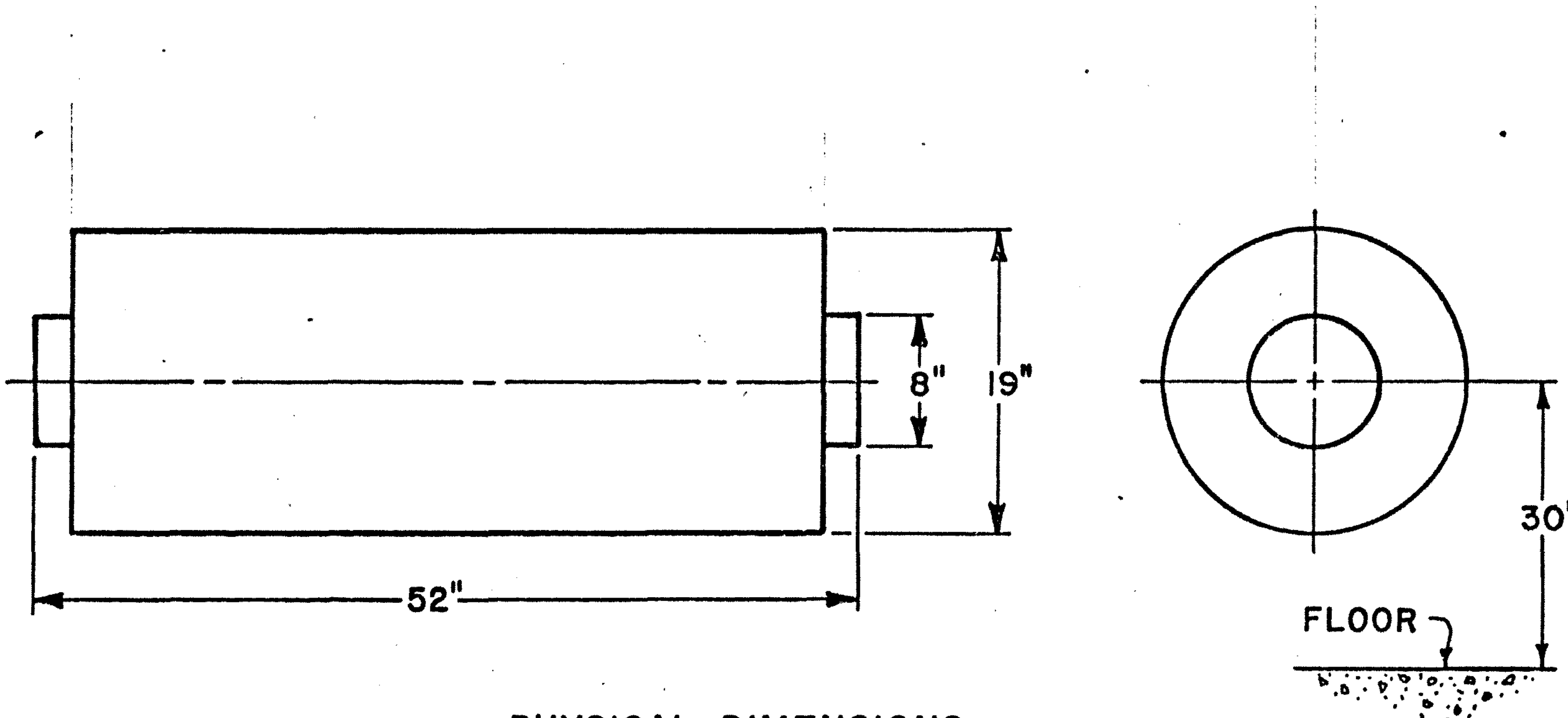

PHYSICAL DIMENSIONS
FIRST HARMONIC BUNCHING CAVITY
FOR BOTH PRECOOLER & ELECTRON COOLING RING
(SUPPORTS NOT SHOWN)

Fig. 4-14 h = 1 Cavity

Exact values for XQ1-XQ4 will change slightly due to detailed matching.

4.8 Acceleration in the Precooler

Single antiproton bunches with longitudinal emittance of approximately 0.075 eV-sec are to be accelerated from 204 MeV to 8 GeV in the Precooler at harmonic number 14. The acceleration system consists of three PPA rf cavities operating over the frequency range 5.01 to 8.802 MHz. This is the same system used for Precooler deceleration.

The stationary bucket necessary to match the bunch shape extracted from the Electron Ring requires 3.8 kV at 5.01 MHz. The acceleration rate will be 8 GeV per second and a bucket area of at least 0.09 eV-sec will be maintained during acceleration. The net accelerating voltage $V \sin \phi_s$ will be 12.7 kV per turn. The acceleration will require about 1 second.

At the beginning of acceleration, just above 204 MeV, a maximum voltage of 30 kV and a synchronous phase angle of 25 degrees are required. As acceleration progresses, the voltage and phase angle both change so that just below 8 GeV the required voltage becomes 13 kV and the synchronous phase angle 75 degrees.

At 8 GeV, a stationary bucket of sufficient size must be established so that the antiproton bunch length is shorter than the Main Ring bucket length (18.9 nsec) into which it is to be injected. If the voltage is raised to 15 kV, a 0.09 eV-sec bunch in equilibrium with the bucket will have a bunch length of 8 nsec, which can be matched easily by a stationary bucket in the Main Ring. The phase-oscillation period in this bucket will be 1.5 msec, so the stationary bucket can be established in 10 msec at the end of the acceleration cycle.

4.9 8-GeV Extraction and Transport

Extraction is carried out in a single-turn mode by a fast kicker and pulsed septum at the upstream end of the east straight section, followed by a non-achromatic horizontal translation to a line parallel to the beam center line in the east straight secction and 1.0668 m from it. A FODO system located in three manholes leads to a left bend that puts the beam directly underneath the 4.5-GeV injection line. The beam is then translated up 1.9666 m by an achromatic system to join the other beam line. The system is designed to contain a beam of transverse emittance 2π mm-mrad in each plane and momentum spread 0.4%. A list of elements is given in Table 4-XI.

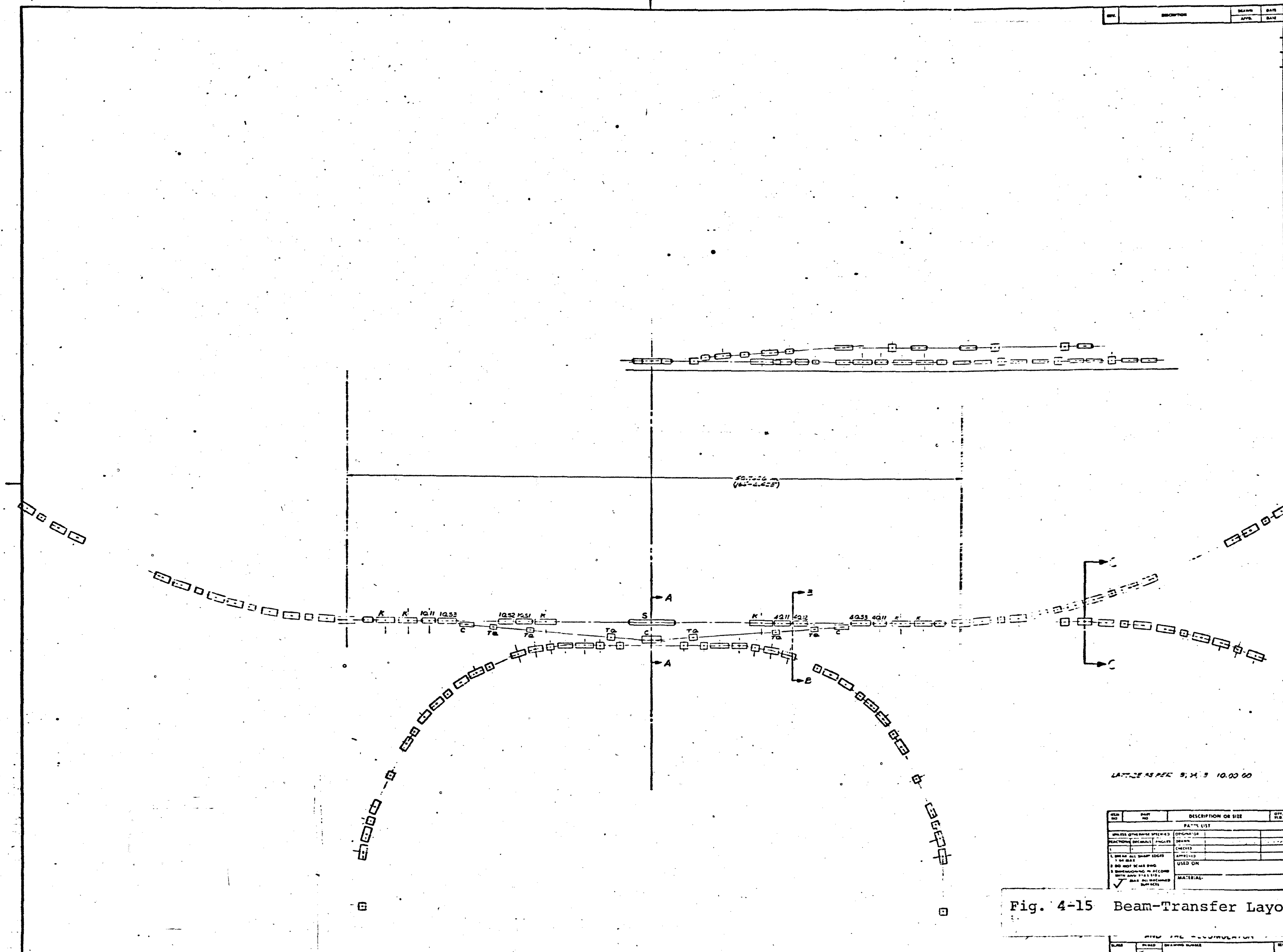

Fig. 4-15 Beam-Transfer Layout

TABLE 4-XI ANTI-PROTON EXTRACTION FROM THE PRECOOLER

	Kicker #1	Kicker #2
Location		
Strength	250 G	250 G
Rise Time		
Aperture		
Effective Length	2m	2m

Method: Single-turn fast extraction, full-aperture kicker

Extraction occurs horizontally, to outside,
at upstream end of East long straight section

Beam Emittances: $E_H = E_V = 7\pi\ 10^{-6}$mm-mrad
i

Momentum Spread: ± 0.1%

Magnet Sequence:

1. Translator
2. Long Straight Transport
3. Bend Left
4. Matching and Vertical Translation
5. Matching FODO
6. Matching and FODO Transport
7. Vertical Translation to Target

1. Translator

2QE3 D1 B1 D2 B2 D3 Q1 D4 Q2 D5 B3

Drifts	Length(m)
D1	0.25
D2	1.0
D3	3.5147
D4	1.5
D5	1.181

Dipoles	Effective Length(m)	Strength $(B/B\rho)(m^{-1})$
B1	1.00	0.033727
B2	1.1217	0.054172
B3	1.675	0.062523

Quadrupoles	Effective Length(ft)	Gradient $(B'/B\rho)(m^{-2})$
Q1	2	0.5296
Q2	2	-0.4697

2. Long Straight Transport

D6 Q3 D2 Q4 D7 QF D8 QD D8 QF D8 QD D9

Drifts	Length (m)
D6	14.332
D7	5.3904
D8	14.0757
D9	10.2205
D2	1.00

Quadrupoles	Effective Length(ft)	Gradient $(B'/B\rho)(m^{-2})$
Q3	2	0.42314
Q4	2	-0.4295
QF	2	0.1602
QD	2'	-0.1602

3. Bend Left

Q5 0 B 0 B 0 Q6 0 B 0 B 0
Q7 0 B 0 B 0 Q8 0 B 0 B 0 Q9/2

Drift	Depth
0	0.5 m

Bending	Effective Depth	Strength $(B/B\rho)$
B	1.3716 m	0.040929 m^{-1}

Quadrupoles	Effective Length(ft)	Strength $(B'/B\rho)(m^{-2})$
Q5	2	0.4216
Q6	2	-0.3443
Q7	4	0.32715
Q8	2	-0.2784
Q9/2	2	0.43036

4. Matching and Vertical Translation

Q9/2 D2 Q10 D11 V3 D12 Q11
D13 Q12 D13 Q11 D12 $\overline{V3}$

Drifts	Lengths(m)

D11	.6954m
D12	5.9185
D13	4.999
D2	1.00

Quadrupole	Effective Length(ft)	Strength $(B'/B\rho)(m^{-2})$
Q9/2	2	0.43036
Q10	4	-0.4687
Q11	2	-0.54850
Q12	2	0.4423

Vertical Dipoles	Effective Length(m)	Strength $(B/B\rho)(m^{-1})$
V3	1.3716	(up) 0.036928
$\overline{V}3$	1.3716	(down) 0.036928

5. Matching FODO

O Q13 D14 Q14 D4 QF/2

Drift	Lengths(m)
O	0.5
D14	1.354
D4	1.5

Quadrupoles	Effective Length(ft)	Strength $(B'/B\rho)(m^{-2})$
Q13	2	-0.45869
Q14	2	0.34931
QF/2	1	0.1602

6. Matching and FODO Transport

QF/2 D9 QD D9 QF
D9 QD D9 QF D8 QD D7
Q4 D6 Q3 D5 (in the middle of $\overline{V}$)

Drifts	Lengths(m)
D5	3.0
D6	3.1962
D7	1.6916
D8	2.574
D9	14.0757

Quadrupoles	Effective Length(ft)	Strength$(B'/B\rho)(m^{-2})$
QF/2	1	0.1602
Q3	2	-0.52436
Q4	2	0.34452

QD	2	-0.1602
QF	2	0.1602

7. Vertical Translation to Target

D1 $\overline{V}1$ D2 Q7 D3 Q2 D4
Q1 D4 Q2 D3 Q1 D2 V1 D1

Drifts	Length(m)
D1	-0.915
D2	3.8359
D3	1.5
D4	3.50

Quadrupoles	Effective Length(ft)	Strength (B/Bρ)(m^{-2})
Q1	2	0.5025
Q2	4	-0.41262

Vertical Dipoles	Effective Length(m)	Strength (B/Bρ)(m^{-1})
V1	1.83	(up) 0.05726
$\overline{V}1$	1.83	(down) 0.05726

5. Electron Cooling Accumulator

5.1 General Structure and Layout

5.1.1 Lattice. The design parameters of the Electron Cooling Accumulator have been chosen to allow efficient electron cooling to be carried out in a range between 200 and 450 MeV, and possibly as high as 1-GeV antiproton energy.

The overall design of this ring is very similar to that of the present Electron Cooling Ring and has essentially the same constraints. The intended mode of operation is to inject $\bar{p}$'s from the Precooler into the Accumulator, precool them with electron cooling and then momentum displace the injected beam into a stack, which will also be electron cooled. Thus the ring needs a straight section appropriate for injection and extraction and another one for cooling. For injection and extraction, it is desirable to have large horizontal dispersion and small beam sizes. The length of this straight section need not be too great. The cooling straight section, on the other hand, should be quite long, zero dispersion, and have $\bar{p}$-beam sizes matched to electron-beam sizes, approximately 1 in. in radius. One would like to have as large a percentage of the circumference as possible filled with electron cooling, subject to several considerations. The expense and difficulty of the cooling system, as well as the nonlinear end effects of solenoid, toroids, and electron beam on the $\bar{p}$'s effectively limit the number of cooling systems to one, and the beam-size variation through the cooling region limits the length of that region. The desire for some superperiodicity produces at least a four-sided figure. The final design of this ring, then, is generally the same as the present cooling ring. It is a racetrack design having two long straight sections. One long straight section will be used for electron cooling; the two short straight sections will be used for injection and extraction and for such functions as a beam dump. The main difference between this new ring and the present one is in the overall circumference, the fraction of the ring used for cooling, and the maximum energy of the ring. The ring has a circumference of some 203 m, and will have 10 m of electron cooling, compared with 135 m and 5 m of cooling the present experiment. The structure and lattice parameters for this ring are listed in Table 5-I, and the lattice functions are plotted in Fig. 5-1. Horizontal and vertical aperture requirements are shown in Figs. 5-2 and 5-3.

The ring has been designed to use the same magnets as in the present Electron Cooling Ring, with new ones to be built to piece out the circumference. A total of 44 4-ft dipoles and 48 2-ft quadrupoles with sizes and apertures as in the present magnets are needed. At present, 24 dipoles and 32 quadrupoles exist. In addition, two 2-ft special quads with a good-field region of 30 cm are required for injection. The totals given here include six standard quadrupoles required for transfer to and from the

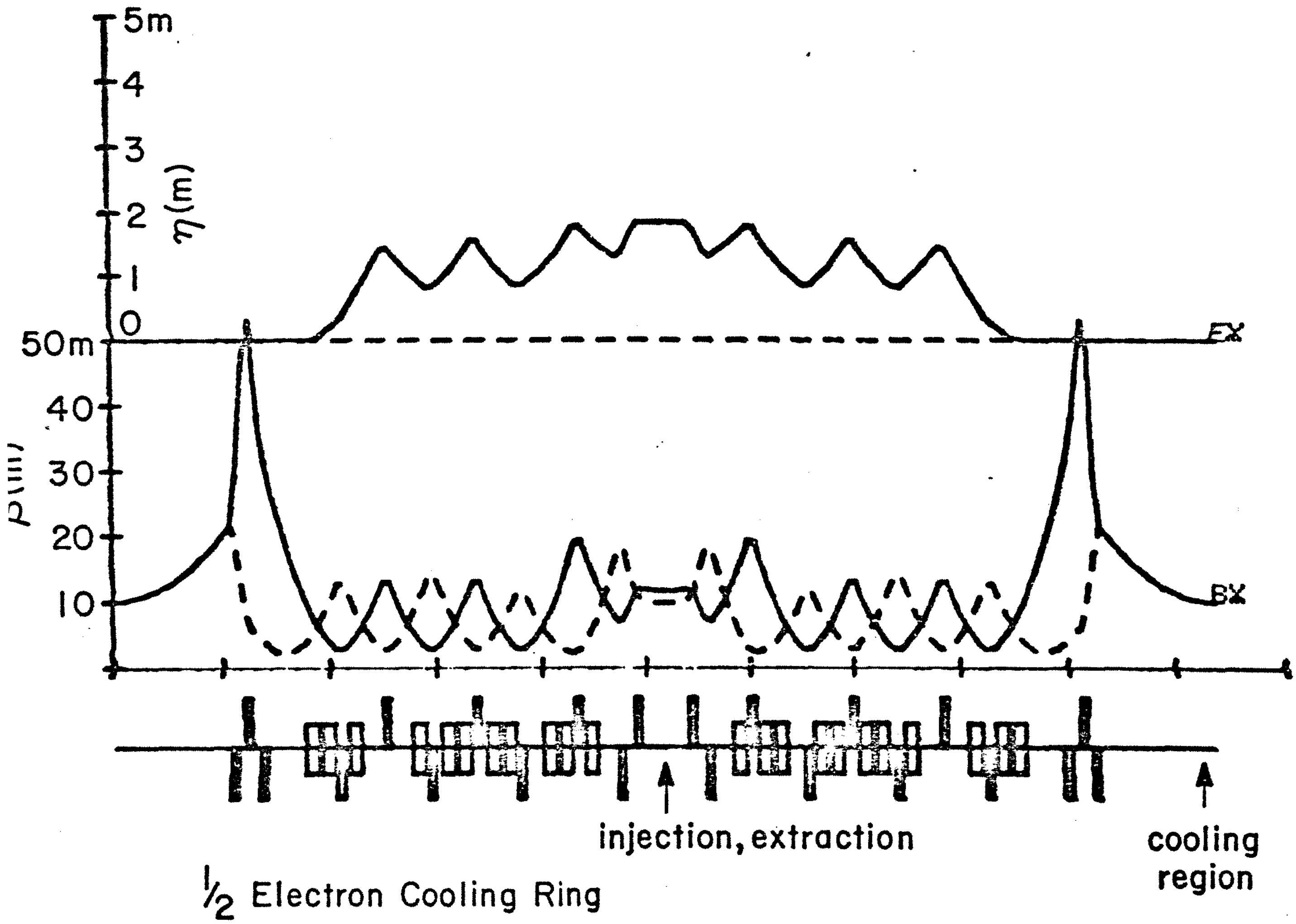

Fig. 5-1 Electron Accumulator Orbit Functions

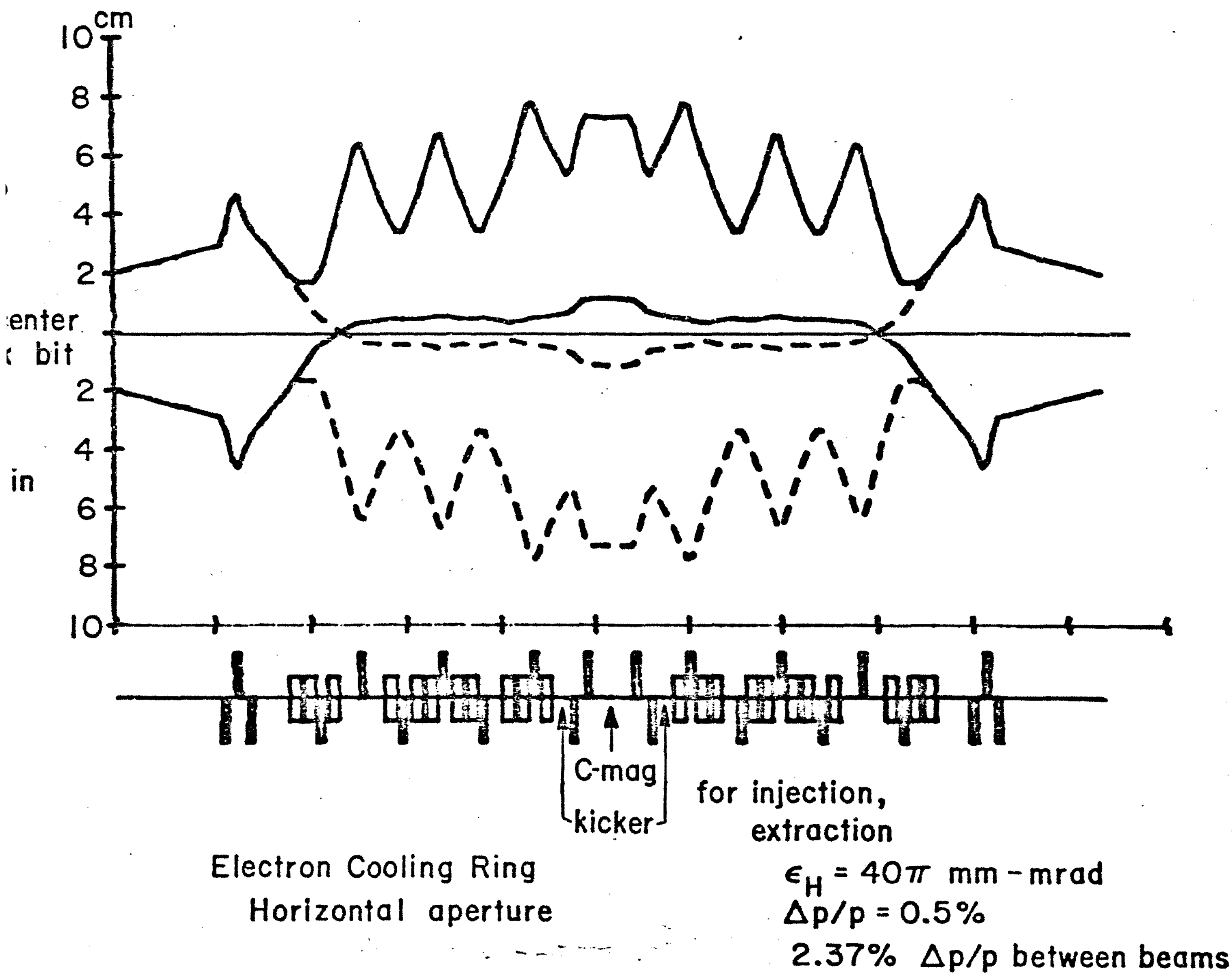

Fig. 5-2 Accumulator Horizontal Aperture Requirements

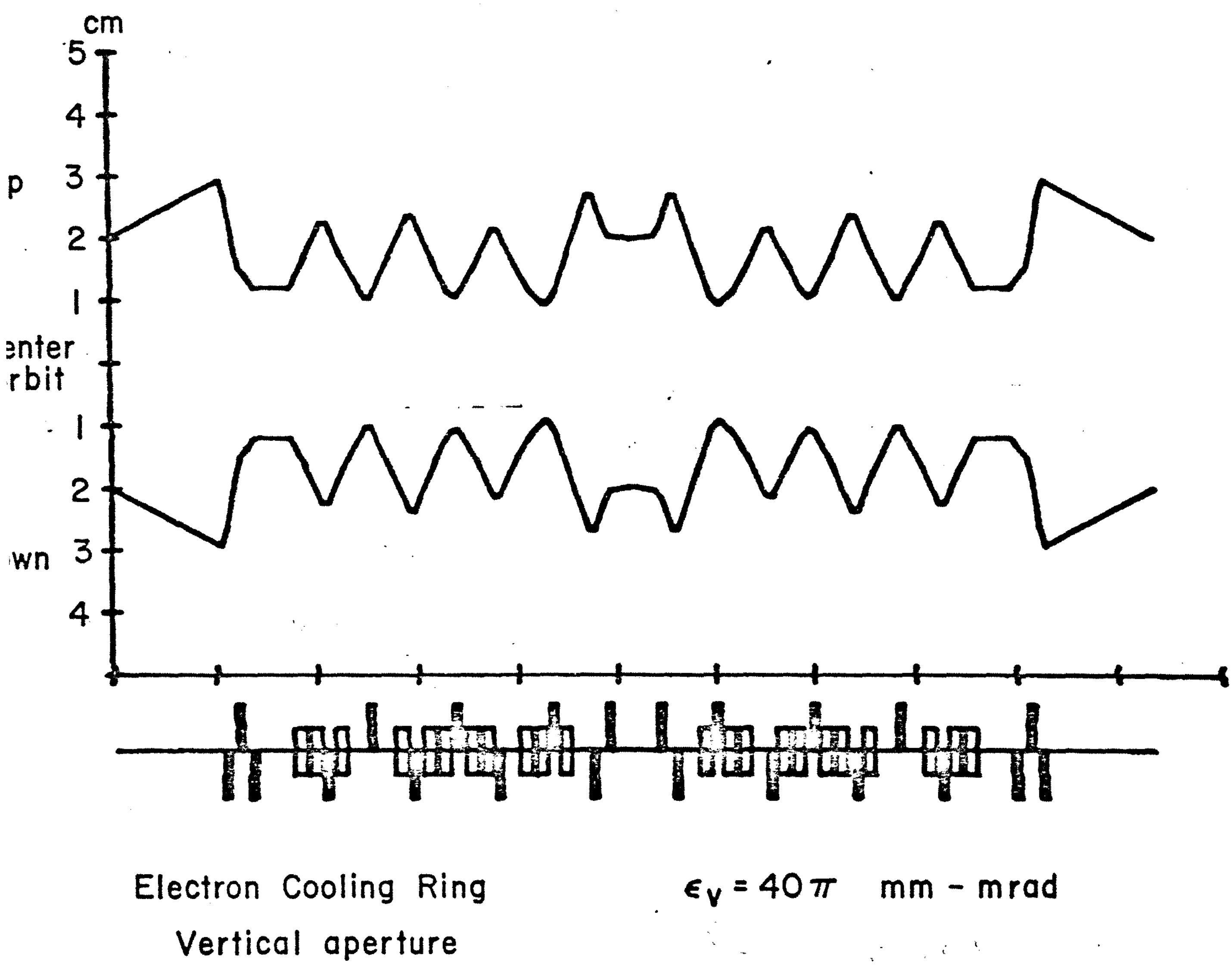

Fig. 5-3 Accumulator Vertical Aperture Requirements

TABLE 5-I ELECTRON COOLING RING ACCUMULATOR PARAMETERS

1. General

Energy	200 MeV - 1.0 GeV
Corresponding bend field	2.35 kG - 6.17 kG
Magnetic bend radius (ρ)	9.17 m
Radius	32.35 m
	= 36/1113 MR radius
Revolution time	1197 - 775 nsec
Superperiodicy	
without electron beam	2
With electron beam	1
Focusing structure	Separated function
	FODO normal cell
Nominal working point	ν_H 4.102
	ν_V 5.367
	γ_T 4.084
Natural chromaticity	ξ_H -6.460
	ξ_V -6.096

2. Magnets

Number of dipoles	44
Length of dipoles	48.00 in.
Effective length of dipoles	51.52 in.
Number of quadrupoles	44
Length of quadrupoles	24.00 in.
Effective length of quadrupoles	26.64 in.
Quadrupole gradients at 1.0 GeV	

QF	28.70 kG/m
QD	-26.47
Q1	-37.89
Q2	43.82
Q3	-9.90
Q9	22.69
Q10	-28.84
Q11	15.07

3. Structure

A. Curved section

Elements in curved section		Length
Dipole	(B)	4 ft
Quadrupole	(Q)	2 ft
Drift space	(O)	1 ft
Drift space	(OO)	2 ft

Cell structure
(QD) 0 (B) 0 (B) 00
(QF) 0 (B) 0 (B) 00

Cell length	28 ft

B. Short straight

Drift space	(SS)	6.90 ft
Drift space	(S1)	3.40 ft
Drift space	(S2)	6.56 ft
Drift space	(S3)	5.77 ft

C. Long straight

Drift space	(LS)	31.80 ft
Drift space	(L1)	2.00 ft
Drift space	(L2)	2.62 ft
Drift space	(L3)	12.00 ft

D. Dispersion suppressor

Drift space	(D1)	1.10 ft
Drift space	(D2)	6.90 ft

E. Quadrant structure (Q)

SS (Q11) S1 (Q10) S2 (B) 0 (Q9) 0 (B) 0 (B)
S3 (QD) 0 (B) 0 (B) 00 (QF) 0 (B) 0 (B)
00 (QD) D1 (B) D2 (QF) D2 (B) D1 (QD) 0 (B)
0 (B) L3 (q3) L2 (Q2) L1 (Q1) LS

F. Ring structure

Q ($\bar{Q}$) Q ($\bar{Q}$)

Length of central orbit — 203.2296 m, 666.76 ft

4. Aperture and Acceptance

Nominal vacuum chamber aperture	$a_H = \pm 89$ mm
	$a_V = \pm 25$ mm
sagitta	21.8 mm
available aperture	$a_H = \pm 78$ mm

Lattice functions

	Maxima	In dipole	L.S.	S.S.
β_H	48.23 m	19.50 m	12.93 m	10.37 m
β_V	19.44	13.25	10.11	11.48
η_H	3.65	3.65	0.06	3.51

Acceptance (using beam size in dipoles)

$a_V = \pm 25$ mm $\qquad A_V = 47\ \pi$ mm-mrad

$a_H = \pm 78$ mm $\qquad A_H = 40\ \pi$ mm-mrad

$\Delta p/p$)beam = $\pm$ 0.25%

$\Delta p/p$(beam-to-beam) 2.37%

(This is the acceptance for two beams as given with a separation of 10 mm at an injection kicker.)

5. Beam angles in electron cooling long straight section

$\theta_{11} = \sqrt{\varepsilon/\pi\beta^*}$ LS $\qquad \theta_H = 1.76$ mrad

θperp $\backsim \gamma\ \Delta p/p$ $\qquad \theta_V = 2.17$ mrad

θperp = 6 mrad - 10 mrad

Precooler ring.

Precooler ring. Finally, two 5-ft kickers with movable shutters and one 5-ft C-magnet are required for injection and extraction. These need to reach fields of 380 G and 2.4 kG, respectively, at an antiproton energy of 450 MeV.

5.1.2 Layout. The accumulator is located south of the Precooler, with the beam line in the South straight section of the Precooler separated from the beam line in the North straight section of the accumulator by 2 m. At this junction, they are in a common building (see Chapter 7).

The North short straight section is occupied by the components for transfer to and from the Precooler described in the previous section. The West straight section is occupied by electron cooling equipment. The first harmonic rf system is small enough that it can be located in a short straight section. Fig. 5-4 is a layout of the Accumulator ring.

5.2 Injection

Injection into the accumulator is a simple single-turn matter, with the 5-ft kicker and 5-ft C magnet described in section 5.1.1.

5.3 Magnets

The Accumulator magnets will be taken from the present Electron Cooling Ring. The 20 additional dipoles and 16 additional quadrupoles will be built from the existing lamination dies and coil forms. The present magnets have shown themselves to be very reliable (none have failed) and of excellent field quality. Measured fields are shown in Figs. 5-5 and 5-6.

5.4 Electron Cooling System

5.4.1 Equipment Description. The Electron Cooling System is basically similar to the one in present use. Its design parameters are given in Table 5-II, and Fig. 5-7 shows an over-all view.

Except for problems of reliability, the existing electron cooling system would be adequate for accumulation at 200 MeV. Our experience tells us that:

(i) a new solenoid design must be adopted to eliminate failures and cooling limitations in the existing units and,

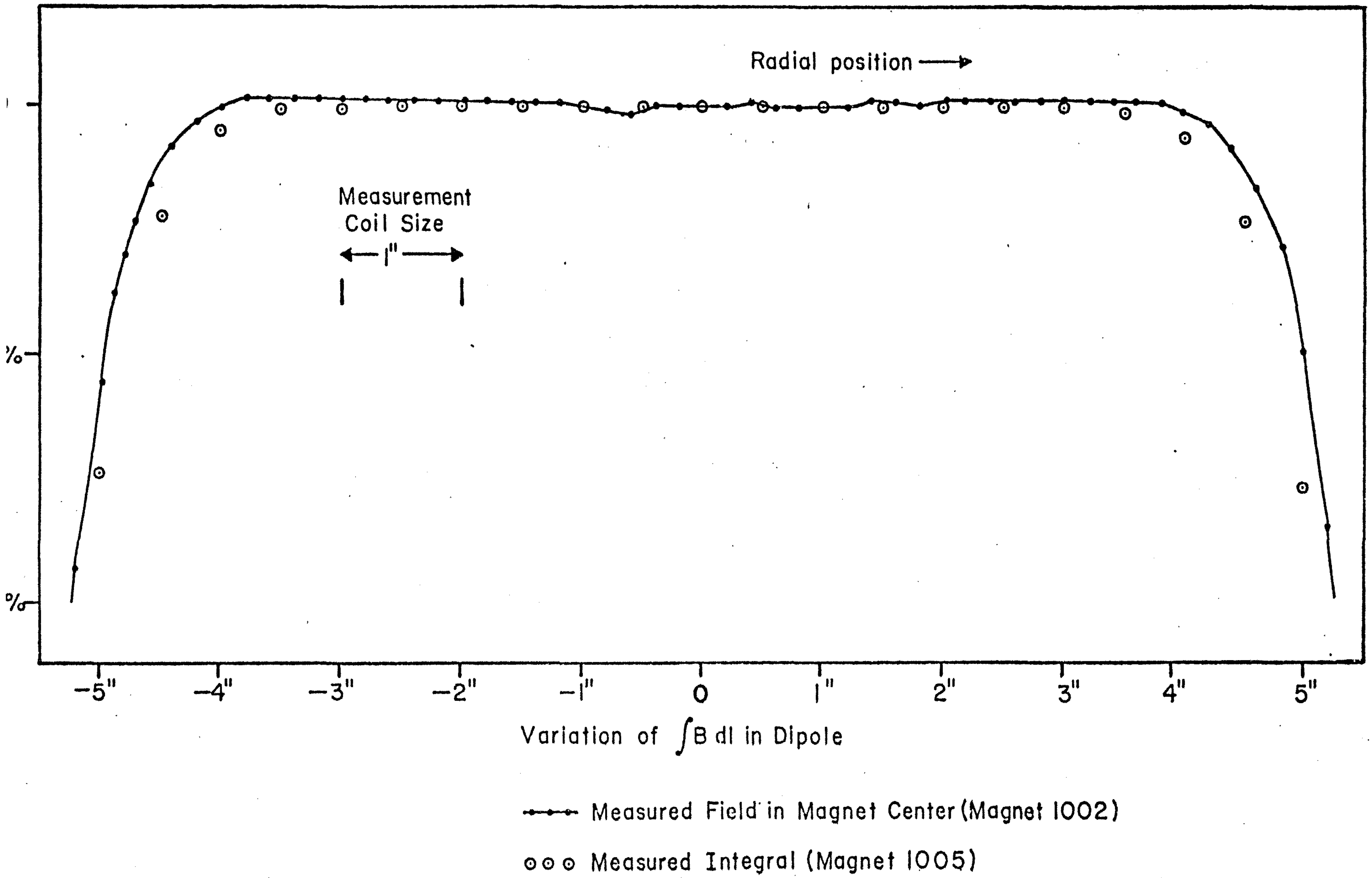

Fig. 5-5 Measured Accumulator Dipole Fields

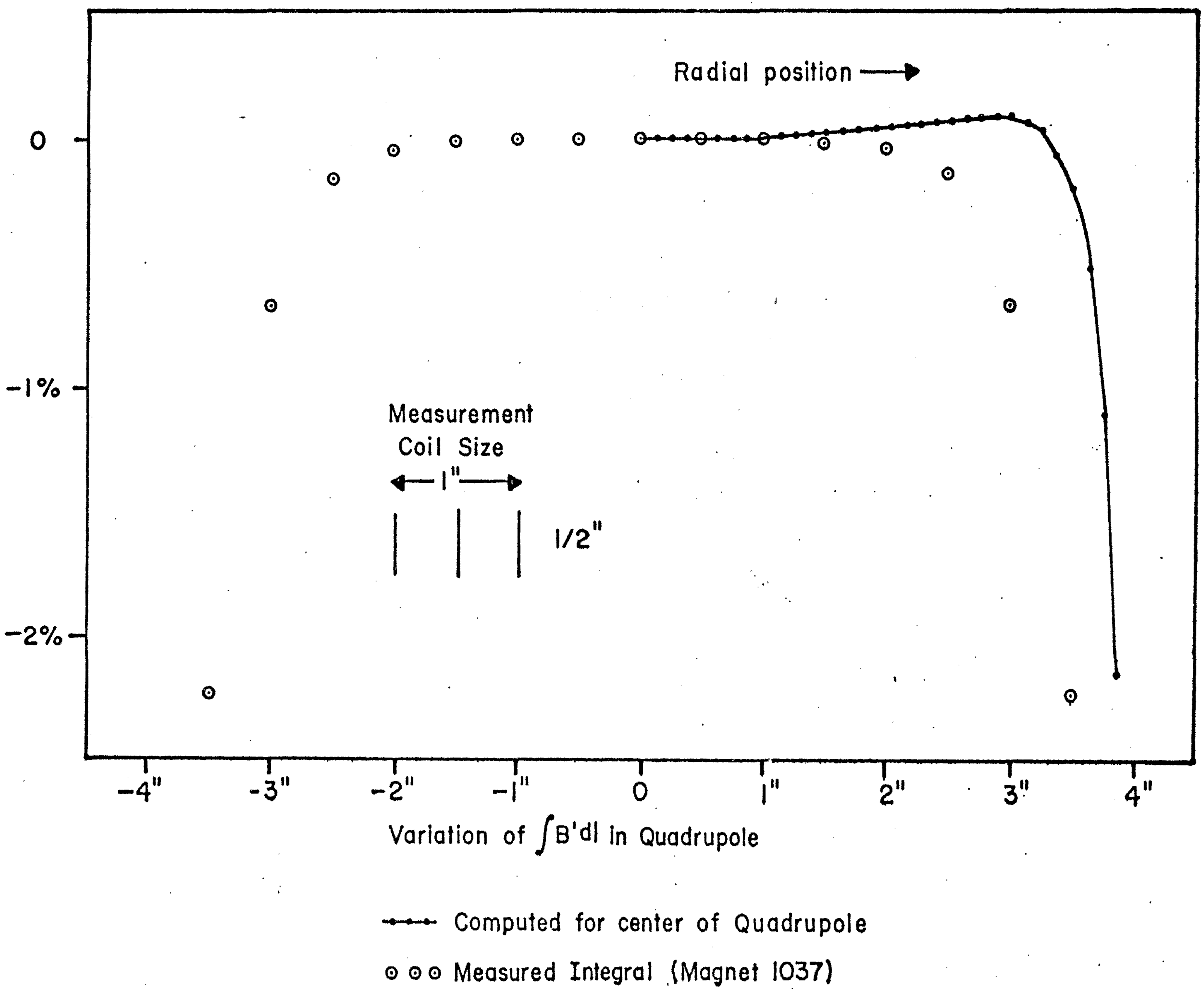

Fig. 5-6   Measured Accumulator Quadrupole Fields

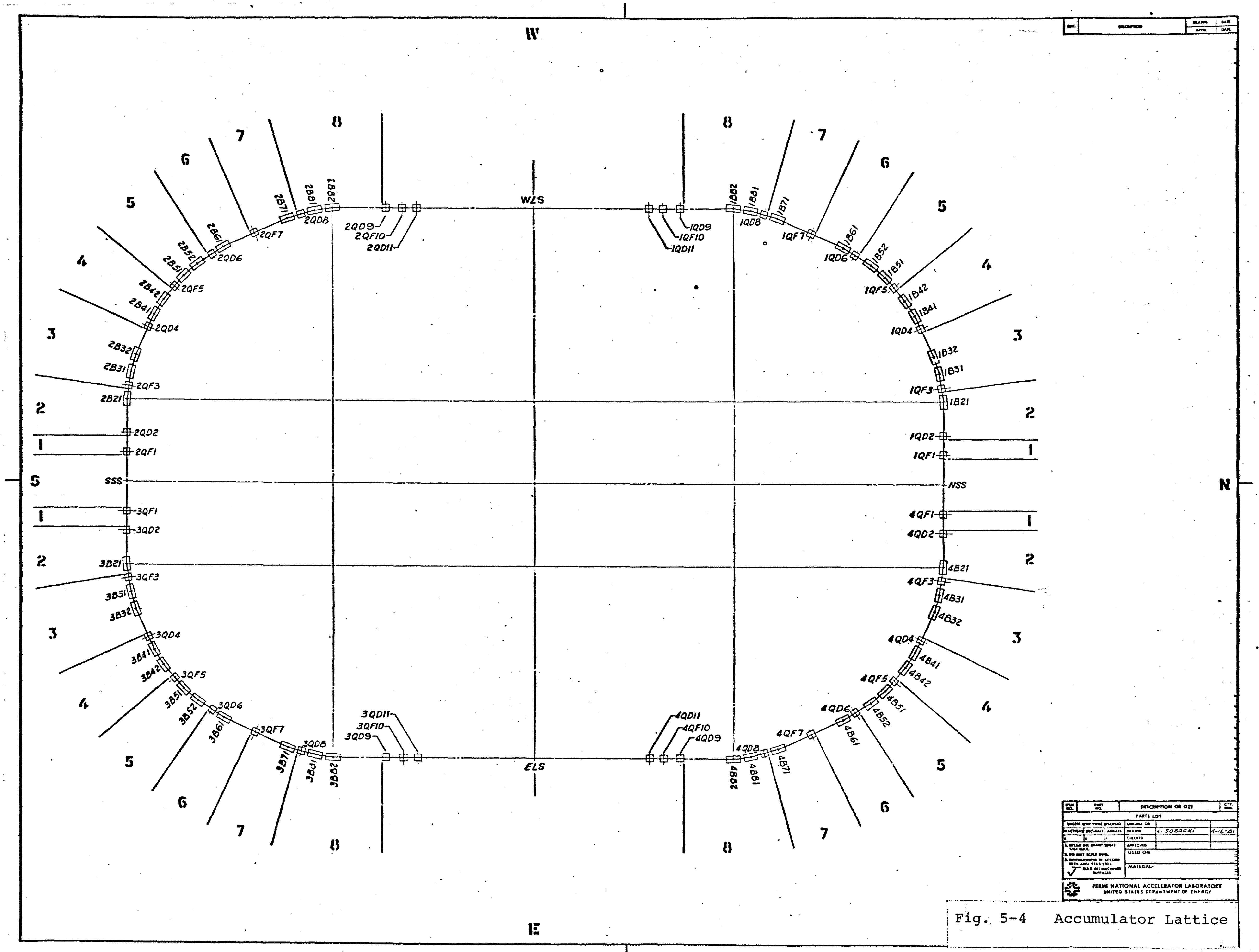

Fig. 5-4 Accumulator Lattice

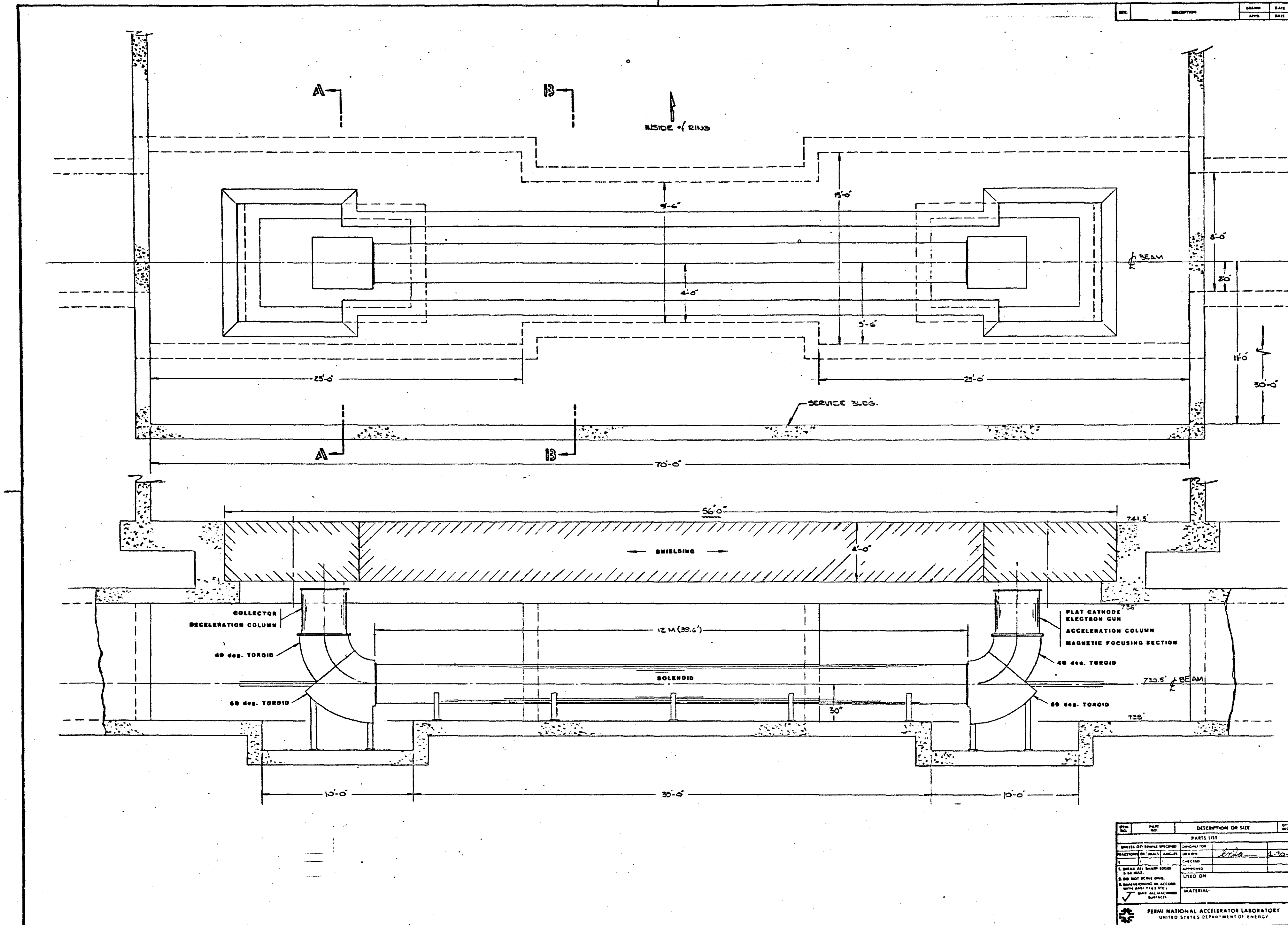

Fig. 5-7 Electron Cooling System

TABLE 5-II ELECTRON COOLING SYSTEM DESIGN PARAMETERS

Beam Current (max)	10A
Cooling Length	12m
Overall Length	16m
Solenoid Guide Field (max)	2kG
Magnet Power Requirement (1.5kG)	120 kW
Collection Inefficiency	$<10^{-3}$
Cathode Diameter	5cm
Beam Diameter (int. region)	5-10cm
High Voltage Supply Power (max)	
collector	3kW
gun	2.5kW
Gun Perveance	1.5 μperv
High-Voltage Insulation	SF6 (atmospheric)
High-Voltage Switching Range	0-10kV (@220kV)

(ii) the high-voltage terminals and columns at the gun and collector ends ought to be accessible for maintenance without breaking the high-vacuum system.

A new solenoid is needed in any case because the length is greater (12 m vs. 5 m for the existing one) and several designs have therefore been developed for constructing long, highly uniform solenoids. The second criterion is one reason for proposing that the cooling system be built with electron gun and collector totally immersed in the solenoid guide field. This allows removal of enough of the solenoid (by sliding off the ends) for direct inspection, baking of the high-voltage section, and modification or repair. The toroid and solenoid-to-beam pipe clearances are also to be made larger. Both gun and collector will be on the same side of the beam. A doglegged gun and collector (as in the existing system) cancels certain abevration of the $\overline{p}$ lattice, which we believe will be managable with electron beams of less than 10A.

The upgrade from our existing equipment will include major improvement of the high-voltage supply. The basic supply is apparently adequate for reliable 220-kV operation. Most of the control and regulation circuitry needs replacement or rebuilding. The significant new capability that must be built into the supply is to switch rapidly (< 100 msec) between stack energy and injection-ejection energy. At 400 MeV (218 keV electron energy), this will be an 8.5 kV change, which will be supplied by a new programmable supply floating at cathode potential.

The other important motivation for building a new electron cooling system is to perform accumulation at higher energy than 200 MeV; for which the existing system is designed. With electron beams greater than 10A at 0.5A/cm^2, one is near to having cooling times limited by longitudinal electron temperature due to space charge (unless the space charge is exactly neutralized). If we take 10A as a resonable current limit, a 5% fraction of the Accumulator circumference (12 m) must contain electron cooling to achieve the desired cooling times at 400 MeV (see table 5-III).

TABLE 5-III ELECTRON COOLING SYSTEM PERFORMANCE PARAMETERS

Beam Current	10A
Fraction of Accum. Circumf. Cooled	5.9%
Transverse Electron Temperature	0.25eV
Longitudinal Electron Temp (max)	0.1eV
T_1 (200 MeV)	1.5 sec
T_1 (400 MeV)	6.3 sec
T_2 (200 MeV)	0.98 sec
T_2 (400 MeV)	3.4 sec

It may be argued that even higher energy electron cooling is feasible with this 12 m interaction constraint. Keeping these possibilities open dictates much of the system design. A higher guide field is needed in proportion to electron momentum to maintain the same low transverse electron temperature. The solenoid in particular is to be designed for greater heat dissipation. A cathode totally immersed in magnetic field was chosen to give the lowest electron temperatures at higher voltages, as well as allowing smaller high-voltage terminals. These features allow transverse temperatures comparable to those obtained at 110 keV (200 MeV) in the existing device up to beam energies of 750 keV (1.4 GeV).

All supplies and signal lines come directly up into the surface service building. All heavy components will be serviced by lifting up. Two important features are dictated by this: The 90^0 toroidal bends (as contrasted to the CERN or Novosibirsk design of 45^0); and the U configuration of gun/collector.

5.4.2 Electron Cooling and Accumulation Rates. The electron cooling system used for accumulation is assumed to be operating in an ideal manner (i.e., full theoretical damping rates). Cooling takes place in two essentially decouples (largely thanks to the highly nonlinear fall off of electron "friction" force with relative momentum), regions of longitudinal phase space, even though the cooling system is in a dispersion-free section. Sections 5.5 and 5.6 give more detail about the stacking and unstacking processes. Two distinct doses of electron cooling are applied for the stacking cycle.

First the fresh hot batches of $\bar{p}$'s are cooled for a time T_1 immediately upon their injection into the Accumulator. The exact value of T_1 depends critically on the phase-space area of the hot beam, the exact manner of approach of the rf stacking bucket to the stack, and the relative height of the stacking bucket to the stack height. The cooling decrement necessary is from 2 to 4 (for 95% of a Gaussian in momentum). For one e-folding, values of T_1 are shown in Table 5-III. It is important to note that for an anticipated 40π x 40π beam emmittance T_1 is dominated by the relative transverse $\bar{p}$ momenta.

The cooled fresh beam is then moved by rf (see section 5.5) 2% to the stack. It may be desirable to form the rf buckets while the T_1 cooling is in progress. The gun high voltage is then stepped by 8.5 kV (for 400 MeV $\bar{p}$) so that it arrives at the stack ahead of the moving bucket. (It requires 240 nsec to move 2%). If the stacking is entirely adiabadic (no dilution), then it is clear that the stack must be cooled by a factor 2 (for time T_2) after each stacking, for a factor 2 cooling during the T_1 step. Alternatively, the fresh beam could simply be parked continguously in momentum next to the stack, with the merging accomplished by electron cooling. Here again, the minimum cooling factor necessary is 2 during T_1 and 2 during T_2.

It is not necessary that the stack be maintained during accumulation in a highly condensed state (ultimately determined by equilibrium with inter-beam scattering). A stack momentum width of $\pm$ 1.0 x 10^{-3} is sufficient and in fact optimal for the cycles described above. The final, ultimate degree of cooling need not be applied to the stack at all. This can be performed after accumulation, on each third of the stack at the ejection energy (see section 5.5.2). Keeping the stack relatively warm allows us to ignore interbeam-scattering effects; for instance, the stack will not appreciably blow up when it is left naked during the T_1 step.

Although an optimum stacking cycle requires about the same factor of momentum cooling of the fresh beam (T_1 step) and, subsequently, the stack (T_2 step), this does not mean thaat T_1 = T_2. The stack cooling step operates on already transversely cooled particles. Since the 40π transverse emittance dominates T_1, this is an important effect. For our conditions we expect T_2 will be one-half to one-third of T_1.

All expected cooling times for the stacking cycle outlined are shown in Table 5-III. Accumulation to $\bar{p}$ energy up to 400 MeV is possible within an 11 sec cycle. We are developing an exact simulation of the cooling/stacking to predict the maximum accumulator enery allowed by this constraint.

5.5 RF Stacking and Unstacking

5.5.1 Injection and Stacking. Antiprotons are injected into the injection orbit of the Electron Accumulator with a kinetic energy of 204 MeV, and momenum spread ± 2.26 x 10^{-3}. The slightly bunched beam is allowed to debunch and is immediately electron-cooled to a momentum spread of 10^{-3}. This results in a total energy spread of $E\beta^2\Delta p/p$ = 372 keV. The rotation period is 1.19 x 10^{-6} sec, resulting in a longitudinal emittance of 0.44 eV-sec. The injected beam is then captured adiabatically in an h = 1, f = 841.36 kHz rf bucket with area 0.5 eV-sec. This results in a phase-oscillation period of 4.3 msec. Adiabatic capture shold be completed in about 25 msec.

The captured beam is decelerated 8.65 MeV to a stacking orbit at 195.35 MeV. This requires a frequency swing of 12.35 kHz. Deceleration will be done with a synchronous phase angle of 5.74 degrees, resulting in a moving-bucket area reduction of 0.82. Constant bucket area is maintained by raising the rf voltage to 427 volts. The accelerating voltage is 427 sin ϕ_s = 42.7 volts per turn, or 35.9 MeV per second, so the stacking requires 0.24 seconds.

In order to minimize the effect of the moving rf bucket on the existing antiproton stack, the rf voltage can be reduced to a very small value well before the momentum reaches the stack momentum, but at momentum sufficiently close so that electron cooling can pull the released antiprotons into the stack.

5.5.2 RF Unstacking and Extraction Antiprotons are to be removed from the cooled stack for extraction by rf unstacking at harmonic-number one. If, for example, three final bunches of antiprotons are desired, a moving bucket with area slightly greater than one-third of the total stack area (longitudinal emittance) is created at the center of the stack and removed at a constant acceleration rate. If the cooled stack has a total momentum spread of 10^{-3}, then the longitudinal emittance will be 0.433 eV-sec and the stack energy spread will bl be ± 179.25 KeV. The synchronous phase angle is 19.27 degrees and the bucket requires application of 100 volts at 827.897 KHz (instantaneous frequency). The acccelerating voltage V sin ϕ_s will be 33 volts per turn or 27.3 MeV/sec, so acceleration by the required 8.65 MeV will require 317 msec.

At approximately 18 msec, the moving bucket has moved 480 kV above the stack and the stack has become sufficiently smooth that it is possible to measure the charge that has been removed by the moving bucket by observing the image current induced in a ring current detector of sufficient bandwidth. This charge is compared with the desired value and the bucket area, which was intentionally slightly too large, can be reduced so that it carries only the intended charge. The charge which is removed from the bucket is sufficiently close to the stack momentum so that it is cooled back into the stack by the electron beam.

Subsequent unstacking buckets will be required to enclose different fractions of the remaining charge, the last one being just adiabatic capture of all of the remaining charge.

After the unstacked charge fractions have been moved to the extraction orbit, it will be necessary to change the electron energy so that the unstacked fraction of the beam can be cooled before extraction. In order to achieve acceptable antiproton bunch lengths at 1 TeV, it necessary that the bunches have longitudinal emittances substantially less than 0.1 eV sec at the start of the several-stage acceleration process. Each extracted bunch will be cooled to an admittance of 0.06 eV-sec just prior to extraction.

After each bunch has been placed in the extraction orbit at 204 MeV, the rf voltage must be raised to a level such that the bunch length will match an rf bucket in the precoder at h=14, 5.01 MHz. Since the h = 14, buckets are 200 nsec long, a total bunch length of 180 nsec is adequate. A 0.06 eV-sec bunch 180 nsec long will have an energy half-height ΔE = 212 keV, matched to a bucket with half-height 907 keV. At h = 1, the required bucket is generated by raising the rf voltage to 3.4 kV. The phase-oscillation period in the final extraction bucket is 1.25 msec, so the adiabatic bunching should be accomplished in about 8 msec.

All rf voltages in the Electron Ring are to be generated by a single ferrite-loaded low-Q cavity capable of generating precisely controlled frequencies, phases, and voltages up to 5 kV at harmonic number one.

6. Colliding Scenario

6.1 General Plan. At present, the Fermilab accelerator operates at slightly greater than 2.5 x 10^{13} protons per pulse with about 1080 bunches (i.e. 1080 of the 1113 main ring buckets occupied). This results in an average proton number per bunch of about 2.5 x 10^{10}. In order to achieve the required 10^{11} protons per bunch, it is proposed that the protons in several groups of four adjacent bunches (quartets) be coalesced and re-captured in normal (h=1113) buckets before injection into the Tevatron. Injection into the Tevatron will be done at 150 GeV, so it is reasonable to do the bunch coalescence at fixed magnetic field at 150 GeV just before injection. It is preferable to do the bunch coalescing at relatively high energy rather than at injection energy (8 Gev) for several reasons: The beam size is smaller relative to the available aperture, the ratio of longitudinal emittance to available rf bucket area is favorable, and the necessity for accelerating heavily populated bunches through transition is eliminated. The advisability of avoiding transition crossing with dense bunches has also been noted in experiments of a similar nature at CERN.

Since it is possible to select which buckets will contain a significant number of protons by selectively expelling unwanted protons before acceleration, the required number of quartets can be established at the desired azimuthal locations before beginning the acceleration cycle. This procedure is absolutely necessary. In order to coalesce the adjacent bunches, it is necessary to reduce their momentum spread to the minimum possible value by lowering the rf amplitude to an extremely small value. If a large fraction of the buckets contain proton bunches, the resultant beam excitation of the high shunt-impedance accelerating cavities prevents lowering the voltage to the required value. Furthermore, it would be extremely difficult to remove the unwanted protons with sufficient precision at 150 GeV and if those protons were to remain in the accelerator, but not well contained in buckets, the injection process into the Tevatron would almost certainly quench the superconducting magnet.

6.2 Coalescing Scenario. The four step procedure for coalescing quartets is shown in Fig. 6-1. (The procedures described here are at 100 GeV instead of 150 GeV because we have well-established accelerator parameters at 100 GeV and the experiments are slightly less expensive in electric-power cost). Step I shows a series of h=1113 (53.102 MHz) buckets, four of which contain bunches of protons. The stationary bucket voltage is 1 MV, resulting in a bucket height of 144 MeV. It is assumed that each of the bunches has a longitudinal emittance of 0.3 eV-sec, consistent with recent measurements. These bunches, initially matched to a 1-MV bucket, will have a half-height of 46.7 MeV and a half width of 4 nsec, roughly as shown.

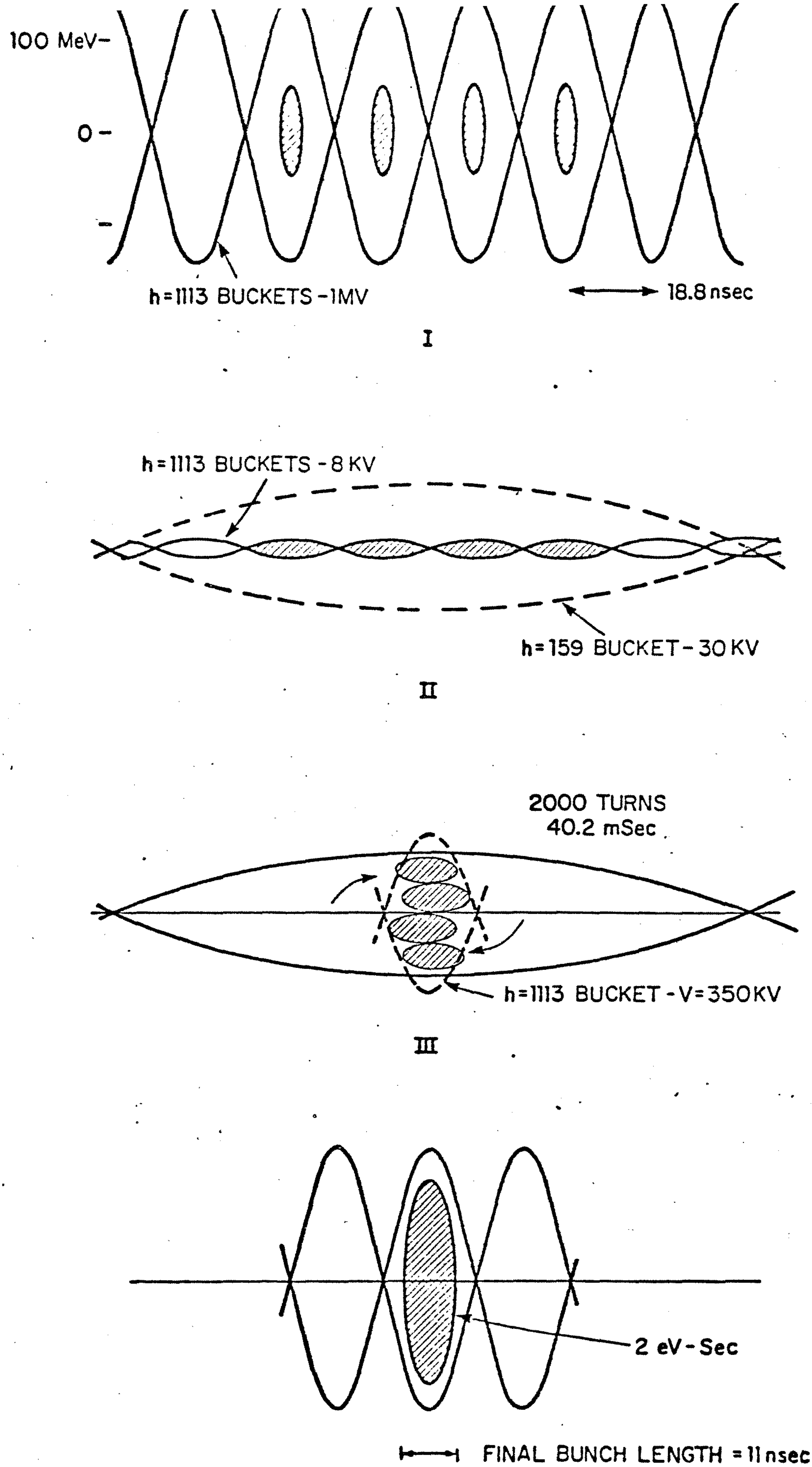

Fig. 6-1 Proton Rebunching

Step II shows the 0.3 eV-sec bunches matched to an rf bucket that has been reduced in amplitude until the bucket area equals the bunch area. The bunch and bucket height are now 12.5 MeV. Shown also in part II is a dashed line representing a subharmonic bucket encompassing seven of the original buckets. Because the original harmonic number h=1113=(3)(7)(53), a 7th subharmonic bucket (h=159) will remain fixed in phase with respect to the original buckets. (Had the original harmonic number been a prime, this subharmonic operation would have been impossible). The subharmonic bucket shown has a height ΔE=66 MeV, requiring the application of 30 kV at 7.58 MHz. When the h=1113 voltage reduction is complete, the voltage creating that bucket is removed and the h=159 voltage is applied suddenly at full amplitude.

Step III shows the proton distribution within the subharmonic bucket after slightly more than one-quarter of one synchrotron period. This requires 2000 turns or 41.8 msec. The distributions with larger momentum deviation are those which started farthest from the bucket center and have consequently lagged slightly due to synchrotron tune spread. Computer simulations of this rotation have established 2000 turns to be an optimum period for establishing the narrowest charge distribution. Initially the charge in the h=159 bucket extends over 4/7 of the bucket length. (In $\Delta\phi$, ΔW coordinates, $\Delta\phi=4\pi/7$ radians). In a 66-MeV bucket, this distribution should reach a maximum energy deviation of 66 $\sin(\Delta\phi/2)$=51.6 MeV. Computer simulations have verified that this indeed happens and the distribution shown in part III is a good representation of the simulation. The rotated charge extends in energy over approximately 104 MeV and in time over about 19 nsec so the phase space area covered is about 2 eV-sec. At this time, the h=159 rf voltage is removed and h=1113 buckets are re-applied at an amplitude which matches as well as possible the rotated distribution. The dashed line in part III represents a 2 eV-sec h=1113 bucket,requiring the application of 340 kV. Because we have coalesced an even number of bunches in an odd-numbered subharmonic bucket, the center of the coalesced bunches have moved azimuthally π radians from the original position and the re-applied h=1113 bucket must be shifted in phase accordingly or the coalesced bunch will arrive at the unstable fixed point.

Part IV of Fig. 6-1 shows the coalesced bunch distribution after the h=1113 rf voltage has been raised to 1 MV. The total bunch width of a 2 eV-sec distribution matched to a 3.36 eV-sec bucket (1 MV) will be 11 nsec and the energy half-height will be 114 MeV. At 100 GeV, this amounts to a total $\Delta p/p$ of 0.12 percent, small with respect to the momentum aperture of the ring, about ±0.5%.

A density dilution of about a factor of two has occurred in the process, so while the final energy half-height is 114 MeV as opposed to 47 MeV for the original bunches, the peak current, as indicated on a beam current detector, will have increased by only a factor of about 1.3.

After acceleration to 1 TeV, this distribution is to be stored in buckets generated by about 1.2 MV. At 1 TeV the 1.2 MV bucket height will be 495 MeV and a 2 eV-sec bunch, matched to such a bucket, will have a total length of 5.7 nsec.

Computer simulations were done also for coalesence of five adjacent bunches in a seventh subharmonic bucket. In that case, all of the center three bunches and about half of each of the outer two bunches could be recaptured, so there is no advantage over coalescing four bunches.

7. Buildings and Structures

7.1 Below-Ground Structures

The existing Target Vault and $\bar{p}$ Hall will be utilized with minor modifications. Summed over the injection and extraction lines, the Precooler, and the Accumulator, the total tunnel length in the project is approximately 3000 ft. Included in this total are several different kinds of tunnels and special sections, which are as follow:

(i) Regular tunnel. The Precooler and Accumulator quadrants are both an 8 ft by 8 ft cross-section tunnel, with the ring center line 2 ft from the larger-radius wall. The tunnels will be cast to follow the wanderings of the rings. A Precooler quadrant is shown in Fig. 7-1 and the entire Accumulator tunnel is shown in Fig. 7-2.

(ii) The long straight sections of the two rings will be housed in special structures designed for the functions in these straight sections.

(a) The South straight section of the Precooler, shown in Fig. 7-3, will have the largest span (18 ft) and the longest length (120 ft). The functions here are similar to those in the Main Ring Transfer Hall. Equipment layout in the south straight section was shown in Fig. 4-15. The tunnel is widened upstream for the junction with the 4.5-GeV injection line. Tunnel cross sections are also shown in Fig. 7-3.

(b) The North straight section contains the 5-9 MHz and the h=1 rf system at its upstream end. It contains the 200-MeV test beam injected into its downstream end. If a stochastic accumulator ring is built in the future, transfer between it and the Precooler will take place in this straight section. The structure surrounding it, also shown on Fig. 7-3, is only slightly enlarged from the regular tunnel because these functions require only moving space for component installation. The equipment is shown in Fig. 4-6.

(c) The East straight section contains stochastic kicker and associated power amplifiers and the 8-GeV extraction line. These components necessitate a tunnel widening, as is shown in Fig. 7-4. There is space between electronics racks for access to the ring and for addition cooling power. The equipment is shown in Fig. 4-7.

(d) The West straight section contains stochastic pickups (which have only small electronics associated with them) and the 53-MHz rf system, located at the upstream end, as shown in Fig. 4-5. The tunnel is widened at this end, as is also shown in Fig. 7-4, to give access to the rf cavities and associated electronics equipment and widened at the other end in case more rf is needed at some later time.

(e) The west straight section of the Accumulator will contain the electron cooling equipment.

(f) The injection tunnel will be 6 ft by 8 ft in cross section, joining the Precooler as shown in Fig. 7-5. An access to the surface will be provided as shown. This beam line rises from the 726-ft 8 in. level of the injection line.

(g) The 8-GeV extraction line will join the injection line in a 50-ft stub shown in Fig. 7-5. The three manholes shown will contain focusing magnets for the FODO extraction line, as described in section 4-9.

7.2 Above-Ground Structures

Service buildings will be provided at each long straight section. The North, East, and West straight sections require only buildings of approximately 1440 ft^2 (gross) and personnel accesses down to the ring. The same is true of the East Accumulator straight section.

The South Precooler straight section will contain power supplies, assembly space, equipment and personnel access, and accelerator control facilities. A structure of 3000 ft^2 gross space is planned.

The West Accumulator straight section will contain power supplies and equipment for the electron cooling system and will require a structure of apporximately 2000 ft^2.

7.3 Utilities and Roads

Existing electric power and cooling water will be utilized and only short feeders are required. No gas service to the project is planned. The roads to be built are shown in the general site plan of Fig. 1-1.

8. Experimental Areas

Two interaction regions have been designed for experiments at the collider, one at B0 and the other at D0.

8.1 B0 Experimental Area

The experimental area at B0 will serve the detector to be built by the Colliding Detector Facility, a collaboration of Italian, Japanese and U.S. laboratories. The scale of the project is set by their proposed apparatus, in particular the Central Detector, whose transverse dimensions determine both the depth of the building and its overall width. The area is divided into 2 distinct regions, the Collision Hall, where the experiment is actually performed and the Assembly Area, where the entire apparatus will be constructed and serviced, and where the Central Detector will be stored during operation of the Tevatron fixed-target program. A bypass is provided around the outside of the collison hall for traffic servicing the Main Ring and the Tevatron. It should be noted that the engineering challenge posed by the weight of the detector and the earth pressure on the walls of this underground area is unique in the history of Fermilab. In general, the building is a concrete structure; the floor which carries the detector is a concrete mat about four feet thick. Plan and elevation views of the B0 area are shown in Figs. 8-1 and 8-2.

The central volume of the Collision Hall which houses the Central Detector and a pair of forward-backward toroids is 50 ft long by 50 ft wide and at its deepest point 40 ft high, dimensions set directly by the detector and its requirements for in-place servicing. Extended forward-backward detectors sit in the volumes at either end of the collision area. Since these devices are smaller transversely than the Central Detector, these sections are 35 ft wide by 30 ft high and 25 ft long; their floor level is raised 5 ft from the central region.

The Assembly Area is separated from the Collision Hall by a 35 ft long tunnel whose tranverse size is the minimum needed for passage of the Central Detector. When the accelerator is operating, the tunnel is plugged at the Collision Hall end by a (retractable) 12 ft thick concrete wall. This thickness of radiation shielding is sufficient to allow people to work in the Assembly Area while the Tevatron is running for fixed-target physics.

The Assembly Area consists of three parts, an underground assembly area (at the same level as the Collision Hall), an above-ground construction area, and two floors of electronics, computer and control rooms for the detector on the side closest to the Collision Hall. The area is served by a 50-ton crane that runs the entire length of the building.

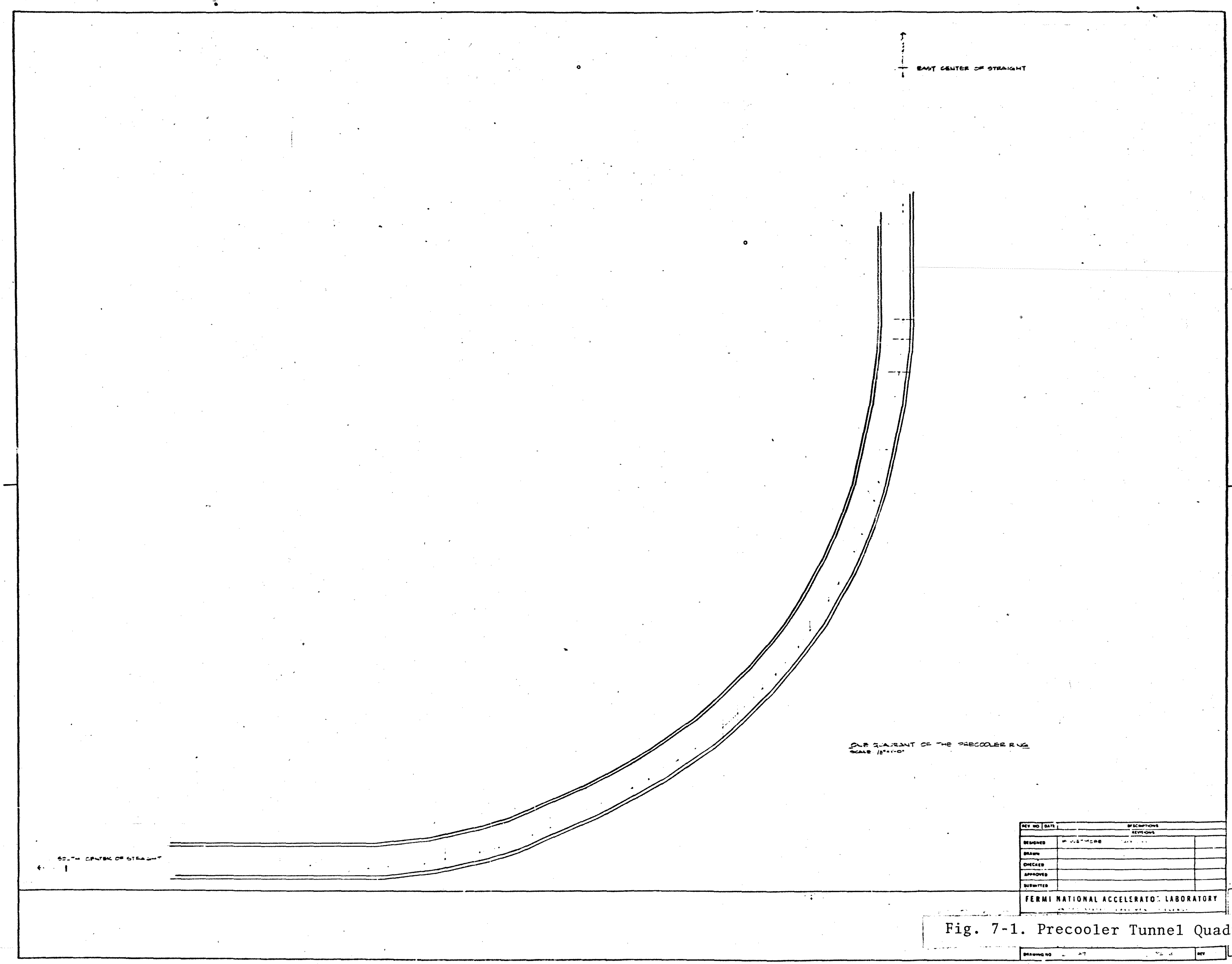

Fig. 7-1. Precooler Tunnel Quadra

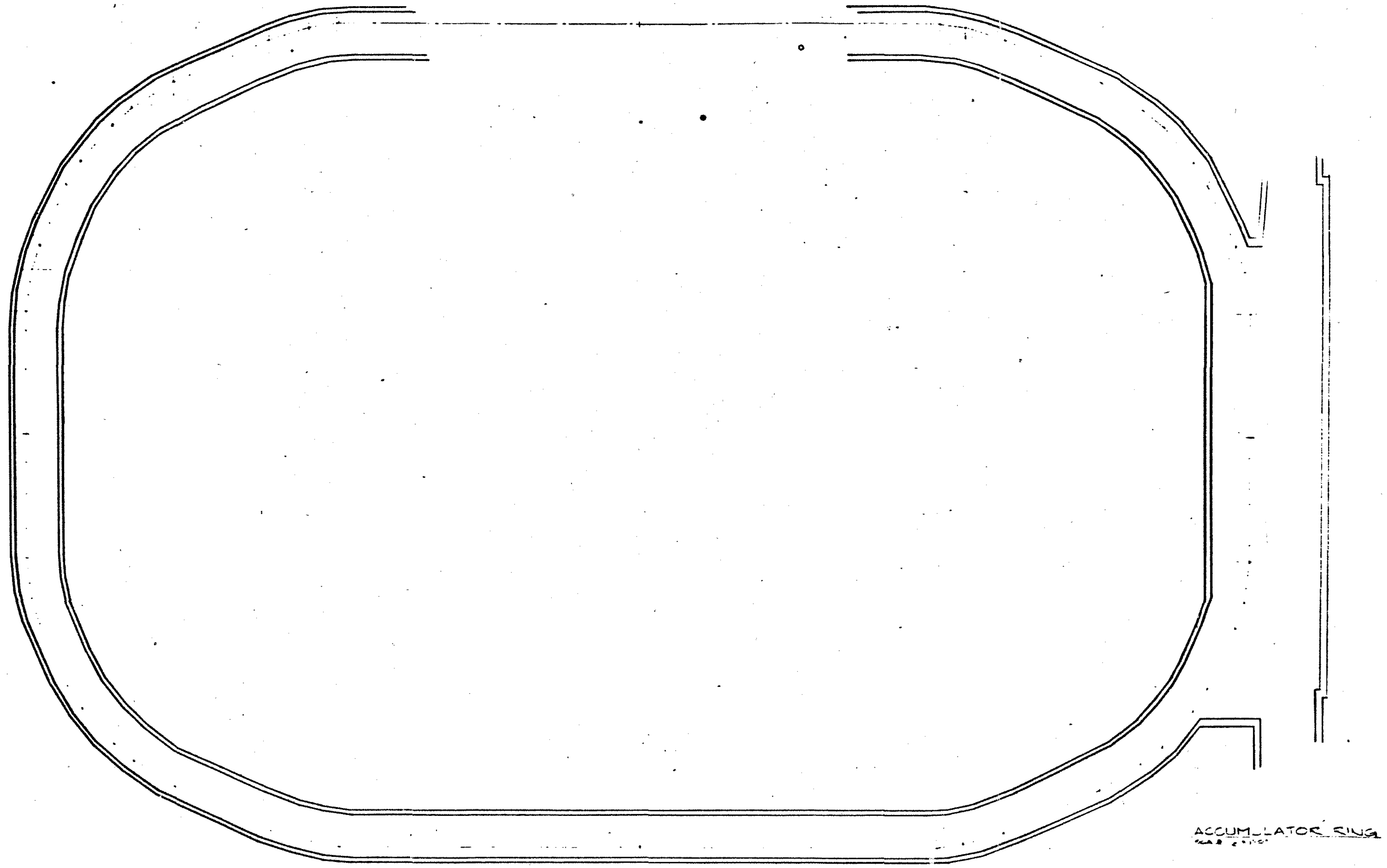

Fig. 7-2 Accumulator Tunnel

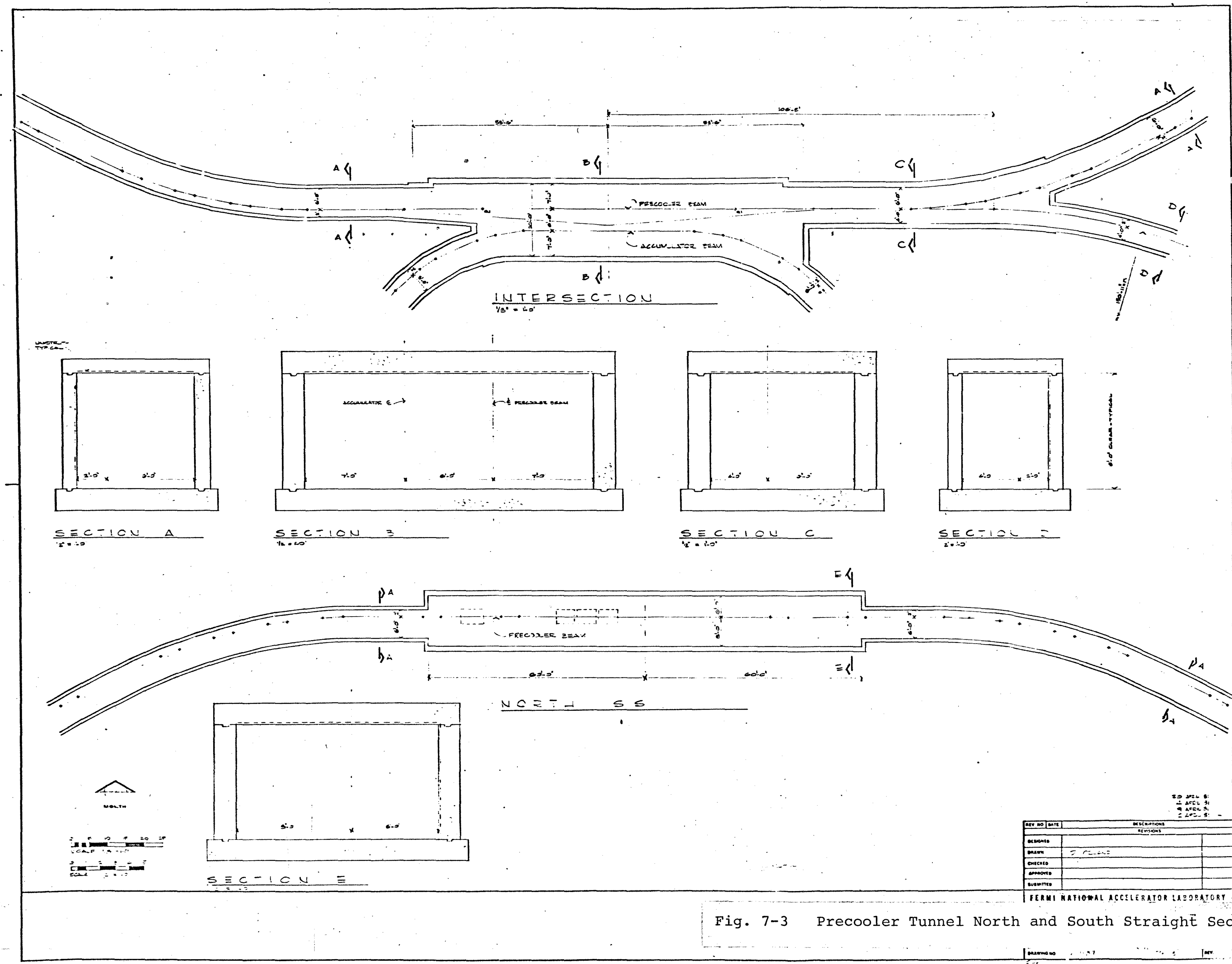

Fig. 7-3 Precooler Tunnel North and South Straight Sections

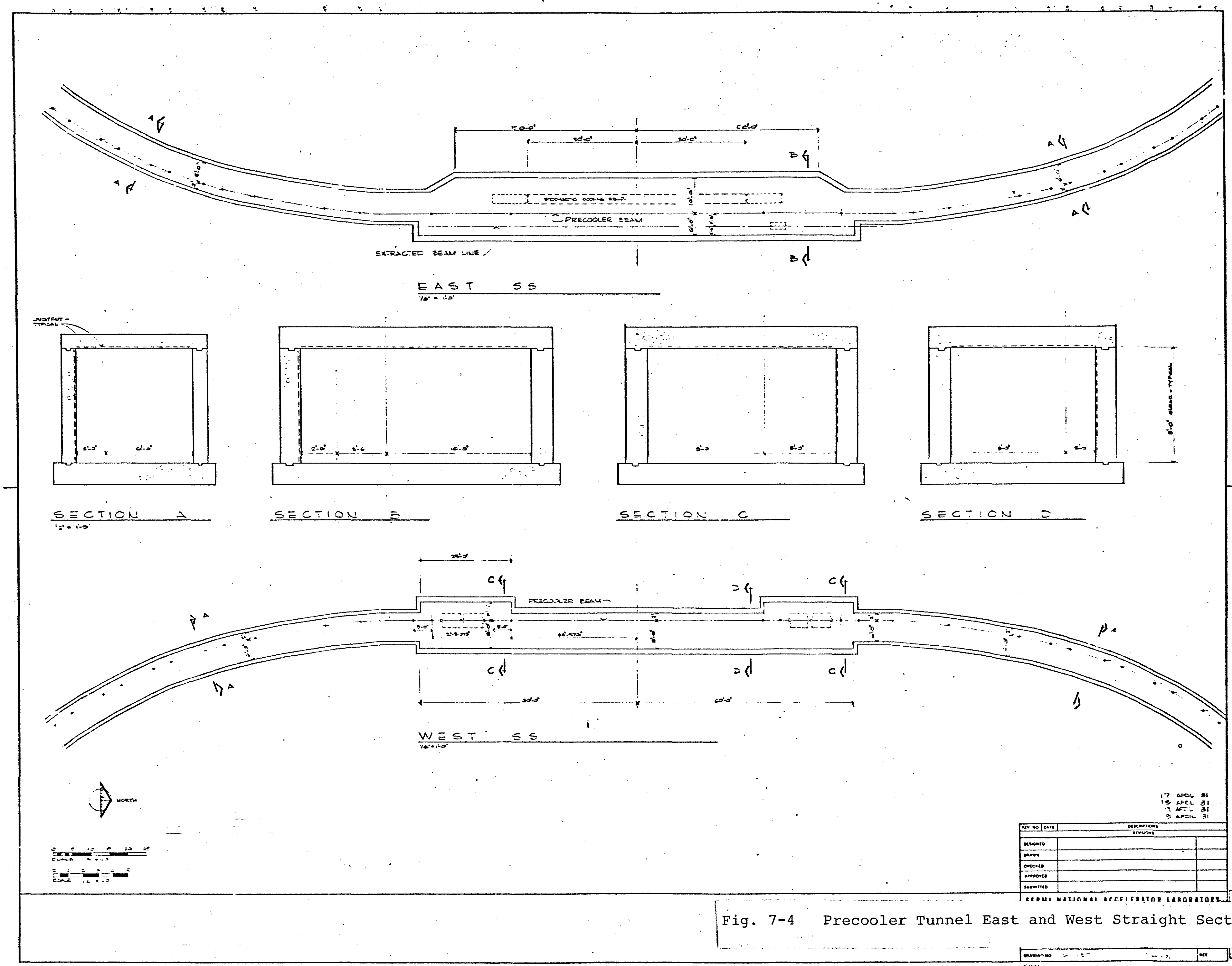

Fig. 7-4 Precooler Tunnel East and West Straight Sections

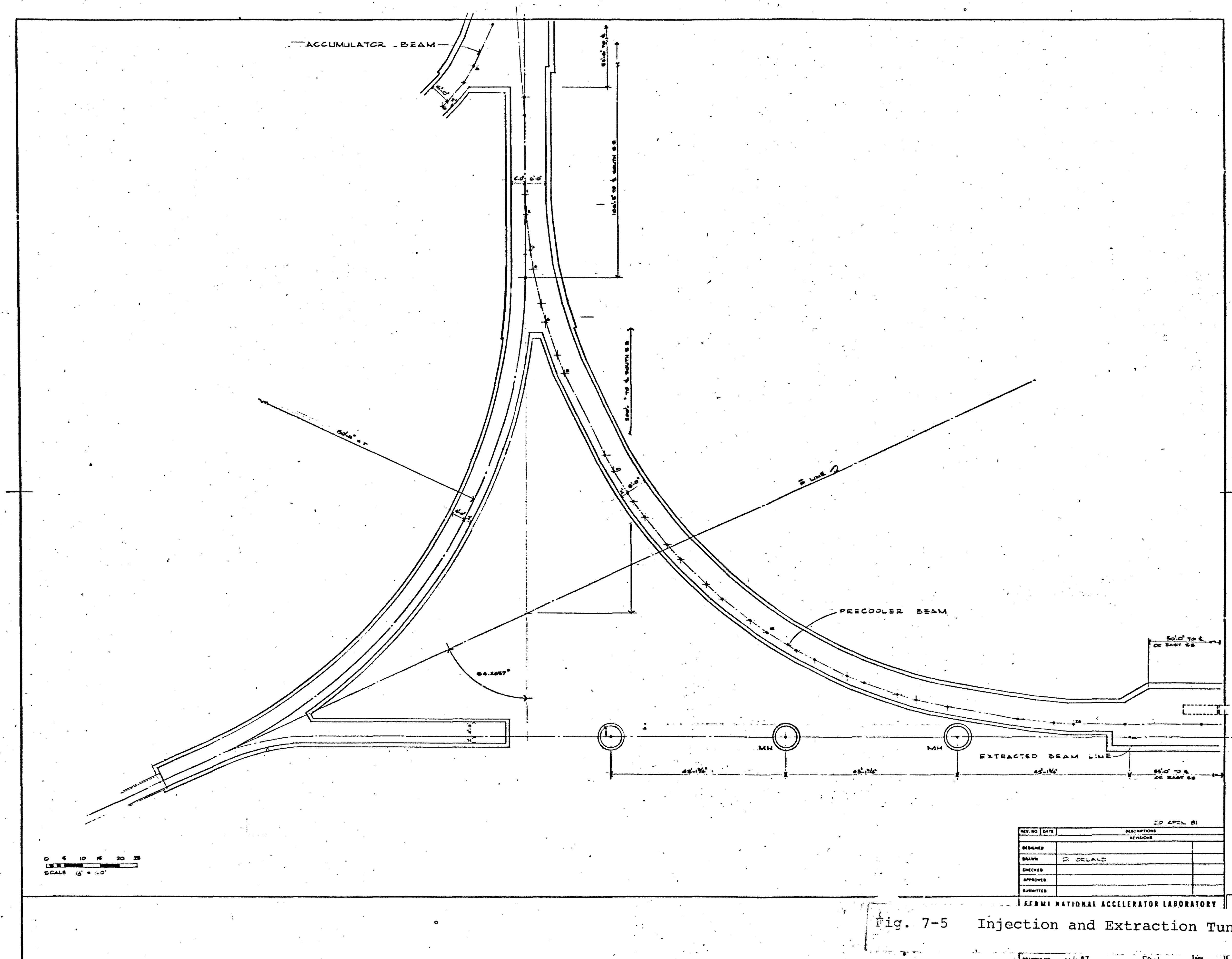

Fig. 7-5 Injection and Extraction Tunnels

The size of the below-ground assembly area is set by the space needed to construct the Central Detector and to service the Central Detector while constructing the forward-backward detectors. As in the Collision Hall, there are two floor levels which differ by 5 ft. The Central Detector sits at the lower level on its own transporter; the forward-backward detectors will be assembled on the higher level and transported to the Collision Hall on a special transfer cart. The two bays at the entrance to the tunnel are at the lower elevation and can both accept either the transfer cart or the concrete shield wall. A labyrinth with a movable plug allows passage for people and light equipment between the Assembly Area and the Collision Hall.

The above-ground section of the assembly building will be used for offices and fabrication of the individual components of the detector. The experiment electronics and control rooms are placed as close to the Collision Hall as possible to reduce the time delays from cable lengths to a minimum.

8.2 D0 Experimental Area

No specific detector has yet been proposed for the D0 interaction region; a nominal detector of diameter 15 ft and length of 20 ft has been considered in the design. The experimental area provided consists of an underground hall 47 ft wide, 24 ft long and 20 ft high. Equipment is lowered to the hall with a 20-ton crane through a hatch with opening 29 ft wide and 20 ft long. The hall is designed to provide an assembly and work area, shielded from the Tevatron beam by 9 ft of high-density concrete. To run the experiment, this shielding is removed to cover the access hatch and the assembled detector is rolled into place. The D0 experimental area is shown in Fig. 8-3.

SCALE 1" = 20'-0"

D–O Experiment Area

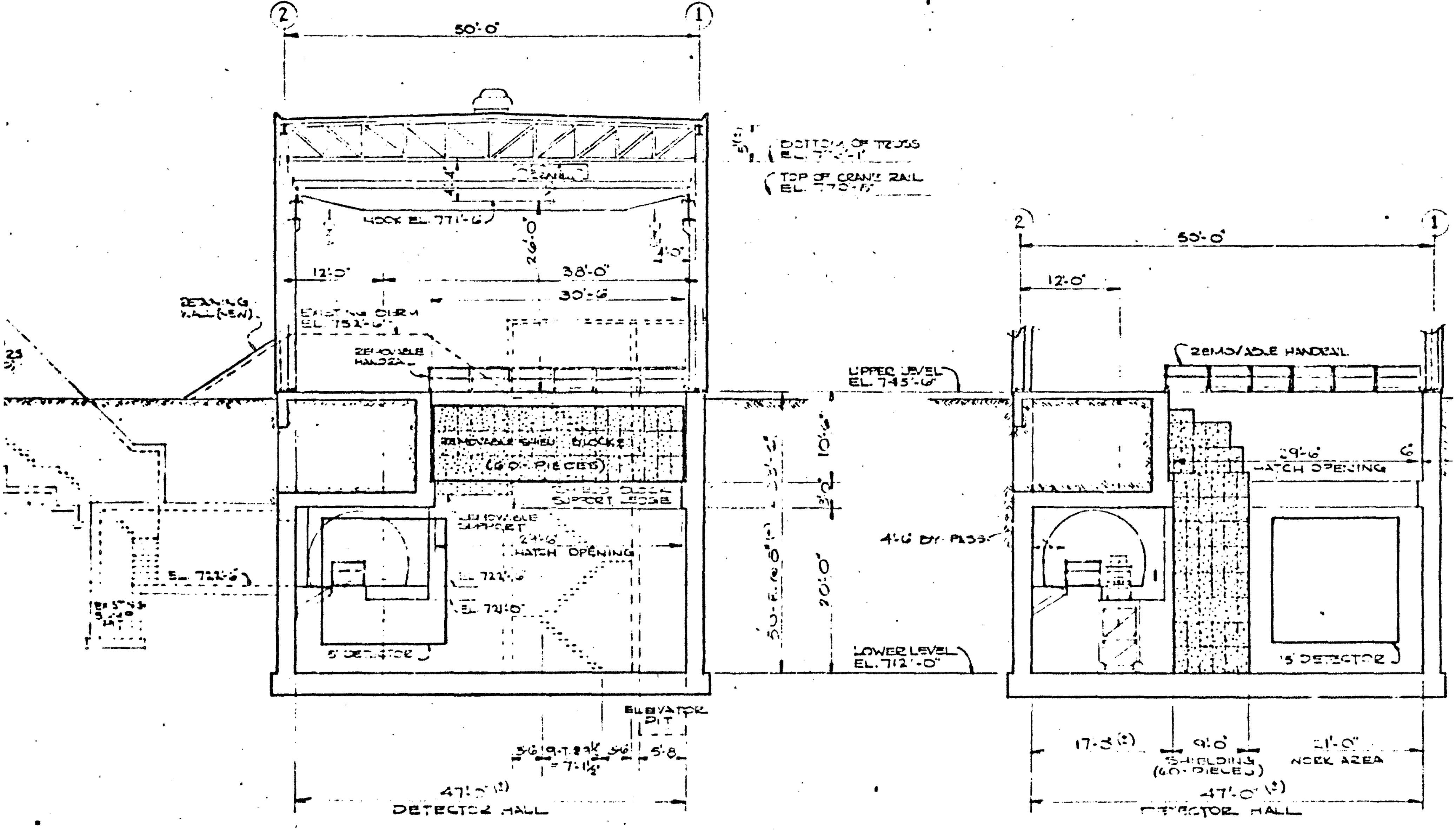

OPERATIONAL PHASE

ASSEMBLY PHASE

SECTION (A)

LOOKING NORTH

SCALE 1/8" = 1'-0"

Fig -3

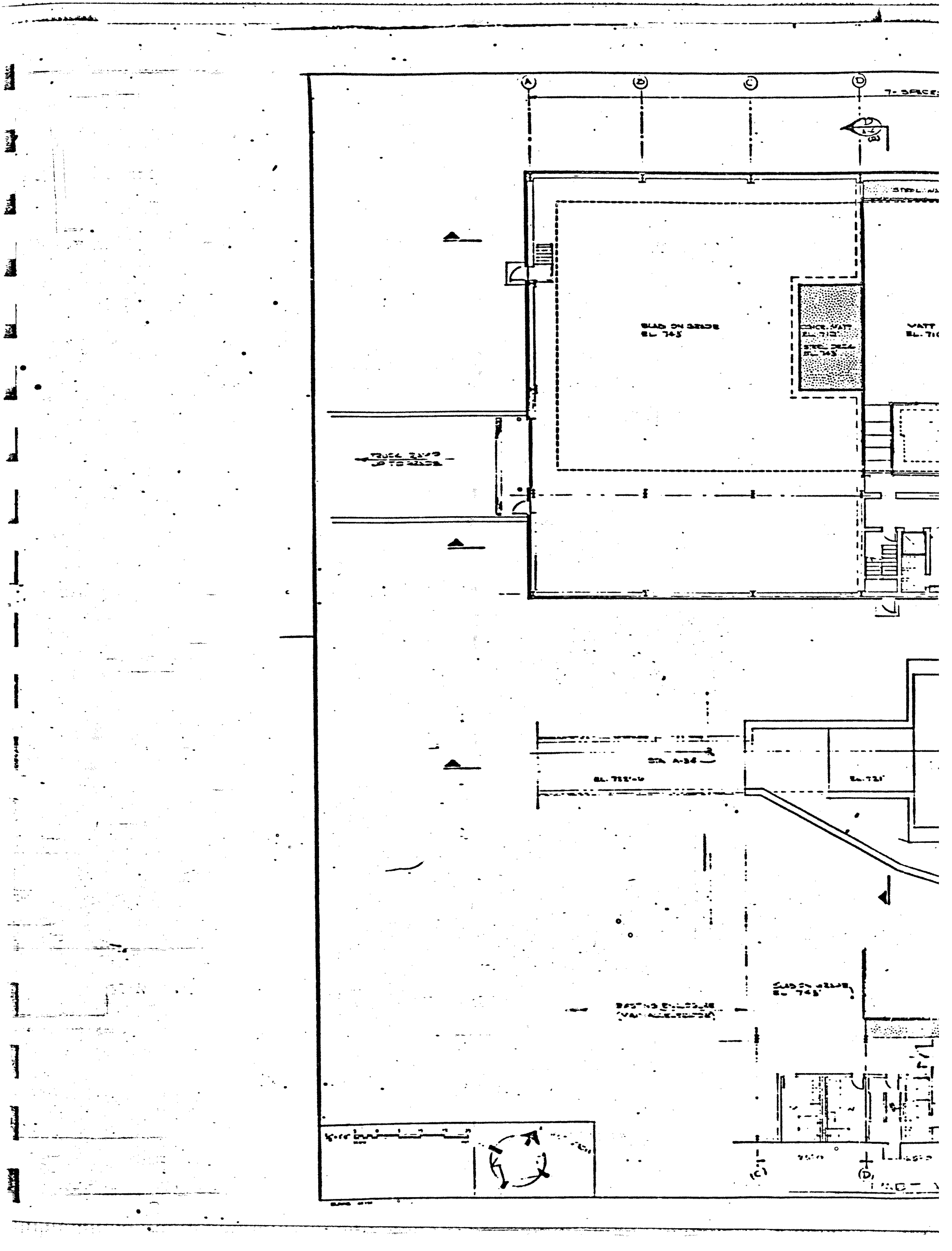

SLAB ON GRADE
EL. 743
STA. A-34

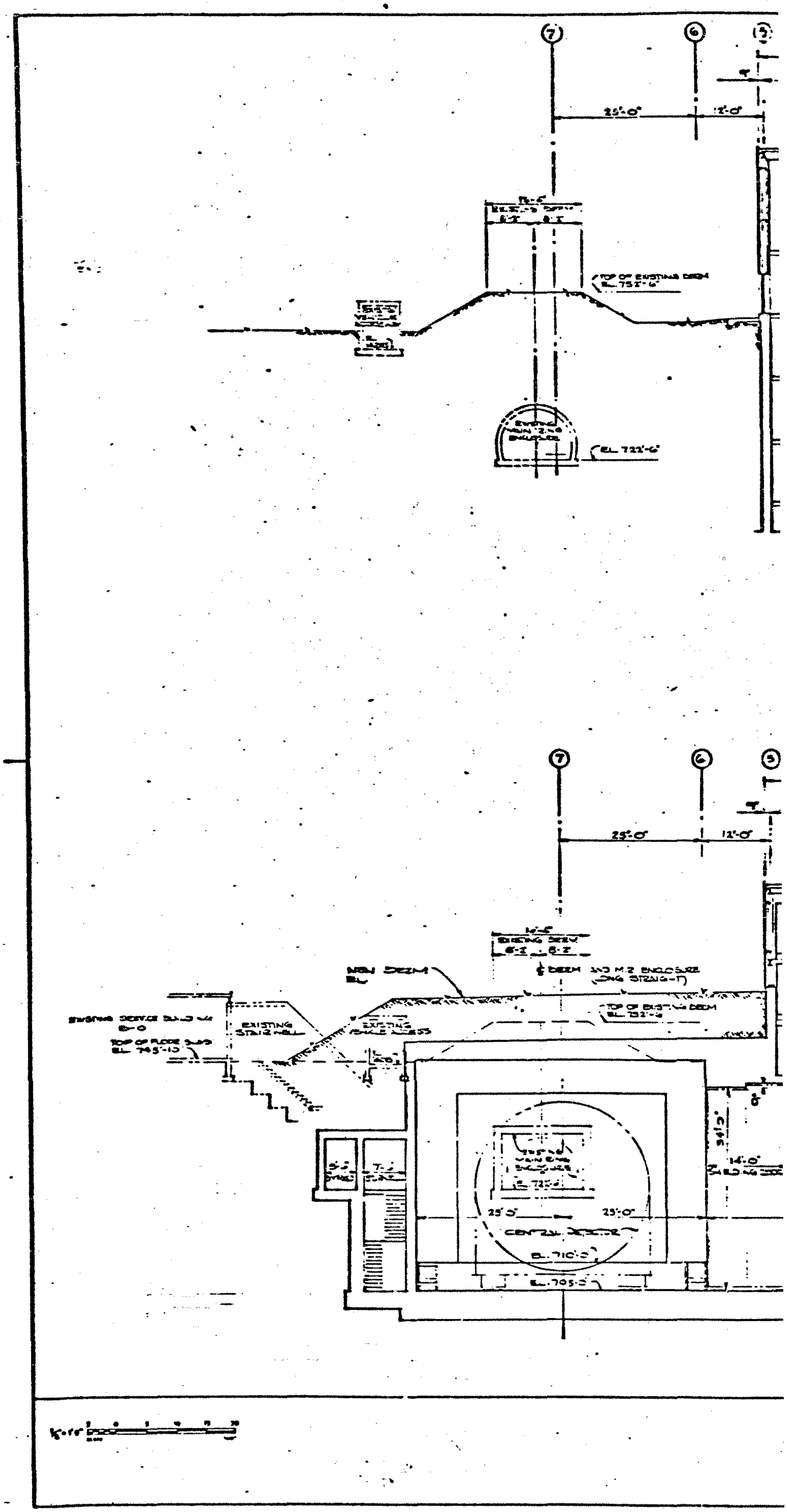

7
6
5
25'-0"
12'-0"
7
6
5
25'-0"
12'-0"
EXISTING
STAIR WELL
25'-0"
25'-0"

Appendix A

Parameters

PROTON-ANTIPROTON SOURCE FOR FERMILAB

APRIL, 30, 1981
02:00 P.M.

LIST OF TABLES

(COMPILED BY A. G. RUGGIERO)

MAIN RING CYCLE

EXTRACTION KINETIC ENERGY	80 GEV
BETA	0.999933
GAMMA	86.264
MOMENTUM (P)	80.933 GEV/C
MAGNETIC RIGIDITY (B-RHO)	2699.6 KG-M
BETATRON TUNES (H AND V)	19.4
TRANSITION ENERGY (GAMMA-T)	18.75
BETATRON EMITTANCE (EPS-H = EPS-V, 95% OF BEAM)	0.3 PI-MM-MRAD
RF FREQUENCY	53.1 MHZ
RF VOLTAGE	4.0 MV
HARMONIC NUMBER (H)	1113
INDIVIDUAL BUNCH AREA (95% OF BEAM)	0.4 EV-SEC
NO. OF PROTONS PER BUNCH	2.7* 10EXP10
BUNCH LENGTH (RMS)	21 CM
BUNCH MOMENTUM SPREAD (RMS)	3.7* 10EXP-4
NO. OF EQUAL BATCHES	13
NO. OF BUNCHES PER BATCH	75
TOTAL NO. OF BUNCHES	975
TOTAL NO. OF PROTONS	2.6325* 10EXP 13
MAJOR BEAM GAP (1)	580 NSEC
MINOR BEAM GAPS (12)	185 NSEC
REVOLUTION TIME	20.96 MICRO-SEC
MAIN RING CYCLE PERIOD	9.85 SEC
FLAT-TOP LENGTH (80 GEV)	1.3 SEC

TARGETRY

TARGETRY MATERIAL	TUNGSTEN (W)
LENGTH OF TARGET	5 CM
CROSS-SECTION RADIUS	1 MM
BETA* ,PROTON (H AND V)	1.0 M
ALPHA*, PROTON (H AND V)	0.0
ETA*, PROTON (DISPERSION)	0.0 M
ETA-PRIME*, PROTON	0.0
SIGMA*, PROTON (RMS SPOT SIZE, H AND V)	0.224 MM
NO. OF P-BATCHES/ MR CYCLE	13
TIME INTERVAL BETWEEN BATCHES	100 MSEC
MAIN RING CYCLE PERIOD	9.85 SEC
NO. OF PROTONS PER BATCH	2.025* 10EXP 12
PBAR-PRODUCTION MOMENTUM	5.3567 GEV/C
KINETIC ENERGY	4.5 GEV
BETA	0.985
GAMMA	5.796
MAGNETIC RIGIDITY (B-RHO)	178.7 KG-M
MOMENTUM SPREAD ACCEPTED	
FULL DELTA P/P, (UNIFORM DISTRIBUTION)	1.0 %
EMITTANCE ACCEPTED (H AND V)	5.0 PI-MM-MRAD
ANGLE ACCEPTED	25 MRAD
BETA*, ANTIPROTON, (H AND V)	0.8 CM
A*, ANTIPROTON SPOT RADIUS	0.2 MM
PP-PBAR INVARIANT CROSS-SECTION	0.8 MB/GEV**2
PP INELASTIC CROSS-SECTION	33 MB
PROTON ABSORPTION LENGTH	10.5 CM
ANTIPROTON ABSORPTION LENGTH	6.0 CM
YIELD, NO.OF PBAR/ NO.OF P	
(FROM TARGET ONLY)	1.15* 10EXP-6
EFFECTIVE YIELD INCLUDING	
COLLECTION LI-LENS	0.8* 10EXP-6
TOTAL NO. OF PBAR/MR CYCLE	2.106* 10EXP 7
PBAR-BUNCH LENGTH (RMS)	21 CM
PBAR-BUNCH AREA (95% OF BEAM)	0.15 EV-SEC
PBAR-BEAM RF BUNCHING	52.31 MHZ
NO. OF PBAR-BUNCHES/BATCH	75
GAP LENGTH (9 BUNCHES)	188 NSEC

PBAR-TRANSPORT TO PRECOOLER

BEAM EMITTANCE (H AND V)	20 PI-MM-MRAD
MOMENTUM SPREAD, DP/P (FULL)	4%

SEQUENCE OF MAGNET SECTORS:

1. VERTICAL TRANSLATION AFTER TARGET

D1	V1	D2	Q1	D3	Q2	D4	Q1	D4
Q2	D3	Q1	D2	V1*	D1			

2. MATCHING PLUS FODO TRANSPORT

D5	Q3	D6	Q4	D7	QD	D8	QF	D9
QD	D9	QF	D9	QD	D9	QF/2		

3. MATCHING

QF/2	D4	Q14	D14	Q13	OS	V3*	D15	Q15
D16	Q16	D17	Q17	Q17	D16	Q18	D18	

4. DISPERSION SUPPRESSOR

O6	B	O	B	O5	QD	O4	B	O3
QF	O2	B	O1	QD/2				

5. TWO REGULAR CELLS

QD/2	O	B	O	B	OO	QF/2
QF/2	OO	B	O	B	O	QD/2
QD/2	O	B	O	B	OO	QF/2
QF/2	OO	B	O	B	O	QD/2

6. ONE CELL WITH TWO MISSING MAGNETS

QD/2	OOO	QF	O	B	O	B	OO	QD/2

7. ONE AND ONE-HALF REGULAR CELL

QD/2	O	B	O	B	OO	QF/2				
QF/2	O	B	O	B	OO	QD2	O	B	O	B

8. LONG STRAIGHT MATCHING

D19	Q19	D20	Q20	D21	Q21	D22	Q22	D21	Q23	D22

9. VERTICAL TRANSLATION

V4	D23	Q24	D24	Q25	D25	Q26	D26	Q27	D27
Q28	D28	V5	D29						

DRIFTS	LENGTHS (METERS)
D1	-0.915
D2	3.8359
D3	1.5
D4	3.5
D5	3.0
D6	3.1962
D7	1.6916
D8	2.574
D9	14.0757
D10	--
D11	--
D12	--
D13	--
D14	1.354
D15	12.719
D16	0.9144
D17	5.2461
D18	0.3048
D19	0.75
D20	5.32814
D21	1.25
D22	3.00
D23	3.5046
D24	0.75
D25	1.15113
D26	0.884
D27	0.60754
D28	2.1712
D29	-1.8288
OS	0.5
O	0.3048
OO	0.72963
O1	0.45
O2	2.2609
O3	1.8025
O4	0.9083
O5	0.2172
O6	0.8172
OOO	4.08243

QUADRUPOLES	EFFECT. LENTGH (METER)	STRENGTH (B'/B-RHO) /M**2
Q1	0.6096	0.5025
Q2	1.2192	-0.41262
QF/2	0.3048	0.1602
Q3	0.6096	-0.52436
Q4	0.6096	0.34452
QD	0.6096	-0.1602
QF	0.6096	0.1602
Q13	0.6096	--
Q14	0.6096	-0.005059
Q15	0.6096	-0.5
Q16	0.6096	0.4727
Q17	0.6096	-0.1662
Q18	0.6096	0.2584
QD	0.6096	-0.53522
QF	0.6096	0.54216
QF/2	0.3048	0.54216
QD/2	0.3048	-0.53522
QF2	0.6096	0.4042
QD2	0.6096	-0.42353
Q19	0.6096	0.47357
Q20	0.6096	-0.799
Q21	1.2192	0.82195
Q22	1.2192	0.62407
Q23	0.6096	-0.849
Q24	0.6096	0.82608
Q25	1.2192	-0.80589
Q26	0.6096	0.78407
Q27	1.2192	-0.89608
Q28	0.6096	0.72807

VERTICAL DIPOLES	EFFECT. LENGTH (METERS)		STRENGTH (B/B-RHO) /M
V1	1.83	UP	0.05726
V1*	1.83	DOWN	0.05726
V3*	1.3716		--
V4	1.3716	DOWN	0.058357
V5	3.6576	UP	0.021884

HORIZ. DIPOLE	EFFECT. LENGTH (METERS)	STRENGTH (B/B-RHO) /M
B	1.3716	0.0409

RF ROTATION AND STACKING

KINETIC ENERGY	4.5 GEV
BETA	0.985
GAMMA	5.796
MOMENTUM, (P)	5.3567 GEV/C
MAGNETIC RIGIDITY (B-RHO)	178.7 KG-M
PRECOOLER RING RADIUS (R)	75.4717 M
RF FREQUENCY (FA)	52.31 MHZ
HARMONIC NUMBER (H)	84
TRANSITION ENERGY (GAMMA-TI)	10.24624

CAPTURE:

PBAR-BUNH AREA (95% OF BEAM)	0.15 EV-SEC
MOMENTUM SPREAD	
FULL DELTA-P/P, (UNIFORM DISTR.)	1.0 %
BUNCH LENGTH (RMS)	21.0 CM
RF VOLTAGE AT CAPTURE	
(STATIONARY BUCKET)	400 KV
PHASE OSCILLATION PERIOD	0.367 MSEC

BUNCH ROTATION:

TIME PERIOD FOR ROTATION	94 MICRO-SEC

BUCKET REDUCTION:

FINAL VOLTAGE	19 KV
(STATIONARY BUCKET)	
BUCKET HALF-HEIGHT, DELTA-P/P	0.12 %
BUCKET AREA	0.154 EV-SEC
TIME TO DROP VOLTAGE TO FINAL VALUE	
AT THE END OF ROTATION	8 MICRO-SEC
PHASE OSCILLATION PERIOD	1.68 MSEC

TRANSFORMATION TO MOVING BUCKET:

RF VOLTAGE FOR MOVING BUCKET	33.0 KV
RF PHASE FOR MOVING BUCKET	173 DEGREES
MOVING BUCKET AREA	0.154 EV-SEC
MOVING BUCKET HALF-HEIGHT, DP/P	0.18 %
PHASE OSCILLATION PERIOD	1.29 MSEC
TIME FOR TRANSFORMATION	1.6 MSEC

STACKING WITH MOVING BUCKET:

MOMENTUM VARIATION SWEPT, DP/P	4.0 %
ENERGY VARIATION	213 MEV
ENERGY GAIN PER TURN	4 KEV
NO. OF REVOLUTION DURING STACKING	53,000
TIME FOR STACKING	85 MSEC
RF FREQUENCY SWING (DF/F)	8.0* 10EXP-4
VARIATION OF RF FREQUENCY	500 HZ/MSEC

TRANSFORMATION TO STATIONARY BUCKET:

RF VOLTAGE FOR STATIONARY BUCKET	19 KV
RF PHASE FOR STATIONARY BUCKET	180 DEGREES
STATIONARY BUCKET AREA	0.154 EV-SEC
STATIONARY BUCKET HALF-HEIGHT, DP/P	0.12 %
PHASE OSCILLATION PERIOD	1.68 MSEC
TIME FOR TRANSFORMATION	1.6 MSEC

ADIABATIC DEBUNCHING

FINAL VOLTAGE	0.0 V
TIME REQUIRED TO TURN OFF RF	1.5 MSEC
FINAL BEAM MOMENTUM SPREAD, DP/P (FULL)	0.17 %

OVERALL STACKING PARAMETERS

NO. OF PULSES STACKED/ MAIN RING CYCLE	13
NO. OF PBARS PER PULSE	1.62* 10EXP 6
FINAL MOMENTUM SPREAD, DP/P (FULL)	2.16 %
STACKING EFFICIENCY (INCLUDING DILUTION DURING BUNCH ROTATION)	0.88
FRACTION OF OVERALL BEAM LOSS	5.0 %

RF CAVITIES REQUIREMENT

NO. OF CAVITIES REQUIRED (MR KIND)	2
VOLTAGE CAN BE PROGRAMMED BY PARAPHASING	
MODEST FREQUENCY TUNING RANGE	
TOTAL LENGTH OF SYSTEM	4.3 M

PRECOOLER PARAMETERS

A. GENERAL

TOP KINETIC ENERGY	8.0 GEV
BETA	0.99448
GAMMA	9.5264
MOMENTUM (P)	8.8889 GEV/C
MAGNETIC RIGIDITY (B-RHO)	296.5 KG-M
BENDING FIELD (B)	12.127 KG
BENDING RADIUS (RHO)	24.449255 M
AVERAGE RADIUS (R)	75.4717
REVOLUTION TIME: 80 GEV	628.71 KHZ
4.5 GEV	622.72 KHZ
200 MEV	357.93 KHZ
SUPERPERIODICITY	2
FOCUSSING STRUCTURE	SEPARATED FUNCTION
NORMAL CELL STRUCTURE	FODO
HORIZONTAL BETATRON TUNE	11.415
VERTICAL BETATRON TUNE	11.393
TRANSITION ENERGY (GAMMA-T)	10.246
NATURAL CHROMATICITY: HORIZONTAL	-18.35
VERTICAL	-17.68

B. MAGNETS

NUMBER OF DIPOLES	112
LENGTH OF DIPOLES	-
EFFECTIVE LENGTH OF DIPOLES	1.3716 M
SAGITTA	0.962 CM

QUADRUPOLES:

TYPE	NUMBER	EFFECT. LENGTH	STRENGTH (B'/B-RHO)
QF	24	2 FT	.542162 M-2
QD	28	2	-.535217
1Q1	4	1.3716 M	.292781
1Q2	4	1.143	-.380244
1Q3	4	1.524	.455736
QD1	4	0.9906	-.468417
QF1	4	0.7874	.403642
QD2 FT	4	2 FT	-.42353
QF2	4	2	.40420
QF9	4	4	.308953
2Q1	4	4	-.359801
2Q2	4	4	.361397
2Q3	4	4	-.406104

C. DRIFT LENGTHS

O	.3048	M
OO	.72963	
OOO	4.08243	
LL	10.00000	
L11	1.96582	
L1	1.1159	
L2	2.67062	
L3	.2667	
O1	.45	
O2	2.26083	
O3	1.80250	
O4	0.90833	
O5	0.217213	
O6	.817217	
LL*	9.9238	
L2*	2.55632	
OOO*	4.10783	
OO*	.64073	
L4	.77763	
L5	.9144	
L6	1.64192	

D. LATTICE STRUCTURE

D1. CELLS:

.BB	OO	B	O	B	O		
.BB*	OO*	B	O	B	O		
.C	QD	.BB	QF	QF	.BB	QD	
.C1	QD1	OOO*	QF1	QF1	.BB	QD2	
.C2	QD2	.BB	QF2	QF2	.BB*	QD	
.C3	QD	.BB	QF	QF	OOO	QD	
.C8	QD	O1	B	O2	QF		
	QF	O3	B	O4	QD		
.DF9	QD	O5	B	O	B	O6	QF9

CELL LENGTH: 9.3841 M

D2. LONG STRAIGHT SECTION:

WITH DISPERSION

.S1	LL*	1Q1	1Q1	L3	1Q2	1Q2	
	L1	L5	L6	1Q3	1Q3	L3	QD1

WITHOUT DISPERSION

.S2	QF9	L3	2Q3	2Q3	L2	L11
	2Q2	2Q2	O	2Q1	2Q1	LL

PRECOOLER INJECTION

KINETIC ENERGY AT INJECTION	4.5 GEV
MOMENTUM	5.3567 GEV/C
MAGNETIC RIGIDITY	178.7 KG-M
EMITTANCE INJECTED (H AND V)	20 PI-MM-MRAD
MOMENTUM SPREAD INJECTED, FULL DP/P	1.0 %
METHOD	VERTICAL INJECTION ON A FULL APERTURE HORIZONTAL ORBIT BUMP
LOCATION OF HORIZ. BUMP	SOUTH LONG STRAIGHT
LOCATION OV VERTICAL INJECT.	MIDDLE OF SOUTH LONG STRAIGHT
ORBIT SEPARATION AT SEPTUM	6.5 CM

STRUCTURE OF HORIZ. BUMP:

K4 O 2(QF2) O B O B OO 2(QD1)
O B O B OO* 2(QF1) O K3
L* 2(QD1) L3 2(1Q3) L2 K2 L1 2(1Q2)
L3 2(1Q1) LS K1 LL* S/2

KICKERS:	K1	K2	K3	K4	
EFF. LENGTH	2.00	1.8288	1.596715	0.477	M
STRENGTH	0.35	0.35	0.35	0.35	KG
RISE TIME	180	180	180	180	NSEC
H. APERT.	10.	3.0	7.0	3.0	IN
V. APERT.	2.5	4.0	3.0	1.5	IN

SEPTUM MAGNET: S

SEPTUM THICKNESS	10 MM
EFFECTIVE LENGTH (2*S/2)	12 FT
STRENGTH	4.0 KG
INJECTION ANGLE	80 MRAD

VERTICAL SEPARATION BETWEEN BEAM AXIS 50 IN

DRIFT ELEMENTS:

O OO OO* L3	SEE TABLE 7
LL*	4.095 M
L*	2.206315
L2	0.72752
L1	1.1159
LS	2.00

QUADRUPOLES:

QF1 QD1 1Q1 1Q2 1Q3 QF2 QD2 — SEE TABLE 7

STOCHASTIC COOLING

MODE	MOMENTUM
BEAM	DEBUNCHED
NO. OF COOLING STEPS (SEE TABLE 9)	3
PRECOOLER RADIUS	75.4717 M
TRANSITION ENERGY (GAMMA-T)	10.24624
NO. OF COOLING DEVICES	1
PICK-UP LONG STRAIGHT SECTION	20. M
KICKER LONG STRAIGHT SECTION	20. M
NO. OF PARTICLES COOLED	2.0* 10EXP 7
NOTCH FILTER	CIRCUMFERENCE LENGTH SHORTED
NO. OF TANKS OF PICK-UPS/KICKERS	8
NO. OF PICK-UPS/KICKERS PER TANK	32
TOTAL NO. OF PICK-UPS/KICKERS	256
IMPEDANCE PER PICK-UP	30 OHM
PER KICKER	80 OHM
LENGTH PER PICK-UP/KICKER	5 CM
OVERALL TRANSVERSE DIMENSION OF TANKS	1 FT
NO. OF PREMPLIFIERS	6
NO. OF MAJOR AMPLIFICATION STATIONS	1
AMPLIFIER TOTAL RATED POWER	10. KW
PRE-AMP NOISE LEVEL	1.8 DB
DISTANCE BETWEEN PICK-UPS AND KICKERS NORMALIZED TO CIRCUMFERENCE	0.4
LOCATION OF PICK-UP STATION	WEST LONG STRAIGHT
LOCATION OF KICKER STATION	EAST LONG STRAIGHT
TIME DISTANCE BETWEEN PICK-UPS AND KICKERS COLLECTION POINT IN STRAIGHT L INE	470 NSEC

D3. ARC SECTOR:

```
.ARC                 .C1  .C2  .C3  .C
                     .C   .C   .C   .C8  .DF9
```

D4. QUADRANT STRUCTURE:

```
.SPH                       .S1  .ARC  .S2
```

D5. SUPERPERIOD:

```
        .SPH           REFLECT  (.SPH)
```

E. LATTIC E FUNCTIONS

	BETA,H	BETA,V	ETA
MAXIMA	60.22 M	56.80 M	-2.74 M
REGULAR CELL:			
MAX	16.	16.	1.3
MIN	2.5	2.5	0.6
MIDDLE OF LONG STRAIGHT "WITH" DISPERSION (.S1)			
	9.9862	10.0506	-2.7427
MIDDLE OF LONG STRAIGHT "WITHOUT" DISPERSION (.S2)			
	10.3516	6.0182	0.00

COOLING STEPS:

STEP		#1	#2	#3
KINETIC ENERGY, GEV		4.5	2.4	0.9
BETA		0.985	0.959	0.860
GAMMA		5.796	3.558	1.959
ETA		0.021	0.070	0.251
REVOLUTION FREQ., KHZ		622.72	606.28	543.70
BANDWITH, MHZ	LOW	100	100	100
	HIGH	500	500	500
LOWER HARMONIC		160	164	183
UPPER HARMONIC		803	825	920
INITIAL DP/P, FULL (%)		2.0	0.494	0.272
FINAL DP/P, FULL (%)		0.288	0.133	0.0464
COOLING TIME, SEC		4.5	1.25	0.75
OVERALL LOOP GAIN (DB)		236	230	220
POWER AT KICKERS (RMS) :				
AMPLIFIER NOISE (KW)		5.0	1.6	0.08
SCHOTTKY SIGNALS (KW)		0.8	0.1	0.015
BEAM TRANSIT TIME FROM P.U. TO KICKERS (NSEC)		640	658	733

DECELERATION IN THE PRECOOLER

SEQUENCE OF EVENTS	TIME	KINET. ENERGY	REF
INJECTION OF 1ST BATCH	0.0 SEC	4.5 GEV	TAB. 5
END OF RF STACKING	1.3	4.5	6
FIRST STEP OF STOCH. COOL.	5.8	4.5	8
FIRST STAGE OF DECELERAT	6.38	4.5-2.4	
SECOND STEP OF STOCH. COOL.	7.63	2.4	8
SECOND STAGE OF DECELERAT.	8.105	2.4-0.9	
THIRD STEP OF STOCH. COOL.	8.855	0.9	8
THIRD STAGE OF DECELERAT.	9.32	0.9-0.204	
BUNCHING PRIOR TRANSFER TO ELECTRON ACCUMULATOR	9.397	0.204	10

NUMBER OF PBAR'S DECELERATED	2.0* 10EXP 7
TRANSITION ENERGY (GAMMA-TI)	10.246
PRECOOLER AVERAGE RADIUS	75.4717 M

FIRST STAGE OF DECELERATION (4.5 - 2.4 GEV)

KINETIC ENERGIES	4.5 - 2.4 GEV
BETA	0.985-0.959
GAMMA	5.796-3.558
MOMENTUM SPREAD, DP/P	
FULL, AFTER COOLING, 4.5 GEV	0.300 %
REVOLUTION PERIOD, 4.5 GEV	1.6 MICRO-SEC
TOTAL BEAM AREA	24 EV-SEC
HARMONIC NUMBER	9
RF FREQUENCY, 4.5 GEV	5.604 MHZ
2.4 GEV	5.470 MHZ
STATIONARY BUCKET, 4.5 GEV FOR CAPTURE:	
VOLTAGE	11.6 KV
SINGLE BUCKET AREA	3.33 EV-SEC
SINGLE BUNCH AREA	2.66 EV-SEC
BUCKET HEIGHT, FULL DP/P	0.556 %
SYNCHROTRON PERIOD	6.38 MSEC
ADIABATIC CAPTURE + TRANSFORMATION TO MOVING BUCKET TIME PERIOD	30 MSEC
DECELERATION RATE	4.0 GEV/SEC
TIME REQUIRED FOR DECELERATION	0.54 SEC

RF PARAMETERS VS. KINETIC ENERGY (K.E.)

K.E.	PHASE ANGLE	VOLTAGE	FREQUENCY
4.5 GEV	0.0 DEG	11.6 KEV	5.604 MHZ
4.4	12.3	29.7	5.601
4.0	10.4	34.9	5.59
3.5	8.0	45.5	5.56
3.0	6.0	60.8	5.52
2.5	4.3	84.4	5.47
2.4	0.0	65.3	5.46

MOVING BUCKET AREA (SINGLE)	3.33 EV-SEC
STATIONARY BUCKET, 2.4 GEV:	
VOLTAGE	65.3 KEV
PHASE ANGLE	0.0 DEG
BUCKET AREA (SINGLE)	3.33 EV-SEC
BUCKET HEIGHT, FULL DP/P	0.93 %
SYNCHROTRON PERIOD	1.14 MSEC
TRANSFORMATION TO STATIONARY BUCKET PLUS ADIABATIC DEBUNCHING TAKES	10 MSEC
TOTAL TIME FOR 1ST STAGE OF DECELERAT.	0.58 SEC
FINAL MOMENTUM SPREAD, 2.4 GEV DEBUNCHED AND FULL, DP/P	0.578 %

SECOND STAGE OF DECELERATION (2.4 - 0.9 GEV)

KINETIC ENERGIES	2.4 - 0.9 GEV
BETA	0.959-0.860
GAMMA	3.558-1.959
MOMENTUM SPREAD, DP/P	
FULL, AFTER COOLING, 2.4 GEV	0.13 %
REVOLUTION PERIOD, 2.4 GEV	1.65 MICRO-SEC
TOTAL BEAM AREA	6.8 EV-SEC
HARMONIC NUMBER	10
RF FREQUENCY, 2.4 GEV	6.067 MHZ
0.9 GEV	5.436 MHZ
STATIONARY BUCKET, 2.4 GEV FOR CAPTURE:	
VOLTAGE	4.54 KV
SINGLE BUCKET AREA	0.75 EV-SEC
BUCKET HEIGHT, FULL DP/P	0.12 %
SYNCHROTRON PERIOD	4.1 MSEC
ADIABATIC CAPTURE + TRANSFORMATION TO MOVING BUCKET TIME PERIOD	30 MSEC
DECELERATION RATE	4.0 GEV/SEC
TIME REQUIRED FOR DECELERATION	0.435 SEC
RF PARAMETERS VS. KINETIC ENERGY (K.E.)	

K.E.	PHASE ANGLE	VOLTAGE	FREQUENCY
2.4 GEV	0.0 DEG	4.54 KV	6.067 MHZ
2.0	16.8	21.9	5.99
1.5	12.6	29.00	5.835
1.0	8.0	45.5	5.54
0.9	0.0	35.0	5.437

MOVING BUCKET AREA (SINGLE)	0.75 EV-SEC
STATIONARY BUCKET, 0.9 GEV:	
VOLTAGE	30.2 KV
PHASE ANGLE	0.0 DEG
BUCKET HEIGHT, FULL DP/P	0.47 %
SYNCHROTRON PERIOD	0.61 MSEC
TRANSFORMATION TO STATIONARY BUCKET PLUS ADIABATIC DEBUNCHING TAKES	10 MSEC
TOTAL TIME FOR 2ND STAGE OF DECELERATION	0.475 SEC
FINAL MOMENTUM SPREAD, 0.9 GEV DEBUNCHED AND FULL, DP/P	0.28 %

THIRD STAGE OF DECELERATION (0.9 - 0.2 GEV)

KINETIC ENERGIES	0.9 - 0.204 GEV
BETA	0.860-0.570
GAMMA	1.959-1.217
MOMENTUM SPREAD, DP/P	
FULL, AFTER COOLING, 0.9 GEV	0.046 %
REVOLUTION PERIOD, 0.9 GEV	1.84 MICRO-SEC
TOTAL BEAM AREA	1.15 EV-SEC
HARMONIC NUMBER	14
RF FREQUENCY, 0.9 GEV	7.61 MHZ
0.2 GEV	5.01 MHZ
STATIONARY BUCKET, 0.9 GEV FOR CAPTURE:	
VOLTAGE	1.17 KV
SINGLE BUCKET AREA	0.09 EV-SEC
BUCKET HEIGHT, FULL DP/P	0. 08 %
SYNCHROTRON PERIOD	2.6 MSEC
ADIABATIC CAPTURE + TRANSFORMATION TO MOVING BUCKET TIME PERIOD	45 MSEC
DECELERATION RATE	2.0 GEV/SEC
TIME REQUIRED FOR DECELERATION	0.41 SEC

RF PARAMETERS VS. KINETIC ENERGY (K.E.)

K.E.	PHASE ANGLE	VOLTAGE	FREQUENCY
0.9 GEV	0.0 DEG	1.15 KV	7.61 MHZ
0.6	21.	8.8	7.01
0.4	17.	10.8	6.31
0.3	15.5	11.9	5.78
0.2	0.0	5.0	5.01

MOVING BUCKET AREA (SINGLE)	0.09 EV-SEC
STATIONARY BUCKET, 200 MEV:	
VOLTAGE	5.0 KV
BUCKET AREA (SINGLE)	0.09 EV-SEC
BUCKET HEIGHT, FULL DP/P	0.19 %
SYNCHROTRON PERIOD	0.61 MSEC
TRANSFORMATION TO STATIONARY BUCKET PLUS ADIABATIC DEBUNCHING TAKES	10 MSEC
TOTAL TIME FOR 3RD STAGE OF DECELERATION	0.465 SEC
FINAL TOTAL BEAM AREA AT 200 MEV AFTER DEBUNCHING	1.25 EV-SEC

ELECTRON RING PARAMETERS

A. GENERAL

KINETIC ENERGY	0.2-1.4 GEV
BENDING FIELD	2.35-7.79 KG
BENDING RADIUS (RHO)	9.17 M
AVERAGE RADIUS	32.35 M
REVOLUTION TIME	1197-740 NSEC
SUPERPERIODICITY:	
WITHOUT ELECTRON BEAM	2
WITH ELECTRON BEAM	1
FOCUSSING STRUCTURE	SEPARATED FUNCTION
NORMAL CELL STRUCTURE	FODO
NORMAL WORKING POINT:	
HORIZONTAL TUNE	4.102
VERTICAL TUNE	5.390
TRANSITION ENERGY (GAMMA-TI)	4.089
NATURAL CHROMATICITY:	
HORIZONTAL	-7.410
VERTICAL	-6.409

B. MAGNETS

NUMBER OF DIPOLES	44
LENGTH OF DIPOLES	48.00 IN
EFFECTIVE LENGTH OF DIPOLES	51.52 IN
NUMBER OF QUADRUPOLES	44
LENGTH OF QUADRUPOLES	24.00 IN
EFFECTIVE LENGTH OF QUADRUPOLES	26.64 IN

QUADRUPOLE GRADIENTS AT 1.4 GEV:

QF	36.24 KG/M
QD	-33.43
Q1	-47.85
Q2	55.33
Q3	-12.50
Q9	28.65
Q10	-36.42
Q11	19.03

D. APERTURE AND ACCEPTANCE

NOMINAL VACCUM CHAMBER APERTURE:		
	HORIZONTAL (HALF)	89 MM
	VERTICAL (HALF)	25 MM
SAGITTA		21.8 MM
AVAILABLE HORIZONTAL APERTURE (HALF)		78 MM

LATTICE FUNCTIONS

	MAXIMA	IN DIPOLE	L.S.	S.S.
BETA H	48.23 M	19.50 M	12.93 M	10.37 M
BETA V	19.44	13.25	10.11	11.48
ETA	3.65	3.55	0.06	3.51

ACCEPTANCE (USING BEAM SIZE IN DIPOLES)

AV = 2*25 MM , EPS V = 47 PI-MM-MRAD
AH = 2*78 MM , EPS H = 40 PI-MM-MRAD
DP/P = 0.5 % (FULL)

DP/P (RF STACKING) = 2.37 % (FULL)

(THIS IS THE ACCEPTANCE FOR TWO BEAMS AS GIVEN ABOVE WITH A SEPARATION OF 10 MM AT THE INJECTION SEPTUM).

FINAL BUNCHING AT 204 MEV

TOTAL BEAM AREA		1.3 EV-SEC
HARMONIC NUMBER		1
RF FREQUENCY		360.36 KHZ
STATIONARY BUCKET:		
VOLTAGE		2.0 KV
SYNCHROTRON PERIOD		3.8 MSEC
BUCKET AREA		3.0 EV-SEC
BUCKET HEIGHT, FULL DP/P		0.46 %
TIME FOR ADIABATIC CAPTURE		10 MSEC
VOLTAGE JUMP	FROM 2.0 TO	3.85
BUCKET AREA		4.14 EV-SEC
BUCKET HEIGHT, FULL DP/P		0.64 %
SYNCHROTRON PERIOD		2.65 MSEC
TIME TO RAISE VOLTAGE		10 MICRO-SEC
90 DEG. BUNCH ROTATION		0.67 MSEC
FINAL MOMENTUM SPREAD, FULL DP/P		0.45 %
FINAL BUNCH LENGTH, FULL		1.0 MICRO-SEC

TRANSFER OF PBARS TO MAIN RING

EXTRACTION METHOD: SINGLE TURN
FAST
FULL APERTURE
EXTRACTION OCCURS HORIZONTALLY TO OUTSIDE, AT UPSTREAM END OF EAST LONG STRAIGHT SECTION

TRANSPORT CHANNEL:

KINETIC ENERGY	8.0 GEV
EMITTANCE (H AND V)	2.0 PI-MM-MRAD
MOMENTUM SPREAD	(+/-) 0.1 %

KICKERS:

	#1	#2
LOCATION		
FIELD	250 G	250 G
RISE TIME	1.5 MICRO-SEC	1.5 MICRO-SEC
APERTURE, H		
V		
EFFECT. LENGTH	2.00 M	2.00 M

SEQUENCE OF MAGNET SECTORS:

1. TRANSLATOR

   2Q3 S1 B1 S2 B2 S3 Q1 S4 Q2 S5 B3

2. LONG STRAIGHT TRANSPORT

   D6 Q3 S2 Q4 S7 QF S8 QD S8 QF S8
   QD S9

3. BEND LEFT

   Q5 OS B OS OS Q6 OS B OS B O
   Q7 OS B OS B Q8 OS B OS B O
   Q9/2

4. MATCHING AND VERTICAL TRANSLATION

   Q9/2 S2 Q10 S11 V3 S12 Q11 S13 Q12 S13 Q11
   S12 V3*

5. MATCHING FODO

OS Q13 D14 Q14 S4 QF/2

6. MATCHING PLUS FODO TRANSPORT

QF/2 S19 QD S19 QF S19 QD S19 QF S18 QD
S17 Q18 S16 Q17 S15 (IN THE MIDDLE OF V1*)

7. VERTICAL TRANSLATION TO TARGET

S21 V1* S22 Q15 S23 Q16 S24 Q15 S24 Q16 S23
Q15 S2 V1 S1

DRIFTS	LENGHTS
S1	0.25 METER
S2	1.0
S3	3.5147
S4	1.5
S5	1.181
S6	14.332
S7	5.3904
S8	14.0757
S9	10.2205
OS	0.5
S10	--
S11	0.6954
S12	5.9185
S13	4.999
S14	1.354
S15	3.0
S16	3.1962
S17	1.6916
S18	2.574
S19	14.0757
S20	--
S21	- 0.915
S22	3.8359
S23	1.5
S24	3.5

QUADRUPOLES	EFFECT. LENGTH (METER)	STRENGTH (B'/B-RHO) /M**2
Q1	0.6096	0.5296
Q2	0.6096	-0.4697
Q3	"	0.42314
Q4	"	-0.4295
QF	"	0.1602
QD	"	-0.1602
Q5	"	0.4216
Q6	"	-0.3443
Q7	1.2192	0.32715
Q8	0.6096	0.2784
Q9/2	"	0.43036
Q10	1.2192	-0.4687
Q11	0.6096	-0.5485
Q12	"	0.4423
Q13	"	-0.45869
Q14	"	0.34931
QF/2	0.3048	0.1602
Q17	0.6096	-0.52436
Q18	"	0.34452
Q15	"	0.5025
Q16	1.2192	-0.41262

HORIZ. DIPOLES	EFFECT. LENGTH (METER)	STRENGTH (B/B-RHO) /M
B1	1.00	0.033727
B2	1.1217	0.054172
B3	1.675	0.062523
B	1.3716	0.040929

VERT. DIPOLES	EFFECT. LENGTH (METER)	STRENGTH (B/B-RHO) /M
V3	1.3716	UP 0.036928
V3*	1.3716	DOWN 0.036928
V1	1.83	UP 0.05726
V1*	1.83	DOWN 0.05726

C. STRUCTURE

C1. CURVED SECTION

ELEMENTS IN CURVED SECTION		LENGTH
DIPOLE	(B)	4 FT
QUADRUPOLE	(Q)	2 FT
DRIFT SPACE	(O)	1 FT
DRIFT SPACE	(OO)	2 FT

CELL STRUCTURE:

(QD)O(B)O(B)OO
(QF)O(B)O(B)OO

CELL LENGTH 28 FT

C2. SHORT STRAIGHT

DRIFT SPACE	(SS)	6.90 FT
" "	(S1)	2.00 FT
" "	(S2)	6.56 FT
" "	(S3)	5.77 FT

C3. LONG STRAIGHT

DRIFT SPACE	(LS)	31.80 FT
" "	(L1)	2.00 FT
" "	(L2)	2.62 FT
" "	(L3)	12.00 FT

C4. DISPERSION SUPPRESSOR

DRIFT SPACE	(D1)	1.10 FT
" "	(D2)	6.90 FT

C5. QUADRANT STRUCTURE (Q)

SS(Q11)S1(Q10)S2(B)O(Q9)O(B)O(B)
S3(QD)O (B)O (B)OO(QF)O(B)O(B)
OO(QD)D1(B)D2(QF)D2(B)D1(QD)O(B)
O(B)L3(Q3)L2(Q2)L1(Q1)LS

C6. RING STRUCTURE

Q(REFLECT Q)Q(REFLECT Q)

LENTGH OF CENTRAL ORBIT 203.2296 M
666.76 FT

Appendix B

Precooler Orbit Listing

```
PCO1  RUN
BRHO   =            17.8601155
BO     =            .730824538
BKO    =            -.25
RHO    =            24.4472550
RHOI   =            1.          /          RHO
RHOK   =            BKO         /          BRHO
LB     =            1.3716
LQ     =            .3048
LQL    =            .6096
LK     =            1.596715
LK2    =            LK          /          2.
XP     =            LK          *          RHOK
X      =            LK2         *          XP
MUX    =            .26633
MUY    =            .26577
B*     =            10.
BX*    =            6.
BY*    =            6.
C   GRADIENTS-- K=GRADIENT/BRHO
KF     =            .539479
KD     =            -.534781
K1     =            .29280
K2     =            -.38038
K3     =            .45570
KD1    =            -.46045
K21    =            -.36028986
K22    =            .36375003
K23    =            -.41305853
KF1    =             .40384
KF9    =             .31345
KD2    =             -.42353
KF2    =             .40420
C   SPECIAL QUADRUPOLE LENGTHS ---
LK1    =             .6058
LK2    =             .5715
LK3    =             .762
LKD1   =             .4953
LKF1   =             .3937
LK21   =             .38910
LK22   =             .40825
LK23   =             .49705
LKF9   =             .33085
C  DRIFT SPACES ---
O      DRF          .3048
OO     DRF          .72963
OOO    DRF          4.08243
LL     DRF          10.
LI1    DRF          1.96582
L1     DRF          1.1159
L2     DRF          2.67062
L3     DRF          .2667
LL*    DRF          9.9238
L2*    DRF          2.55632
OOO*   DRF          4.10703
OO*    DRF          .64073
L4     DRF          .77763
L5     DRF          .9144
L6     DRF          1.64192
   IPC      AGN      --
B      MAG          LB          0.          1.          RHOI      *
```

```
: |     ICE     INI'      ---
 .BD    BML          OO    B     O     B     O
 BBB*   BML          O     BK    O     BK    O
 .BB*   BML          OO*   B     O     B     O
 .BB9   BML          O5    B     O     B     O6
 .DF    BML          QD    .BB   QF
 .DF*   BML          QD1   BBB*  QF1
 .DF1   BML          QD1   OOO*  QF1
 .FD1   BML          QF1   .BB*  QD2
 .FD    BML          QF    .BB   QD
 .C     BML          .DF   .FD
 .C1    BML          .DF1  .FD1
 .C2    BML          QD2   .BB   QF2   QF2   .BB   QD
 .C3    BML          QD    .BB   QF    QF    OOO   QD
 .CB    BML          QD    O1    B     O2    QF    QF    O3    B     O4    QD
 .DF9   BML          QD    .BB9  QF9
 .ARC   BML          .C1   .C2   .C3   .C    .C    .C    .C    .CB   .DF9
 .S1    BML          LL*   1Q1   1Q1   L3    1Q2   1Q2   L1    L5    L6    1Q3
                     1Q3   L3    QD1
 .S2    BML   -1     LL    2Q1   2Q1   O     2Q2   2Q2   L11   L2    2Q3   2Q3
                     O     QF9
 .SPH   BML          .S1   .ARC  .S2
 .MM    BML          .C8   QD    .BB9
 .SS1   BML   -1     .S1   .DF1  QF1   CC3R
 .SS2   BML          .C8   .DF9  .S2
C
P  NORMAL CELLS ---
 DO     SUB
 QF     MAG          LQ          KF          1.
 QD     MAG          LQ          KD          1.
 C      MMM          .C
        END
        FITQ         DO    C     KF    KD         1     1MUX          MUY
 CR     REF          C
 QD2    MAG          LQ          KD2         1.
 QF2    MAG          LQ          KF2         1.
 CC3    MMM          .BB*  QD2   .C2   .C3
 CC3R   REF          CC3
        CYC          .C
C
P  DISPERSION SUPPRESSOR ---
 MF     SUB
 A1     =            -.27763
 A2     =             .2004968
 A3     =            -.47483
 D1     =            .72963      +           A1
 D4     =            .72963      +           A2
 D5     =            .72963      +           A3
 D2     =            1.9812      -           A1
 D3     =            1.9812      -           A2
 D6     =            .3048       -           A3
 O1     DRF          D1
 O2     DRF          D2
 O3     DRF          D3
 O4     DRF          D4
 O5     DRF          D5
 O6     DRF          D6
 TM     TRKB   O  16 .MM   C                        O   16


        END
        SOLV   2    2 MF    TM        O   16
                                                             O          00001
```

SYNCH RUN PCB1

```
================================================================================================================
***  BRHO    =                //  17.8681155
***  BO      =                //  .730824538
***  BKO     =                //  -.25
***  RHO     =                //  24.4492550
***  RHOI    =                //  1.         /           RHO
***  RHOK    =                //  BKO        /           BRHO
***  LB      =                //  1.3716
***  LQ      =                //  .3048
***  LQL     =                //  .6096
***  LK      =                //  1.596715
***  LK2     =                //  LK         /           2.
***  XP      =                //  LK         *           RHOK
***  X       =                //  LK2        *           XP
***  MUX     =                //  .26633
***  MUY     =                //  .26577
***  B*      =                //  10.
***  BX*     =                //  6.
***  BY*     =                //  6.
         GRADIENTS-- K=GRADIENT/BRHO
***  KF      =                //  .539479
***  KD      =                //  -.534781
***  K1      =                //  .29280
***  K2      =                //  -.38038
***  K3      =                //  .45590
***  KD1     =                //  -.46845
***  K21     =                //  -.36028786
***  K22     =                //  .36375003
***  K23     =                //  -.41305853
***  KF1     =                //   .40384
***  KF9     =                //   .31345
***  KD2     =                //   -.42353
***  KF2     =                //   .40420
         SPECIAL QUADRUPOLE LENGTHS ---
***  LK1     =                //   .6858
***  LK2     =                //   .5715
***  LK3     =                //   .762
***  LKD1    =                //   .4953
***  LKF1    =                //   .3937
***  LK21    =                //   .38710
***  LK22    =                //   .40825
***  LK23    =                //   .49705
***  LKF9    =                //   .33085
         DRIFT SPACES ---
***  D       DRF              //  .3048
***  DD      DRF              //  .72963
***  DDD     DRF              //  4.08243
***  LL      DRF              //  10.
***  L11     DRF              //  1.96582
***  L1      DRF              //  1.1159
***  L2      DRF              //  2.67062
***  L3      DRF              //  .2667
***  LL*     DRF              //  9.9238
***  L2*     DRF              //  2.55632
***  DDD*    DRF              //  4.10783
***  DD*     DRF              //  .64073
***  L[illegible]    D[illegible]           //  77[illegible]
     L[illegible]    D[illegible]           /[illegible] .714[illegible]
***  LA      DRF              //  1.44192
```

```
P  STRAIGHT SECTION NO.  1 --- WITH DISPERSION
 SR1    SUB
 1Q1    MAG           LK1       K1        1.
 1Q2    MAG           LK2       K2        1.
 1Q3    MAG           LK3       K3        1.
 QD1    MAG           LKD1      KD1       1.
 QF1    MAG           LKF1      KF1       1.
 T1     TRKB    0  18 .SS1 CR


        END
 BX2    =             4.
        SOLV    4   1 SR1  T1              18 7000   -6
                      X           11                         0.        .01
                      WAIST       18                         0.        .0000001
                      BX                                     B*        .001
                      BY                                     B*        .001
                      K1   K2   K3   KD1  KF1      1 -1.     1.        .01
C
P  STRAIGHT SECTION NO.  2 --- WITHOUT DISPERSION
 SR2    SUB
 QF9    MAG           LQL       KF9       1.
 2Q3    MAG           LQL       K23       1.
 2Q2    MAG           LQL       K22       1.
 2Q1    MAG           LQL       K21       1.
 T2     TRKB    0  29 .SS2 C


        END
        SOLV    4   1 SR2  T2        0  29
                      AX          29                         0.        .0001
                      AY                                     0.        .0001
                      BX                                     B*        .01
                      BY                                     B*        .01
                      K21  K22  K23  KF9           1 -1.     1.        .01
C
C  BETATRON FUNCTIONS THROUGH ONE QUADRANT, STARTING AT CENTER OF NO. 1 STRAIGHT
        CYC        -2 .SPH
        FIN
```

```
***  BK     MAG            //  LK       0.        1.        RHOK      $

         LATTICE DEFINITION ---
***  .BB    BML            //  OD   B    O    B    O
***  BBB*   BML            //  O    BK   O    BK   O
***  .BB*   BML            //  OO*  B    O    B    O
***  .BB9   BML            //  O5   B    O    B    O6
***  .DF    BML            //  QD   .BB  QF
***  .DF*   BML            //  QD1  BBB* QF1
***  .DF1   BML            //  QD1  OOO* QF1
***  .FD1   BML            //  QF1  .BB* QD2
***  .FD    BML            //  QF   .BD  QD
***  .C     BML            //  .DF  .FD
***  .C1    BML            //  .DF1 .FD1
***  .C2    BML            //  QD2  .BB  QF2  QF2  .BB  QD
***  .C3    BML            //  QD   .BB  QF   QF   OOO  QD
***  .C8    BML            //  QD   O1   B    O2   QF   QF   O3   B    O4   QD
***  .DF9   BML            //  QD   .BB9 QF9
***  .ARC   BML            //  .C1  .C2  .C3  .C   .C   .C   .C   .C8  .DF9
***  .S1    BML            //  LL*  1Q1  1Q1  L3   1Q2  1Q2  L1   L5   L6   1Q3
  *                        //  1Q3  L3   QD1
***  .S2    BML     -1     //  LL   2Q1  2Q1  O    2Q2  2Q2  L11  L2   2Q3  2Q3
  *                        //  O    QF9
***  .SPH   BML            //  .S1  .ARC .S2
***  .MM    BML            //  .C8  QD   .BB9
***  .SS1   BML     -1     //  .S1  .DF1 QF1  CC3R
***  .SS2   BML            //  .C8  .DF9 .S2
```

POS	S(M)	NUX	NUY	BETAX(M)	BETAY(M)	ETAX(M)	ETAY(M)	ETAS(M)	ALPHAX	ALPHAY	DETAX	DETAY
0	0.0000	0.00000	0.00000	9.98616	10.05056	-2.74271	0.00000	0.00000	0.00000	0.00000	.00000	0.00000
1 LL*	9.9238	.12450	.12399	19.84799	19.84920	-2.74271	0.00000	0.00000	-.97376	-.98739	.00000	0.00000
2 1Q1	10.6096	.13007	.12708	18.52435	24.24133	-2.55603	0.00000	0.00000	2.03441	-5.70830	.53815	0.00000
3 1Q1	11.2954	.13700	.13281	12.76701	36.98583	-2.02140	0.00000	0.00000	5.17173	-13.72037	1.00305	0.00000
4 L3	11.5621	.14073	.13386	10.16300	44.66823	-1.75389	0.00000	0.00000	4.59210	-15.08502	1.00305	0.00000
5 1Q2	12.1336	.15214	.13562	6.52372	56.79947	-1.27874	0.00000	0.00000	2.03727	-5.25590	.67691	0.00000
6 1Q2	12.7051	.16825	.13721	5.11048	55.71285	-.96406	0.00000	0.00000	.53712	7.07787	.43571	0.00000
7 L1	13.8210	.20685	.14092	4.22569	41.05851	-.47785	0.00000	0.00000	.25577	6.05444	.43571	0.00000
8 L5	14.7354	.24269	.14502	3.96874	30.75299	-.07944	0.00000	0.00000	.02527	5.21581	.43571	0.00000
9 L6	16.3773	.30571	.15677	4.56563	16.09762	.63597	0.00000	0.00000	-.38075	3.70995	.43571	0.00000
10 1Q3	17.1393	.33269	.16504	4.08761	14.62229	.87122	0.00000	0.00000	.75973	-1.60598	.16808	0.00000
11 1Q3	17.9013	.37241	.17212	2.12978	21.90306	.88097	0.00000	0.00000	1.37806	-8.77714	-.14305	0.00000
12 L3	18.1680	.39632	.17387	1.49119	26.83821	.84282	0.00000	0.00000	1.01555	-9.72736	-.14305	0.00000
13 QD1	18.6633	.46677	.17644	.93153	33.62608	.81949	0.00000	0.00000	.15734	-3.44819	.04796	0.00000
14 QD1	19.1586	.54767	.17876	1.15503	33.15831	.89124	0.00000	0.00000	-.62573	4.35616	.24453	0.00000
15 OOO*	23.2665	.68044	.22060	26.62542	7.53544	1.89572	0.00000	0.00000	-5.57472	1.88141	.24453	0.00000
16 QF1	23.6602	.68265	.22960	29.38567	6.56816	1.93200	0.00000	0.00000	-1.20750	.62652	-.06121	0.00000
17 QF1	24.0539	.68479	.23929	28.57248	6.50713	1.84803	0.00000	0.00000	3.31175	-.46829	-.36313	0.00000
18 OO*	24.6946	.68865	.25423	24.50056	7.10415	1.61536	0.00000	0.00000	3.04307	-.58835	-.36313	0.00000
19 B	26.0662	.69936	.28132	16.94351	9.12548	1.15601	0.00000	.07740	2.46718	-.82480	-.30702	0.00000
20 O	26.3710	.70236	.28649	15.47721	9.64539	1.06243	0.00000	.07740	2.34151	-.88092	-.30702	0.00000
21 B	27.7426	.72007	.30653	9.84450	12.37420	.68001	0.00000	.12593	1.76731	-1.10545	-.25090	0.00000
22 O	28.0474	.72528	.31034	8.80606	13.06476	.60354	0.00000	.12593	1.63765	-1.16019	-.25090	0.00000
23 QD2	28.3522	.73104	.31400	8.17060	13.26272	.53847	0.00000	.12593	.47249	.51928	-.17743	0.00000
24 QD2	28.6570	.73700	.31776	8.21477	12.44814	.49467	0.00000	.12593	-.61702	2.11808	-.11096	0.00000
25 OO	29.3866	.75037	.32837	9.20818	9.59194	.41370	0.00000	.12593	-.74221	1.79651	-.11096	0.00000
26 B	30.7582	.77158	.35871	11.55965	5.47048	.30005	0.00000	.14559	-.97307	1.20362	-.05485	0.00000
27 O	31.0630	.77567	.36820	12.16850	4.77834	.28333	0.00000	.14559	-1.02443	1.06718	-.05485	0.00000
28 B	32.4346	.79169	.43078	15.29376	2.68253	.24660	0.00000	.16010	-1.25582	.45842	.00127	0.00000
29 O	32.7394	.79479	.44976	16.07465	2.44498	.24699	0.00000	.16010	-1.30665	.32092	.00127	0.00000
30 QF2	33.0442	.79777	.47005	16.27074	2.37982	.24275	0.00000	.16010	.67137	-.10447	-.02900	0.00000
31 QF2	33.3490	.80082	.48982	15.27643	2.57556	.22942	0.00000	.16010	2.54704	-.54574	-.05817	0.00000
32 OO	34.0786	.80947	.52812	11.81696	3.64019	.18698	0.00000	.16010	2.17155	-.91340	-.05817	0.00000
33 B	35.4502	.83403	.57166	6.73112	7.07843	.14569	0.00000	.16907	1.51036	-1.58939	-.00206	0.00000
34 O	35.7550	.84177	.57807	5.85115	8.09361	.14506	0.00000	.16907	1.36068	-1.74122	-.00206	0.00000
35 B	37.1266	.87462	.59881	3.02142	13.77433	.18070	0.00000	.17786	.67547	-2.39393	.05405	0.00000
36 O	37.4314	.91182	.60215	2.64307	15.27907	.19718	0.00000	.17786	.54502	-2.54287	.05405	0.00000
37 QD	37.7362	.93098	.60522	2.47919	16.07576	.21871	0.00000	.17786	.00070	-.02748	.08784	0.00000
38 QD	38.0410	.95014	.60829	2.64218	15.31147	.25117	0.00000	.17786	-.54427	2.49329	.12601	0.00000
39 OO	38.7707	.98763	.61688	3.69758	11.92402	.34311	0.00000	.17786	-.70727	2.14940	.12601	0.00000
40 B	40.1423	1.03076	.64107	7.09321	6.88623	.55431	0.00000	.20267	-1.57476	1.51775	.18212	0.00000
41 O	40.4471	1.03716	.64861	8.09876	6.00557	.60982	0.00000	.20267	-1.72427	1.37153	.18212	0.00000
42 B	41.8187	1.05790	.69982	13.74832	3.13275	.89796	0.00000	.24462	-2.37603	.71968	.23824	0.00000
43 O	42.1235	1.06125	.71641	15.25500	2.73705	.97057	0.00000	.24462	-2.54636	.57199	.23824	0.00000
44 QF	42.4283	1.06432	.73491	16.04492	2.56461	1.01824	0.00000	.24462	-.00150	.00991	.07322	0.00000
45 QF	42.7331	1.06740	.75345	15.25686	2.72656	1.01483	0.00000	.24462	2.54351	-.55015	-.09547	0.00000
46 OOO	46.8155	1.17838	.86286	2.64891	15.18103	.62506	0.00000	.24462	.54404	-2.50060	-.09547	0.00000
47 QD	47.1203	1.19749	.86595	2.48581	15.95660	.61132	0.00000	.24462	-.00087	-.00160	.00496	0.00000
48 QD	47.4251	1.21659	.86904	2.65003	15.18292	.62811	0.00000	.24462	-.54680	2.49771	.10564	0.00000

POS	S(M)	NUX	NUY	BETAX(M)	BETAY(M)	ETAX(M)	ETAY(M)	ETAS(M)	ALPHAX	ALPHAY	DETAX	DETAY
50 B	49.5263	1.29699	.90226	7.10988	6.76354	.88847	0.00000	.28897	-1.57642	1.51044	.16175	0.00000
51 O	49.8311	1.30337	.90995	8.11641	5.88785	.93777	0.00000	.28897	-1.72503	1.36256	.16175	0.00000
52 B	51.2027	1.32407	.96241	13.76943	3.05016	1.19798	0.00000	.34854	-2.37701	.70307	.21787	0.00000
53 O	51.5075	1.32742	.97945	15.27667	2.66709	1.26438	0.00000	.34854	-2.54721	.55374	.21787	0.00000
54 QF	51.8123	1.33049	.99844	16.06598	2.50097	1.29852	0.00000	.34854	.00123	.00039	.00521	0.00000
55 QF	52.1171	1.33356	1.01742	15.27522	2.66660	1.26753	0.00000	.34854	2.54743	-.55288	-.20770	0.00000
56 OO	52.8468	1.34221	1.05456	11.81631	3.73406	1.11599	0.00000	.34854	2.17171	-.91014	-.20770	0.00000
57 B	54.2184	1.36677	1.09736	6.73121	7.13624	.86971	0.00000	.40389	1.51015	-1.56640	-.15159	0.00000
58 O	54.5232	1.37450	1.10373	5.85136	8.13607	.82351	0.00000	.40389	1.36651	-1.71391	-.15159	0.00000
59 B	55.8948	1.42735	1.12446	3.02192	13.71513	.65416	0.00000	.44499	.67545	-2.34724	-.09547	0.00000
60 O	56.1996	1.44455	1.12782	2.64358	15.19011	.62506	0.00000	.44499	.54581	-2.49191	-.09547	0.00000
61 QD	56.5044	1.46370	1.13091	2.47973	15.95982	.61132	0.00000	.44499	.00064	.00860	.00496	0.00000
62 QD	56.8092	1.48285	1.13400	2.64278	15.17997	.62811	0.00000	.44499	-.54440	2.50742	.10564	0.00000
63 OO	57.5388	1.52034	1.14267	3.69834	11.77654	.70519	0.00000	.44499	-.70231	2.15716	.10564	0.00000
64 B	58.9104	1.56346	1.16730	7.09413	6.73440	.88847	0.00000	.48934	-1.57477	1.51315	.16175	0.00000
65 O	59.2152	1.56786	1.17502	8.09968	5.85736	.93777	0.00000	.48934	-1.72427	1.36427	.16175	0.00000
66 B	60.5868	1.59060	1.22788	13.74914	3.02135	1.19798	0.00000	.54891	-2.37675	.70015	.21787	0.00000
67 O	60.8916	1.59395	1.24509	15.25578	2.64036	1.26438	0.00000	.54891	-2.54627	.54981	.21787	0.00000
68 QF	61.1964	1.59702	1.26427	16.04560	2.47567	1.29852	0.00000	.54891	-.00136	-.00042	.00521	0.00000
69 QF	61.5012	1.60010	1.28345	15.25738	2.64090	1.26753	0.00000	.54891	2.54002	-.55074	-.20770	0.00000
70 OO	62.2308	1.60875	1.32091	11.80597	3.70730	1.11599	0.00000	.54891	2.10654	-.91083	-.20770	0.00000
71 B	63.6024	1.63333	1.36392	6.73122	7.11872	.86971	0.00000	.60426	1.51527	-1.57244	-.15159	0.00000
72 O	63.9072	1.64106	1.37030	5.85301	8.12260	.82351	0.00000	.60426	1.36602	-1.72113	-.15159	0.00000
73 B	65.2788	1.69385	1.39103	3.02794	13.72873	.65416	0.00000	.64536	.67475	-2.35973	-.09547	0.00000
74 O	65.5836	1.71101	1.39439	2.64991	15.21167	.62506	0.00000	.64536	.54550	-2.50556	-.09547	0.00000
75 QD	65.8884	1.73011	1.39748	2.48645	15.98872	.61132	0.00000	.64536	-.00036	-.00143	.00496	0.00000
76 QD	66.1932	1.74921	1.40056	2.65036	15.21336	.62811	0.00000	.64536	-.54629	2.50297	.10564	0.00000
77 OO	66.9228	1.78659	1.40923	3.70835	11.81510	.70519	0.00000	.64536	-.70374	2.15455	.10564	0.00000
78 B	68.2944	1.82961	1.43372	7.10688	6.77525	.88847	0.00000	.68971	-1.57535	1.51410	.16175	0.00000
79 O	68.5992	1.83600	1.44140	8.11273	5.89741	.93777	0.00000	.68971	-1.72467	1.36598	.16175	0.00000
80 B	69.9708	1.85671	1.49380	13.76205	3.05184	1.19798	0.00000	.74928	-2.37627	.70540	.21787	0.00000
81 O	70.2756	1.86006	1.51083	15.26833	2.66742	1.26438	0.00000	.74928	-2.54560	.55583	.21787	0.00000
82 QF	70.5804	1.86313	1.52982	16.05708	2.50008	1.29852	0.00000	.74928	.00143	.00238	.00521	0.00000
83 QF	70.8852	1.86620	1.54882	15.26664	2.66442	1.26753	0.00000	.74928	2.54010	-.55059	-.20770	0.00000
84 OO	71.6149	1.87486	1.58600	11.80947	3.72824	1.11599	0.00000	.74928	2.17006	-.90744	-.20770	0.00000
85 B	72.9865	1.89943	1.62888	6.72726	7.12201	.86971	0.00000	.80463	1.51770	-1.56298	-.15159	0.00000
86 O	73.2913	1.90717	1.63526	5.84797	8.11971	.82351	0.00000	.80463	1.36760	-1.71032	-.15159	0.00000
87 B	74.6629	1.96005	1.65603	3.02075	13.68799	.65416	0.00000	.84573	.67474	-2.34298	-.09547	0.00000
88 O	74.9677	1.97725	1.65939	2.64284	15.16031	.62506	0.00000	.84573	.54513	-2.48749	-.09547	0.00000
89 QD	75.2725	1.99640	1.66249	2.47937	15.92883	.61132	0.00000	.84573	.00007	.00804	.00496	0.00000
90 QD	75.5773	2.01556	1.66559	2.64276	15.15083	.62811	0.00000	.84573	-.54477	2.50199	.10564	0.00000
91 OO	76.3069	2.05304	1.67429	3.69931	11.75487	.70519	0.00000	.84573	-.70308	2.15237	.10564	0.00000
92 B	77.6785	2.09615	1.69095	7.09766	6.72428	.88847	0.00000	.89008	-1.57508	1.50954	.16175	0.00000
93 O	77.9833	2.10255	1.70668	8.10391	5.84737	.93777	0.00000	.89008	-1.72547	1.36092	.16175	0.00000
94 B	79.3549	2.12327	1.75958	13.75706	3.02087	1.19798	0.00000	.94965	-2.37007	.69802	.21787	0.00000
95 O	79.6597	2.12662	1.77679	15.26464	2.64109	1.26438	0.00000	.94965	-2.54706	.54796	.21787	0.00000
96 QF	79.9645	2.12969	1.79596	16.05499	2.47751	1.29852	0.00000	.94965	-.00145	-.00230	.00521	0.00000
97	[illegible]	[illegible]	[illegible]	[illegible]	[illegible]	[illegible]	[illegible]	[illegible]	[illegible]	[illegible]	[illegible]	[illegible]
98 OO	80.9989	2.14141	1.85252	11.81295	3.71394	1.11599	0.00000	[illegible]	[illegible]	[illegible]	[illegible]	

POS	S(M)	NUX	NUY	BETAX(M)	BETAY(M)	ETAX(M)	ETAY(M)	ETAS(M)	ALPHAX	ALPHAY	DETAX	DETAY
100 O	82.6753	2.17370	1.90182	5.85619	8.13885	.82351	0.00000	1.00500	1.36700	-1.72429	-.15159	0.00000
101 B	84.0469	2.22647	1.92251	3.02880	13.75428	.65416	0.00000	1.04610	.67546	-2.36334	-.09547	0.00000
102 O	84.3517	2.24362	1.92586	2.65035	15.23945	.62506	0.00000	1.04610	.54616	-2.50927	-.09547	0.00000
103 QD	84.6565	2.26272	1.92894	2.48652	16.01737	.61132	0.00000	1.04610	.00073	-.00050	.00496	0.00000
104 QD	84.9613	2.28182	1.93202	2.65006	15.24005	.62811	0.00000	1.04610	-.54565	2.50836	.10564	0.00000
105 O1	85.4113	2.30636	1.93709	3.24031	13.07941	.67565	0.00000	1.04610	-.76601	2.29305	.10564	0.00000
106 B	86.7829	2.35558	1.95898	6.26083	7.65801	.85893	0.00000	1.08880	-1.43733	1.65334	.16175	0.00000
107 O2	89.0438	2.39273	2.04223	15.26297	2.67413	1.22462	0.00000	1.08880	-2.54446	.55111	.16175	0.00000
108 QF	89.3486	2.39580	2.06116	16.05129	2.50780	1.24280	0.00000	1.08890	.00167	-.00296	-.04298	0.00000
109 QF	89.6534	2.39887	2.08008	15.26100	2.67786	1.19864	0.00000	1.08890	2.54746	-.55765	-.24556	0.00000
110 O3	91.4559	2.42551	2.15251	7.67191	6.27875	.75603	0.00000	1.08880	1.66206	-1.44008	-.24556	0.00000
111 B	92.8275	2.46513	2.17875	4.03505	11.12420	.45786	0.00000	1.12250	.77008	-2.08706	-.18944	0.00000
112 O4	93.7358	2.51001	2.18984	2.64132	15.31292	.28579	0.00000	1.12250	.54430	-2.52438	-.18944	0.00000
113 QD	94.0406	2.52917	2.19290	2.47828	16.09640	.23470	0.00000	1.12250	-.00057	-.00333	-.14716	0.00000
114 QD	94.3454	2.54833	2.19597	2.64204	15.31685	.19533	0.00000	1.12250	-.54557	2.51837	-.11223	0.00000
115 O5	94.5626	2.56083	2.19831	2.90222	14.24543	.17096	0.00000	1.12250	-.65225	2.41424	-.11223	0.00000
116 B	95.9342	2.61598	2.21821	5.61357	8.49008	.05557	0.00000	1.12849	-1.32556	1.77523	-.05611	0.00000
117 O	96.2390	2.62404	2.22431	6.46726	7.45333	.03846	0.00000	1.12849	-1.47526	1.62619	-.05611	0.00000
118 B	97.6106	2.64952	2.26527	11.43511	3.89585	-.00000	0.00000	1.12921	-2.14050	.96340	-.00000	0.00000
119 O6	98.4278	2.65936	2.30618	15.27483	2.65176	-.00000	0.00000	1.12921	-2.54975	.55894	-.00000	0.00000
120 QF9	99.0374	2.66534	2.34559	16.63920	2.42427	-.00000	0.00000	1.12921	.37017	-.17160	-.00000	0.00000
121 QF9	99.6470	2.67149	2.38196	14.37666	3.10295	-.00000	0.00000	1.12921	3.17026	-.98401	.00000	0.00000
122 O	99.9518	2.67511	2.39618	12.51548	3.76173	-.00000	0.00000	1.12921	2.73577	-1.17735	.00000	0.00000
123 2Q3	100.5614	2.68365	2.41865	10.85077	4.74143	-.00000	0.00000	1.12921	-.06715	-.34810	-.00000	0.00000
124 2Q3	101.1710	2.69213	2.43912	12.70157	4.52767	-.00000	0.00000	1.12921	-3.11015	.68092	-.00000	0.00000
125 L2	103.8416	2.71223	2.56298	35.37746	3.19632	-.00000	0.00000	1.12921	-5.37272	-.18241	-.00000	0.00000
126 L11	105.8075	2.71904	2.64338	59.76350	5.16273	-.00000	0.00000	1.12921	-7.03230	-.81789	-.00000	0.00000
127 2Q2	106.4171	2.72062	2.65979	60.21664	7.10217	-.00000	0.00000	1.12921	6.32254	-2.50478	.00000	0.00000
128 2Q2	107.0267	2.72243	2.67062	45.69035	11.83209	-.00000	0.00000	1.12921	16.43026	-5.59854	.00000	0.00000
129 O	107.3315	2.72362	2.67420	36.22539	15.47891	-.00000	0.00000	1.12921	14.62273	-6.43173	.00000	0.00000
130 2Q1	107.9411	2.72697	2.67938	24.13221	21.64973	-.00000	0.00000	1.12921	6.07153	-3.20444	.00000	0.00000
131 2Q1	108.5507	2.73149	2.68367	20.01194	22.63451	-.00000	0.00000	1.12921	.76604	1.66163	.00000	0.00000
132 LL	118.5507	2.85374	2.84745	10.35156	6.01817	-.00000	0.00000	1.12921	.00000	.00000	.00000	0.00000
133 REFL	237.1013	5.70748	5.69489	9.98616	10.05056	-2.74271	0.00000	2.25842	-.00000	.00000	.00000	0.00000

```
CIRCUMFERENCE =   474.2027 M        THETX =    6.28318532 RAD      NUX =   11.41496      DNUX/(DP/P) =   -18.28241
       RADIUS =    75.4717 M   THETY( 132) =   0.00000000 RAD      NUY =   11.38979      DNUY/(DP/P) =   -17.87367
(DS/S)/(DP/P) =    .0095251
                                 TGAM = (   10.24624,     0.00000)

MAXIMA    --- BETX( 127) =    60.21664    BETY(   5) =    56.79947    ETAX(   1) =    -2.74271    ETAY( 133) =     0.00000
MINIMA    --- BETX(  13) =      .93153    BETY(  30) =     2.37982    ETAX( 118) =     -.00000    ETAY( 133) =     0.00000

***        FIN     0    0  // CORE USE SUMMARY                          MAXIMUM              USED        UNUSED
                              STORE   (ELEMENT STORAGE)                  9600 (LMAX)        3789          5811
                              INFF    (ELEMENT DEFINITIONS)               400 (MAX)          152           248

END OF SYNCH RUN PC81
```

Appendix C

Accumulator Orbit Listing

```
          SYN      UN                       GE     ECT    :OOL     RIN     CUM     OR
*****************************************************************************************************************************

                                16 APRIL 81. DE JOHNSON.
                                THIS HAS REAL EFFECTIVE LENGTHS INCLUDING SAGITTA
 ***   BRHO     =               //  56.574
 ***   BZ       =               //  6.1683960
 ***   BL       =               //  1.3097
 ***   QL       =               //  0.6767

 ***   O        DRF             //  0.2266
 ***   OP       DRF             //  0.2154
 ***   OO       DRF             //  0.5314
 ***   OD1      DRF             //  0.2577
 ***   OD2      DRF             //  2.0243
 ***   NSS      DRF             //  2.2637
 ***   OS1      DRF             //  0.9706
 ***   OS2      DRF             //  1.9218
 ***   OS3      DRF             //  1.6794
 ***   WLS      DRF             //  9.6590
 ***   OL1      DRF             //  0.5425
 ***   OL2      DRF             //  0.7321
 ***   OL3      DRF             //  3.5794

 ***   GF       =               //  28.6961
 ***   GD       =               //  -26.4708
 ***   G1       =               //  15.0678
 ***   G2       =               //  -28.8425
 ***   G3       =               //  22.6898
 ***   G9       =               //  -9.0982
 ***   G10      =               //  43.8154
 ***   G11      =               //  -37.8895

 ***   1B21     MAG           1 //  BL          0.         BRHO      BZ        $
   *                            //  0.08255     0.479      2.8
 ***   1B31     MAG           1 //  BL          0.         BRHO      BZ        $
   *                            //  0.08255     0.479      2.8
 ***   1B32     MAG           1 //  BL          0.         BRHO      BZ        $
   *                            //  0.08255     0.479      2.8
 ***   1B41     MAG           1 //  BL          0.         BRHO      BZ        $
   *                            //  0.08255     0.479      2.8
 ***   1B42     MAG           1 //  BL          0.         BRHO      BZ        $
   *                            //  0.08255     0.479      2.8
 ***   1B51     MAG           1 //  BL          0.         BRHO      BZ        $
   *                            //  0.08255     0.479      2.8
 ***   1B52     MAG           1 //  BL          0.         BRHO      BZ        $
   *                            //  0.08255     0.479      2.8
 ***   1B61     MAG           1 //  BL          0.         BRHO      BZ        $
   *                            //  0.08255     0.479      2.8
 ***   1B71     MAG           1 //  BL          0.         BRHO      BZ        $
   *                            //  0.08255     0.479      2.8
 ***   1B81     MAG           1 //  BL          0.         BRHO      BZ        $
   *                            //  0.08255     0.479      2.8
 ***   1B82     MAG           1 //  BL          0.         BRHO      BZ        $
   *                            //  0.08255     0.479      2.8

 ***   1QF1     MAG             //  QL          G1         BRHO
 ***   1QD2     MAG             //  QL          G2         BRHO
 ***   1QF3     MAG             //  QL          G3         BRHO
 ***   1QD4     MAG             //  QL          GD         BRHO
 ***   1QF5     MAG             //  QL          GF         BRHO
```

```
***  1QD6    MAG          //  QL           GD          BRHO
***  1QF7    MAG          //  QL           GF          BRHO
***  1QD8    MAG          //  QL           GD          BRHO
***  1QD9    MAG          //  QL           G9          BRHO
***  1QF10   MAG          //  QL           G10         BRHO
***  1QD11   MAG          //  QL           G11         BRHO
***  .R/4    BML          //  NSS  1QF1 OS1  1QD2 OS2  1B21 O    1QF3 O    1B31 OP
       *                  //  1B32 OS3  1QD4 O    1B41 OP   1B42 OO   1QF5 O    1B51
       *                  //  OP   1B52 OO   1QD6 OD1  1B61 OD2  1QF7 OD2  1B71 OD1
       *                  //  1QD8 O    1B81 OP   1B82 OL3  1QD9 OL2  1QF10OL1  1QD11
       *                  //  WLS
***          PAGE         //
```

*** RING CYC -2 // .R/4

POS	S(M)	NUX	NUY	BETAX(M)	BETAY(M)	ETAX(M)	ETAY(M)	ETAS(M)	ALPHAX	ALPHAY	DETAX	DETAY
0	0.0000	0.00000	0.00000	10.37395	11.43059	3.50552	0.00000	0.00000	0.00000	0.00000	.00000	0.00000
1 NSS	2.2637	.03419	.03112	10.86791	11.87889	3.50552	0.00000	0.00000	-.21821	-.19804	.00000	0.00000
2 1QF1	2.9404	.04437	.03973	9.90972	13.71960	3.29392	0.00000	0.00000	1.57614	-2.63179	-.61904	0.00000
3 0S1	3.9110	.06272	.04921	7.18134	19.37269	2.69308	0.00000	0.00000	1.23488	-3.19254	-.61904	0.00000
4 1QD2	4.5877	.07829	.05459	7.22257	19.11478	2.57821	0.00000	0.00000	-1.30049	3.54354	.27296	0.00000
5 0S2	6.5095	.10935	.07925	13.59736	8.11422	3.10278	0.00000	0.00000	-2.01660	2.18055	.27296	0.00000
6 1B21	7.8192	.12212	.11866	19.49652	3.51891	3.55241	0.00000	.47376	-2.50296	1.29447	.41600	0.00000
7 0	8.0458	.12392	.12932	20.65000	2.97130	3.64667	0.00000	.47376	-2.58740	1.12217	.41600	0.00000
8 1QF3	8.7225	.12902	.17371	20.33300	2.20961	3.58987	0.00000	.47376	3.02681	.07149	-.58131	0.00000
9 0	8.9491	.13085	.19009	18.98691	2.20057	3.45814	0.00000	.47376	2.91356	-.03159	-.58131	0.00000
10 1B31	10.2588	.14450	.27490	12.23247	3.02077	2.79274	0.00000	.91860	2.26125	-.58866	-.43827	0.00000
11 0P	10.4742	.14742	.28577	11.28151	3.29504	2.69834	0.00000	.91860	2.15360	-.68467	-.43827	0.00000
12 1B32	11.7839	.17175	.33431	6.51094	5.77298	2.21964	0.00000	1.26811	1.50130	-1.18917	-.29522	0.00000
13 0S3	13.4633	.23516	.36819	2.87790	10.94660	1.72384	0.00000	1.26811	.66200	-1.89146	-.29522	0.00000
14 1QD4	14.1400	.27521	.37760	2.75597	11.15177	1.70485	0.00000	1.26811	-.46914	1.61024	.23809	0.00000
15 0	14.3666	.28778	.38094	2.99131	10.43855	1.75880	0.00000	1.26811	-.56946	1.53723	.23809	0.00000
16 1B41	15.6763	.34129	.40578	5.23212	6.80393	2.16293	0.00000	1.54637	-1.14730	1.21132	.38114	0.00000
17 0P	15.8917	.34755	.41101	5.74692	6.29892	2.24503	0.00000	1.54637	-1.24266	1.13321	.38114	0.00000
18 1B42	17.2014	.37545	.45380	9.74513	3.86084	2.83586	0.00000	1.90753	-1.82051	.71049	.52418	0.00000
19 00	17.7328	.38334	.47789	11.80498	3.21580	3.11441	0.00000	1.90753	-2.05576	.50337	.52418	0.00000
20 1QF5	18.4095	.39211	.51188	11.82736	3.42336	3.10080	0.00000	1.90753	2.02529	-.83348	-.56362	0.00000
21 0	18.6361	.39528	.52185	10.93164	3.82651	2.97308	0.00000	1.90753	1.92755	-.94566	-.56362	0.00000
22 1B51	19.9458	.41977	.56240	6.63466	7.05592	2.33077	0.00000	2.28464	1.36452	-1.49645	-.42058	0.00000
23 0P	20.1612	.42517	.56705	6.06684	7.72189	2.24017	0.00000	2.28464	1.27160	-1.59534	-.42058	0.00000
24 1B52	21.4709	.47100	.58833	3.48221	12.50076	1.78456	0.00000	2.57026	.70857	-2.01849	-.27754	0.00000
25 00	22.0023	.49797	.59456	2.85094	14.76063	1.63708	0.00000	2.57026	.47935	-2.23419	-.27754	0.00000
26 1QD6	22.6790	.53668	.60164	2.97325	14.60049	1.62103	0.00000	2.57026	-.67282	2.45371	.22925	0.00000
27 0D1	22.9367	.54968	.60457	3.35247	13.36778	1.68010	0.00000	2.57026	-.79873	2.32979	.22925	0.00000
28 1B61	24.2464	.59563	.62492	6.26996	7.89329	2.07268	0.00000	2.83644	-1.43646	1.81008	.37229	0.00000
29 0D2	26.2707	.63018	.69597	14.08773	2.78509	2.82631	0.00000	2.83644	-2.42550	.71336	.37229	0.00000
30 1QF7	26.9474	.63754	.73781	14.06556	2.62948	2.74667	0.00000	2.83644	2.45569	-.46589	-.60311	0.00000
31 0D2	28.9717	.67240	.81985	6.17166	6.41233	1.52580	0.00000	2.83644	1.44388	-1.40283	-.60311	0.00000
32 1B71	30.2814	.71944	.84510	3.25396	10.72319	.83194	0.00000	3.00284	.79147	-1.85709	-.46006	0.00000
33 0D1	30.5391	.73285	.84876	2.87923	11.70789	.71338	0.00000	3.00284	.66267	-1.96400	-.46006	0.00000
34 1QD8	31.2158	.77288	.85758	2.75661	11.84460	.46862	0.00000	3.00284	-.46871	1.77661	-.27621	0.00000
35 0	31.4424	.78545	.86074	2.99175	11.05746	.40603	0.00000	3.00284	-.56897	1.69709	-.27621	0.00000
36 1B81	32.7521	.83897	.88444	5.23087	7.04556	.13886	0.00000	3.03958	-1.14649	1.33675	-.13317	0.00000
37 0P	32.9675	.84522	.88951	5.74531	6.48805	.11018	0.00000	3.03958	-1.24180	1.25154	-.13317	0.00000
38 1B82	34.2772	.87314	.93202	9.74085	3.79584	.02972	0.00000	3.04735	-1.81932	.78433	.00988	0.00000
39 0L3	37.8566	.90764	1.13914	28.43385	3.63267	.06507	0.00000	3.04735	-3.40306	-.73875	.00988	0.00000
40 1QD9	38.5333	.91106	1.16558	35.83717	4.48629	.07447	0.00000	3.04735	-7.82789	-.48882	.01808	0.00000
41 0L2	39.2654	.91386	1.18946	48.23016	5.35004	.08771	0.00000	3.04735	-9.10010	-.69100	.01808	0.00000
42 1QF10	39.9421	.91608	1.20613	43.36396	8.79731	.08414	0.00000	3.04735	15.42026	-4.99168	-.02833	0.00000
43 0L1	40.4846	.91854	1.21363	28.25358	15.08031	.06877	0.00000	3.04735	12.43297	-6.58989	-.02833	0.00000
44 1QD11	41.1613	.92329	1.21962	20.14707	19.32980	.05942	0.00000	3.04735	.74682	.96565	.00000	0.00000
45 WLS	50.8203	1.02538	1.34184	12.93357	10.00261	.05942	0.00000	3.04735	-.00000	-.00000	.00000	0.00000
46 REFL	101.6406	2.05077	2.68368	10.37395	11.43059	3.50552	0.00000	6.09471	-.00000	.00000	.00000	0.00000

CIRCUMFERENCE = 203.2812 M THETX = 6.28318525 RAD NUX = 4.10154 DNUX/(DP/P) = -6.45980
(DS/S)/RDDZ85 = .0899533 M THETY(45) = 0.00000000 RAD NUY = 5.36736 DNUY/(DP/P) = -6.09567
TGAM = (4.08373, 0.00000)

MAXIMA --- BETX(41) = 48.23016 BETY(3) = 19.37269 ETAX(7) = 3.64667 ETAY(46) = 0.00000
MINIMA --- BETX(14) = 2.75597 BETY(9) = 2.20057 ETAX(38) = .02972 ETAY(46) = 0.00000